

INVESTIGATION OF THE STABILITY AND SEPARATION OF WATER-IN-OIL EMULSION

by

António Luzaiadio Bucu André

Thesis submitted in partial fulfilment of the requirements for the degree of

**MASTER OF SCIENCE IN ENGINEERING
(CHEMICAL ENGINEERING)**



in the Department of Process Engineering
at the University of Stellenbosch

Supervised by
Dr. Raymond Els

STELLENBOSCH
December 2009

Declaration

By submitting this dissertation electronically, I declare that the entirety of the work contained therein is my own, original work, that I am the owner of the copyright thereof (unless to the extent explicitly otherwise stated) and that I have not previously in its entirety or in part submitted it for obtaining any qualification.

December 2009

Copyright © 2009 Stellenbosch University

All rights reserved

ABSTRACT

The study of water-in-oil emulsion stability and separation was carried out for this thesis. The main objectives were as follows: to rank crude oil samples in terms of creating stable emulsions; to assess the effect of the brine pH on emulsion stability; to investigate the influence of different organic acids on emulsion stability; and to determine the efficiency of an electric separator in removing water droplets from a flowing organic liquid.

Seven crude oil samples from different sources such as A, C, H, M, P, U, and V were used to investigate the water-in-crude-oil emulsion. Two crude oil blends were also used. Brine solution comprising 4 wt% NaCl and 1 wt% CaCl₂ was used. In this study the gravity settling, critical electric field (CEF) and centrifuge test methods were used to estimate the emulsion stability created by the crude oil and crude oil blend samples. The experiments were carried out at 60°C. In the gravity test method, the brine pH, stirring speed, stirring time and water-cut (the fraction of water in the emulsion) were changed in 2^{IV-1} factorial design. The parameters for the centrifuge and CEF test methods were selected on the basis of the gravity test method. The crude oil samples were ranked in terms of creating stable emulsion in the following order V, U, P, H, A, M and C. The crude oil blends created more stable emulsions than their respective constituents. The ranking order of the crude oil samples did not correlate to asphaltenes, resins, wax or total acid number (TAN). There was a good correlation between the test methods used. There was an increase and decrease in the brine pH when different crude oil samples were in contact with the brine. It is believed that the structure of the surfactants present in crude oil may explain the emulsion-forming characteristics of different crude oil deposits around the world.

To account for the effect of organic acids on emulsion stability, different organic acids were used. In this case, a mixture of equal volumes of heptane and toluene (here referred to as heptol) was used as the model for crude oil. The brine solution composition was the same as the one used in the crude oil experiments. Equal volumes of heptol and brine were mixed for a period of time and then separated. The brine pH was changed from acidic to basic. In this regard, gas

chromatography and liquid chromatography were used to analyse the concentration of the acids in the brine and heptol samples. It was found that the partitioning coefficient for acids containing a straight-chain hydrocarbon moiety decreased with an increase in molecular weight. However, the partitioning coefficient depended on the structure of the acid. The presence of a benzene ring in the organic acid increased the partitioning coefficient. Organic acids with rings created an interface layer when the heptol sample was mixed with basic brine solution. This confirmed that the emulsion of water and crude oil starts with the formation of a film, and it also provides insight into the formation of naphthenate soap. It is believed that the naphthenic acids that cause stable emulsions have rings. More organic acids should be tested. It is recommended that the interaction of asphaltenes, resins and naphthenic acids should be investigated at different pH levels, temperatures and pressures.

The separation of water droplets from a flowing organic liquid was carried out using a direct current (d.c.) electric separator. The separator used centrifugal forces and a d.c. electric field to enhance the removal of water drops from a flowing organic liquid. For this, vegetable oil, crude oil blend and heptane were used as the continuous phase. The experiments were carried out at room temperature (for heptane and vegetable oil) and at 70°C (for vegetable oil and crude oil blend). The flow rate to the separator was kept constant. The separator removed water droplets from flowing organic liquids. A maximum of 97% (at 100 V) of water droplets was removed from the heptane liquid; a maximum of 28% (at 100 V) of water droplets was removed from the vegetable oil at 70°C and 5% (at 100 V) of water droplets was removed from the crude oil blend. The d.c. electric field enhanced the efficiency of the separator in removing water droplets. The break-up of the droplets is suspected to decrease the efficiency of the separator. This separator can easily be installed into existing process lines and does not require much space. However, further improvements are needed in the design of this separator.

Emulsions created in the petroleum industries are quite complex to deal with. The identification of the structure of the components in crude oil is a matter that still has to be investigated. An improvement in the techniques may lead to a better understanding of the cause of the ultra-stable emulsion encountered in the petroleum and related industries.

OPSOMMING

Die studie van die stabiliteit en skeiding van water-in-olie-emulsies is vir hierdie tesis uitgevoer. Die hoofdoelstellings was as volg: om ruolie-monsters in terme van die skepping van stabiele emulsies te klassifiseer; om die effek van die pekel-pH op emulsie-stabiliteit te assesser; om die invloed van verskillende organiese sure op emulsie-stabiliteit te ondersoek; en om die doeltreffendheid van 'n elektriese skeier in die verwydering van waterdruppels uit 'n vloeiende organiese vloeistof te bepaal.

Sewe ruolie-monsters uit verskillende bronne soos was A, C, H, M, P, U en V gebruik om die water-in-ruolie-emulsie te ondersoek. Twee ruolie-mengels is ook gebruik. 'n Pekeloplossing wat 4 wt% NaCl en 1 wt% CaCl₂ bevat, is gebruik. In hierdie studie is die gravitasie-afsakkings-, kritieke elektriese veld- (KEV-) en sentrifuge-toetsmetodes gebruik om die emulsie-stabiliteit te beraam wat deur die ruolie- en ruolie-mengsel-monsters geskep is. Die eksperimente is teen 60°C uitgevoer. In die gravitasietoetsmetode is die pekel-pH, roertempo en watersnyding (die fraksie van water in die emulsie) is in 'n 2^{IV-1}-faktoriaalontwerp ondersoek. Die parameters vir die sentrifuge- en KEV-toetsmetodes is op grond van die gravitasietoetsmetode resultate gekies. Die ruolie-monsters is in terme van die skepping van 'n emulsie stabiliteit geklassifiseer in die volgende orde V, U, P, H, A, M, en C. Die ruolie-mengsels het meer stabiele emulsies gerorm as die respektiewe samestellende dele. Die rangorde van emulsie stabiliteit van die ruolie-monsters het nie met asfaltene, hars, waks of totale suurgetal gekorreleer nie. Daar was 'n goeie korrelasie tussen die toetsmetodes wat gebruik is. Daar was 'n toename of afname in die pekel-pH wanneer verskillende ruolie-monsters in kontak met die pekel was. Die aanname is dat die struktuur van die surfaktante wat in die ruolie teenwoordig is, die emulsievormende karaktereienskappe van verskillende ruolie-neerslae regoor die wêreld kan verklaar.

Om die effek van organiese sure op emulsie-stabiliteit te verklaar, is verskillende organiese sure gebruik. In hierdie geval is 'n mengsel van gelyke hoeveelhede heptaan en toluen (voortaan verwys na as heptol) as die model vir ruolie gebruik. Die pekeloplossing-samestelling was

dieselfde as die een wat in die ruolie-eksperimente gebruik is. Gelyke hoeveelhede heptol en pekel is vir 'n tydperk gemeng en toe geskei. Die pekel-pH is van suurvormend tot basies verander. Gaschromatografie en vloeistofchromatografie is gebruik om die konsentrasie van die sure in die pekel- en heptoloplossings te analiseer. Daar is gevind dat die verdelingskoëffisiënt vir sure wat 'n reguitketting-koolwaterstofhelfte bevat met 'n toename in molekulêre gewig afneem. Die verdelingskoëffisiënt het egter van die struktuur van die suur afgehang. Die teenwoordigheid van 'n benseenring in die organiese suur het die verdelingskoëffisiënt verhoog. Organiese sure met ringe het 'n tussenvlaklaag geskep toe die heptolmonster met die basiese pekeloplossing gemeng is. Dit het bevestig dat die emulsie van water en ruolie met die vorming van 'n vlies begin, en gee ook insig in die vorming van naftenaatseep. Dit blyk dat die naftenaatsure wat stabiele emulsies veroorsaak, ringe het. Meer organiese sure moet getoets word. Daar word aanbeveel dat die interaksie van asfaltene, hars en naftenaatsure teen verskillende pH-vlakke, temperature en drukke getoets word.

Die skeiding van waterdruppels uit 'n vloeiende organiese vloeistof is uitgevoer met behulp van 'n gelykstroom- elektriese skeier. Die skeier het sentrifugiese kragte en 'n wisselstroom- elektriese veld gebruik om die verwydering van waterdruppels uit 'n vloeiende organiese vloeistof te verhoog. Hiervoor is plantolie, 'n ruolienmengsel en heptaan gebruik as die deurlopende fase. Die eksperimente is teen kamertemperatuur (vir heptaan en plantolie) en teen 70°C (vir plantolie en ruolie-mengsel) uitgevoer. Die vloeitempo na die skeier is konstant gehou. Die skeier het waterdruppels uit die vloeiende organiese vloeistowwe verwyder. N' maksimum van 97% (by 100 V) van die water drupples is verweider van die heptaan vloeistof; a maksimum van 28% (by 100 V) van die water druppels was verweider van die plantolie by 70°C en 5% (by 100 V) van die water druppels was verweider van die rudie mengsel. Die gelykstroom- elektriese veld het die doeltreffendheid van die skeier om waterdruppels te verwyder, verhoog. Daar word vermoed dat die afbreek van die waterdruppels die doeltreffendheid van die skeier verlaag. Die skeier kan met gemak in bestaande proseslyne geïnstalleer word en benodig nie veel spasie nie. Verdere verbeterings is egter nodig ten opsigte van die ontwerp van hierdie skeier.

Emulsies wat in die petroleumbedrywe geskep word, is kompleks om te hanteer. Die identifikasie van die struktuur van die komponente in ruolie verg verdere ondersoek. 'n

Verbetering in hierdie tegnieke kan tot beter begrip lei van die oorsaak van die ultrastabiele emulsie wat in die petroleum- en verwante bedrywe aangetref word.

ACKNOWLEDGEMENTS

I would like to thank God for leading me to Stellenbosch University. I had great times here. I would also like to thank my family for giving me the go-ahead for this work, especially my mum and daughter. I love you.

I would like to extend my gratitude to my supervisor, Dr Raymonds Els, for the support and opportunities that he gave me. This eventually enriched my understanding of the research area. During the research I received a lot of attention from the Department of Process Engineering, and would also like to extend my acknowledgements to them. I would say that studying at Stellenbosch University was a good experience.

I would like to extend a profound gratitude to the postgraduate fellows in A601, for showing courage in times of need. I would say that this was indeed a good experience for me.

I would like to thank the following people for the attention and moral support I received from them: John Fraser, Mike Turner, Paul Rodgers, Sandra McMinn, Daniela Miranda, Manasses Bandi (Passaro), Edgar Filipe (Tchetcherette), Dionisio Fula (Tejota), Ivan Chingalula (Man Gil) and Ilda Cangolo (Furacão).

Last but the least, I would like to thank everyone who was not included in this section, for believing that I would get this far.

Antonio Luzaiadio

September 2009

TABLE OF CONTENTS

ABSTRACT.....	II
OPSOMMING.....	IV
ACKNOWLEDGEMENTS.....	VII
TABLE OF CONTENTS	VIII
LIST OF FIGURES.....	XI
LIST OF TABLES.....	XIV
1 INTRODUCTION.....	1
2 LITERATURE REVIEW	4
2.1 CRUDE OIL.....	4
2.1.1 Crude oil origin and chemistry.....	4
2.2 EMULSIONS.....	8
2.2.1 Stability mechanisms	11
2.2.1.1 Steric stabilisation	12
2.2.1.2 Marangoni-Gibbs effect	12
2.2.1.3 Rigid film formation	13
2.2.2 Process of emulsion breaking	13
2.2.2.1 Ostwald ripening.....	14
2.2.2.2 Coalescence.....	14
2.2.2.3 Sedimentation or creaming.....	15
2.3 NAPHTHENIC ACIDS	16
2.3.1 Origin and structure	16
2.3.2 Characterisation of naphthenic acids.....	17
2.4 FORMATION OF NAPHTHENATE SOAPS	18
2.5 INTERFACIAL ACTIVITY OF NAPHTHENIC ACIDS	20
2.6 THEORY OF ELECTROSTATIC	21
2.6.1 General rules at dielectric interfaces	22
2.6.1.1 Electric fields normal to the interface	22
2.6.1.2 Electric fields parallel to an interface	23
2.6.1.3 Interfacial charges	24
2.6.2 Spheres in external fields.....	24
2.7 ELECTRIC SEPARATORS	27
2.8 FACTORS AFFECTING ELECTROCOALESCENCE.....	28
2.8.1 The electric field.....	28
2.8.2 The electrode	29
3 WATER-IN-CRUDE-OIL EMULSION STUDIES	30
3.1 EXPERIMENTS	31

3.1.1	<i>Chemicals and materials</i>	31
3.1.2	<i>Experimental design</i>	32
3.1.3	<i>Methods</i>	33
3.2	RESULTS AND DISCUSSION	34
3.2.1	<i>Gravity test method</i>	34
3.2.2	<i>The critical-electric-field and centrifuge methods</i>	40
4	THE ROLE OF ORGANIC ACIDS IN EMULSION STABILITY	43
4.1	EXPERIMENTS	44
4.1.1	<i>Materials</i>	44
4.1.2	<i>Preliminary experiments</i>	45
4.1.3	<i>Experimental procedure</i>	47
4.1.3.1	<i>Naphthenic acids</i>	47
4.1.3.2	<i>Mixture of acids</i>	48
4.1.3.3	<i>5β-Cholanic and 4-heptylbenzoic acid</i>	49
4.1.4	<i>Determination of the partitioning coefficient</i>	50
4.2	RESULTS AND DISCUSSION	50
4.2.1	<i>Influence of naphthenic acids on emulsion stability</i>	50
4.2.2	<i>Influence of cocktail acids on the emulsion stability</i>	55
4.2.3	<i>Influence of 5β-cholanic acid on the emulsion stability</i>	58
4.2.4	<i>Influence of 4-heptylbenzoic acid on the emulsion</i>	61
4.2.5	<i>Comparison of the partitioning coefficients of different acids</i>	64
5	DETERMINATION OF THE EFFICIENCY OF AN ELECTRIC SEPARATOR	66
5.1	EXPERIMENTAL SET-UP AND PROCEDURE	67
5.1.1	<i>The electric separator</i>	67
5.1.2	<i>The separating plant and operation</i>	69
5.1.3	<i>Physical properties of the liquid used</i>	70
5.1.4	<i>Experiments with heptane</i>	72
5.1.5	<i>Experiments with vegetable oil at room temperature</i>	72
5.1.6	<i>Experiments at higher temperature</i>	73
5.2	RESULTS AND DISCUSSION	74
5.2.1	<i>Experiments with heptane</i>	74
5.2.2	<i>Experiments with vegetable oil</i>	76
5.2.3	<i>Influence of the crude oil blend on the efficiency</i>	77
6	CONCLUSIONS	78
7	REFERENCES	80
8	NOMENCLATURE	87
9	APPENDIX A: EXPERIMENTAL DATA	88
9.1	WATER-IN-CRUDE-OIL EMULSION STUDIES	88
9.1.1	<i>Gravity test method</i>	88
9.1.2	<i>Critical-electric-field test method</i>	92
9.1.3	<i>Centrifuge test method</i>	93
9.2	ROLE OF ORGANIC ACID IN EMULSION STABILITY	94

9.2.1	<i>Standard graphs for calibration</i>	94
9.2.2	<i>Data for naphthenic acid experiments</i>	99
9.2.3	<i>Data for cocktails</i>	100
9.2.4	<i>Data for HBA experiments</i>	101
9.2.5	<i>Data for CA samples</i>	101
9.3	NOVEL ELECTRIC SEPARATOR EVALUATION	102
9.3.1	<i>Heptane</i>	102
9.3.2	<i>Crown oil at room temperature</i>	103
9.3.3	<i>Crown oil at $\pm 70^{\circ}\text{C}$</i>	103
9.3.4	<i>Crude oil blend</i>	103
10	APPENDIX B: CHEMICAL STRUCTURES OF THE ACIDS	104
11	APPENDIX C: STATISTICAL ANALYSIS OF THE RESULTS OF THE GRAVITY TEST METHOD	105
11.1	SAMPLE H CRUDE OIL	105
11.2	SAMPLE M CRUDE OIL	107
11.3	SAMPLE U CRUDE OIL	110
11.4	SAMPLE P CRUDE OIL	112
11.5	SAMPLE C CRUDE OIL	114
11.6	SAMPLE A CRUDE OIL	116
11.7	SAMPLE V CRUDE OIL	118
12	APPENDIX D: EQUIPMENT USED	122
13	APPENDIX E: PUBLISHED PAPER	124

LIST OF FIGURES

Figure 1-1: The outline of the research project.....	3
Figure 2-1: Typical SARA method for crude oil	6
Figure 2-2: Hypothetical structure of an asphaltene molecule, adapted from Spiecker (2001).....	7
Figure 2-3: Hypothetical structure of a resin molecule, adapted from Spiecker (2001).....	8
Figure 2-4: Schematic of the solvation of asphaltenes by resins, adapted from Spiecker (2001).....	10
Figure 2-5: Adsorption of asphaltene aggregates on the oil water interface, adapted from Spiecker (2001)	11
Figure 2-6: Emulsion stability by steric mechanism, adapted from Spiecker (2001)	12
Figure 2-7: Emulsion stability in terms of the Marangoni-Gibbs effect (Spiecker 2001)	13
Figure 2-8: Types of naphthenic acids.	17
Figure 2-9: Equilibrium of naphthenate and the reservoir water	20
Figure 2-10: Electric fields normal to the interface, adapted by Crowley (1999)	22
Figure 2-11: Electric fields normal to a metal surface, adapted by Crowley (1999)	23
Figure 2-12: Electric fields parallel to an interface, adapted from Crowley (1999)	23
Figure 2-13: Interfacial charge between two media, adapted from Crowley (1999)	24
Figure 2-14: Spheres in external fields, adapted from Crowley (1999).....	25
Figure 2-15: Sectional drawing of a horizontal separator that combines heat, electrical and mechanical separating methods adapted from Eow and Ghadiri (2002b).....	28
Figure 3-1: Other important properties of crude oil from the different wells, as supplied by the source...	32
Figure 3-2: Model of the experimental approach used (adapted from Montgomery 2005).....	33
Figure 3-3: Change in the pH of the brine under acidic conditions, after the separation of the emulsion..	35
Figure 3-4: Change in the pH of the brine under basic conditions, after the separation of the emulsion ...	35
Figure 3-5: Pareto chart for the sample V crude oil experiments	37
Figure 3-6: Normal probability plot for the experiments with sample V crude oil	38
Figure 3-7: Overall effects for the gravity test method for different crude oil samples.....	40
Figure 3-8: Volume [mL] of water centrifuged from a sample of 10 mL emulsion created by different crude oil samples.....	41

Figure 3-9: Critical electric field (V/cm) values needed to break the emulsion formed by different crude oil samples	41
Figure 4-1: Chromatogram of the mixture of all the acids.....	46
Figure 4-2: Confirmation of the 4-heptylbenzoic acid after elution with blank heptol sample.	47
Figure 4-3: Chromatogram of the standard naphthenic acid with all the peaks.....	51
Figure 4-4: Amplified chromatogram of the standard naphthenic acid.	51
Figure 4-5: Some of the hypothetical carboxylic acids identified in the naphthenic acid sample	52
Figure 4-6: The shift of brine pH with NA	53
Figure 4-7: Graph of concentration vs. brine pH of the four acids from the naphthenic acid sample	54
Figure 4-8: The partition coefficient of the NA samples at different brine pH	55
Figure 4-9: The shift of the brine pH with cocktail acid.....	56
Figure 4-10: Ratio of the acids with IS vs. brine pH	56
Figure 4-11: Partitioning coefficient vs. brine pH with the cocktail of acids	57
Figure 4-12: Chromatogram of CA in aqueous pH at pH of 3.2.....	58
Figure 4-13: Shift of the brine pH with CA	58
Figure 4-14: Final concentration of CA vs. brine pH	59
Figure 4-15: Formation of “scale” at pH of 11 when CA was used.....	60
Figure 4-16: Partitioning coefficient of CA vs. brine pH	60
Figure 4-17: Chromatogram of organic phase that contained HBA	61
Figure 4-18: Shift of the brine pH with HBA	62
Figure 4-19: Graph of the final concentration vs. brine pH for the HBA samples	62
Figure 4-20: Effect of brine pH on the samples containing HBA.....	63
Figure 4-21: Graph of the partitioning coefficient vs. brine pH for the HBA samples.....	63
Figure 4-22: Comparison of the partitioning coefficient of different carboxylic acids	64
Figure 5-1: Sectional drawing of the separator and flow pattern.....	68
Figure 5-2: Process flow diagram	70
Figure 5-3: Graph of current vs. voltage for the tap water.....	71
Figure 5-4: Outlet flow rate at different percentages of the needle valve opening in separator	73
Figure 5-5: Specific gravity determination of the two layers in the vegetable oil experiments.....	74
Figure 5-6: Performance of the separator in removing tap water from heptane at room temperature	75
Figure 5-7: Performance of the separator in removing distilled water from vegetable oil at room temperature	76

Figure 5-8: The efficiency of the separator with crude oil and vegetable oil at 20% water-cut	77
Figure 9-1: Graph of peak area vs. concentration, used for NA_18.7.	94
Figure 9-2: Graph of peak area vs. concentration, used for NA_20.7.	95
Figure 9-3: Graph of peak area vs. concentration, used for NA_20.928.	95
Figure 9-4: Graph of peak area vs. concentration, used for NA_22.4.	96
Figure 9-5: Graph of concentration vs. integrated area, used for the HBA samples.....	96
Figure 9-6: Graph of concentration vs. integrated area, used for the CA samples.	97
Figure 9-7: Graph of UDA/DDA vs. percentage of standard.	97
Figure 9-8: Graph of TDA/DDA vs. percentage of standard.....	98
Figure 9-9: Graph of HA/DDA vs. percentage of standard.	98
Figure 11-1: Pareto chart of standard effects for the gravity settling method with sample H crude oil. ..	106
Figure 11-2: Normal probability plot of the results with sample H crude oil.	107
Figure 11-3: Pareto chart of standardised effects for the experiments with sample M crude oil.....	108
Figure 11-4: Probability plot for the experiment with sample M crude oil.	109
Figure 11-5: Surface response for the results with sample M crude oil.....	110
Figure 11-6: Pareto chart of standardised effects for the experiments with sample U crude oil.	111
Figure 11-7: Probability plot of the results with sample U crude oil.	112
Figure 11-8: Pareto chart of standardised effects of the results with sample P crude oil.	113
Figure 11-9: Normal probability plot of the experimental results with sample P crude oil.....	114
Figure 11-10: Pareto chart of the standardised effects of the experiments with sample C crude oil	115
Figure 11-11: Probability plot for the experiments with sample C crude oil.....	116
Figure 11-12: Pareto chart of standardised effects of the experiment with sample A crude oil.	117
Figure 11-13: Normal probability plot for the results with sample A crude oil.....	118
Figure 11-14: Pareto chart of standardised effects for the experiments with sample V crude oil.	119
Figure 11-15: Normal probability plot for the results with sample V crude oil.....	120
Figure 11-16: Surface response for the results with V crude oil.....	121
Figure 12-1: The critical electric field cell.....	122
Figure 12-2: The electric separator	122
Figure 12-3: Crude oil blend in the mixing tank.....	123
Figure 12-4: The centrifuge used in the experiment	123

LIST OF TABLES

Table 3-1: Physical properties of crude oil from the different wells, as measured in the laboratory	31
Table 3-2: Operating parameters used for the gravity test method.....	33
Table 3-3: Ranking of the crude oil samples in terms of creating emulsion.....	39
Table 4-1: Standard composition of the NA samples.	48
Table 4-2: Standard composition of the cocktail of acids.....	49
Table 4-3: Standard composition of the organic phase for CA samples.....	49
Table 4-4: Standard composition of the organic phase for HBA samples.....	49
Table 4-5: Mass percentage and the concentration of the components in the NA sample.....	52
Table 5-1: Physical properties of the liquids used	71
Table 9-1: Data of the experiments with sample A during the gravity test.	88
Table 9-2: Data of the experiments with sample M during the gravity test.....	89
Table 9-3: Data of the experiments with sample C during the gravity test.....	89
Table 9-4: Data of the experiments with sample U during the gravity test.	90
Table 9-5: Data of the experiments with sample V during the gravity test.	90
Table 9-6: Data of the experiments with sample P during the gravity test.	91
Table 9-7: Data of the experiments with sample H during the gravity test.	91
Table 9-8: Data of the experiments with crude oil sample V during the CEF test.	92
Table 9-9: Data of the experiments with crude oil sample H during the CEF test.	92
Table 9-10: Data of the experiments with crude oil sample C during the CEF test.....	92
Table 9-11: Data of the experiments with blend 1 during the CEF test.....	92
Table 9-12: Data of the experiments with blend 2 during the CEF test.....	93
Table 9-13: Data of the centrifuge experiments with sample V.	93
Table 9-14: Data of the centrifuge experiments with sample H.	93
Table 9-15: Data of the centrifuge experiments with sample H.	93
Table 9-16: Data of the centrifuge experiments with Blend 1.	94
Table 9-17: Data of the centrifuge experiments with Blend 2.	94

Table 9-18: Data of the experiments with NA_18.70.	99
Table 9-19: Data of the experiments with NA_20.70.	99
Table 9-20: Data of the experiments with NA_20.928.	99
Table 9-21: Data of the experiments with NA_22.4.	100
Table 9-22: Values for the partitioning coefficient of the NA sample.....	100
Table 9-23: Experimental data for the standard used in the cocktail.	100
Table 9-24: Experimental data for the cocktail samples.	101
Table 9-25: Data of the experiments with HBA samples.	101
Table 9-26: Data of the experiments with CA samples, the concentration are based on brine.....	101
Table 9-27: Experimental data of the experiment with heptane in the plant.	102
Table 9-28: Experimental data for the experiment with vegetable oil at room temperature.....	103
Table 9-29: Experimental data for the experiment with vegetable oil at 70°C.....	103
Table 9-30: Experimental data for the experiments with crude oil blend at 70°C.....	103

1 INTRODUCTION

The production of highly acidic crude oil is carried out in different places in the world. From an operational point of view in crude oil production, the presence of naphthenic acids causes several problems (Havre 2002; Ese & Kilpatrick 2004; Hurtevent et al. 2006). These acids are amphiphilic molecules in that they tend to accumulate at the water crude oil interface and stabilise emulsions. These acids in contact with a basic brine solution create naphthenate soap, which under certain conditions plugs the lines in the process equipment, leading to line shut-down (Hurtevent et al. 2006). Under certain conditions the soap stabilizes the water-in-crude-oil emulsion.

The partitioning of naphthenic acids into process water poses environmental problems. It is believed that naphthenic acid together with other surfactants present in the crude oil enhance the emulsion stability (Havre 2002; Langevin et al. 2004). The acidic value of crude oil is reported in total acid number (TAN). Crude oil fields with high TAN values have been reported to cause ultra stable emulsions (Hurtevent et al. 2006). However, crude oil fields with low TAN values have been reported to create more stable emulsions than those with high TAN values (Hurtevent et al. 2006). It is believed that the structure of the naphthenic acids and other surfactants is a key to explaining the formation of the ultra-stable emulsion (Havre 2002).

The separation or removal of water droplets from crude oil is one of the most important stages in the processing of crude oil. The price of crude oil depreciates with the increase in the volume of water content (water-cut) and the presence of acids (Langevin et al. 2004). As a result of the presence of surfactant in the crude oil, the separation of water drops from crude is a challenging process. There are many methods available; to name a few: chemical demulsifier, electric separation, heat treatment and filtration. Of these, electric treatment has the lowest power consumption and is simple to operate. The separation of water droplets from crude oil takes place in large horizontal electrostatic separators; a long time is needed to complete the separation. Previous works by Eow, Ghadiri and Sharif (2000), Eow, Ghadiri and Williams (2001) and Eow

Chapter 1: Introduction

and Ghadiri (2002a; 2002b; 2003a; 2003b) led to the design of vertical separators. These separators were tested with sunflower oil and a good separation was achieved, as reported by Eow and Ghadiri (2002a; 2002b). Different studies carried out by these authors show that droplet break-up poses a challenge in designing electric separators. Droplet break-up decreases the efficiency of these separators. The separators need to be investigated further, as many parameters are yet to be optimised.

Against this background it is evident that a better understanding is needed of the emulsion stability and possible separation method. This thesis focuses on an investigation of water-in-oil emulsion stability and separation. The main objectives are therefore as follows:

- To rank the crude oil in terms of creating stable emulsions and to assess the influence of crude oil blends.
- To assess the effect of brine pH on emulsion stability.
- To investigate the influence of different organic acids on emulsion stability. Here a prediction of a possible mechanism influencing the emulsion stability is expected.
- To determine the efficiency of the electric separator in removing water droplets from a flowing organic phase.

The thesis was split into three parts. The first part of this research (Chapter 3) focuses on the investigation of the water-in-crude-oil emulsion. The second part (Chapter 4) focuses on the investigation of the behaviour of different organic acids in the water-in-oil emulsion. The third part (Chapter 5) focused on the determination of the efficiency of the so-called electric separator in removing dispersed water droplets from a continuous organic fluid. The research outline is simplified in Figure 1-1.

Chapter 1: Introduction

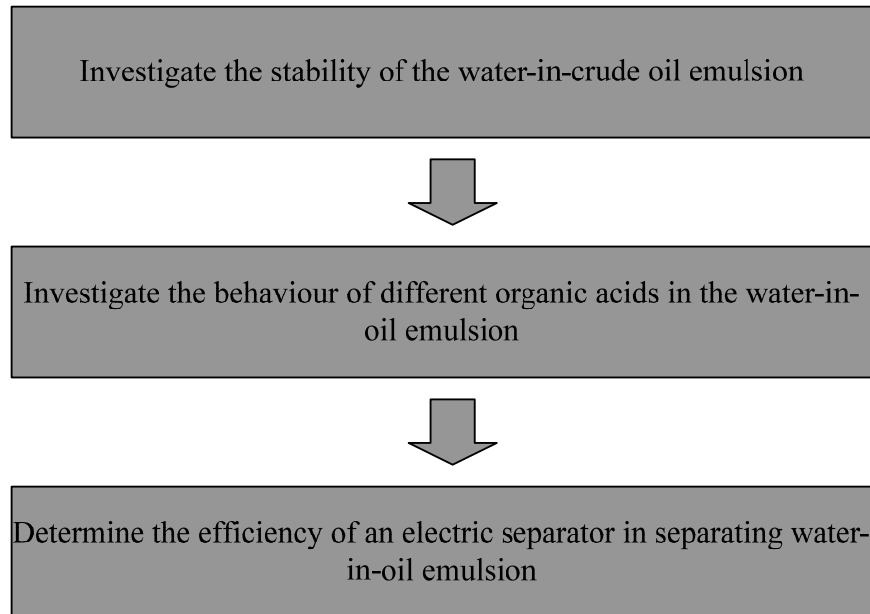


Figure 1-1: The outline of the research project

The thesis is supported with a Literature Review (Chapter 2), which describes a summary of the research results and/or theory that have been published up to date. Chapter 6 presents the general conclusion of the thesis.

The references are found in Chapter 7. The nomenclatures of the symbols used are presented in Chapter 8. The thesis contains appendices in which extra information is presented for supporting the claims made in the thesis main body.

2 LITERATURE REVIEW

This section outlines the basic theory on the studies of emulsion. Information on the naphthenic acids and electric separators is presented.

2.1 CRUDE OIL

Petroleum, etymologically, means rock oil or mineral oil, but in modern technical usage it has a wider meaning that includes natural gas, mineral wax and bitumen in addition to crude oil (Hobson 1973). As a result of the variety and complexity of its components, petroleum or crude oil processing, is a subject of interest in the petroleum and allied industries. Thus, it is of prime importance to provide a comprehensive background on the origin and chemistry of crude oil. Crude oil is a valuable liquid mineral, as experts point out that crude oil is the stock for many chemicals and can be fractionated into gasoline, diesel, asphalt, etc., which can then be used to generate valuable components that are beneficial to the society, using different unit operations. This section summarises the most important features of crude oil, including its origin, possible main components and some related information.

2.1.1 Crude oil origin and chemistry

Petroleum, a mixture of organic compounds and primary hydrocarbons, comes from underground rock formations ranging in age from ten to several hundred million years. The process by which it is formed and developed is not yet fully understood. Studies indicate that petroleum is formed mainly from microscopic-sized marine animals and plants. When these organisms died in water with low oxygen content, they did not decompose. Their remains thus sank to the bottom to be buried under accumulations of sediment. Their conversion to petroleum remains a subject of research today. The theory held generally is that bacteria converted the fats of the marine life into fatty acids (Hobson 1973). These, in turn, were changed by mechanisms

Chapter 2: Literature Review

still unknown to the asphaltic material called kerogen. Then, over millions of years, heat and pressure, plus probably catalytic agents in the rock, changed the kerogen to crude oil and gas. The formation of crude oil from organic matter as referred to above is a fact that likely has much more acceptance, though the reason why it is formed still has to be uncovered. Crude oil is generally found with water and gas (which may be dissolved or in the form of a gas-cap), and they are layered as a result of their differing densities.

Crude petroleum is primarily a liquid of widely varying physical and chemical properties; common colours are green, brown and black, and occasionally almost white or straw colour, as reported by Bland and Davidson (1967). Its specific gravity can range from 0.73 to 1.02; however, most crude oils are between 0.80 and 0.95. Viscosity varies too. Data for a large number of crudes indicate kinematic viscosities from 0.007 to 13 stokes at 100°F, though most of them range from 0.023 to 0.23 stoke. Principal elements in crude petroleum are carbon and hydrogen, usually in a carbon-hydrogen ratio of between 6 and 8. The hydrocarbons are mainly liquids and gases, with some solids in dispersion or solution. Among the many other materials usually present are small amounts of sulphur, nitrogen and oxygen in the form of hydrocarbon derivatives; traces of metals such as nickel, vanadium and iron; and water (emulsified in the oil and sometimes as high as 30%). The water is generally in the form of saturated solutions of calcium and magnesium sulphates and sodium and magnesium chlorides. The major compounds available in the crude oil are asphaltenes, resins, aromatics and saturates, as proved in the SARA method. In the SARA (saturates, aromatics, resins, asphaltenes) method, the crude-oil is separated into four major fractions: saturates (including waxes), aromatics, resins and asphaltenes based on their solubility and polarity, as shown in Figure 2-1.

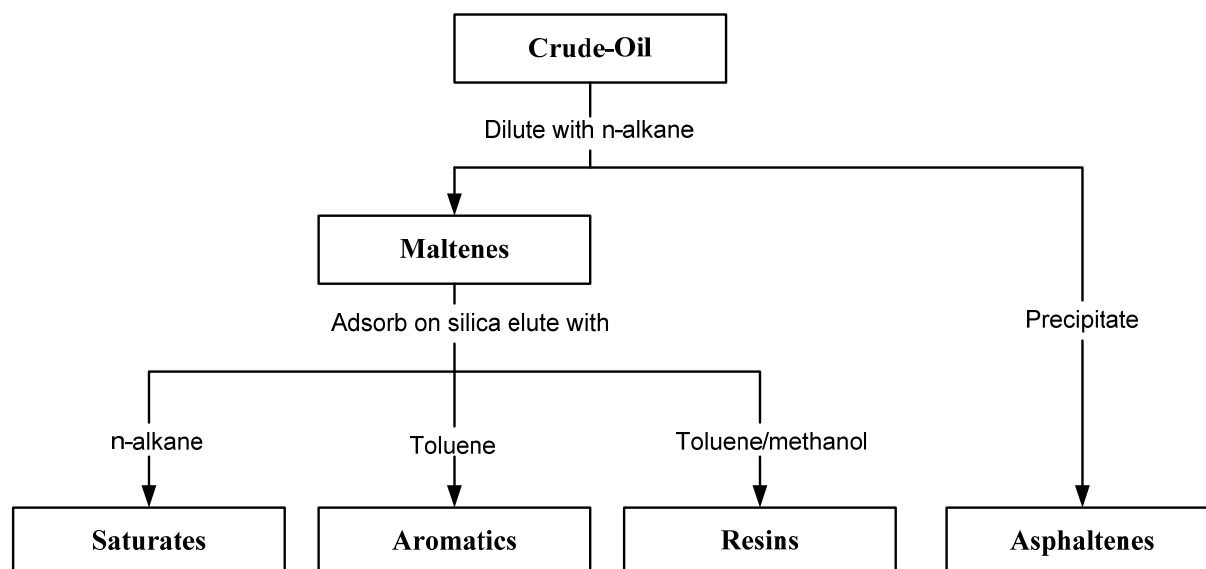


Figure 2-1: Typical SARA method for crude oil

Asphaltenes are considered to be the most polar of the four fractions presented in Figure 2-1. They are defined as the portion of crude oil insoluble in n-alkanes such as n-heptane or n-pentane, yet soluble in benzene or toluene. The solubility class definition of asphaltenes generates a broad distribution of molecular structures that can vary greatly from one crude oil to another (Yen, Erdman & Pollack 1961; Mitchell & Speight 1973). Normally, asphaltenes are characterised by fused ring aromaticity, small aliphatic side chains, and polar heteroatoms containing functional groups. Many studies have indicated the presence of carboxylic acids, carbonyls, phenols, and pyrrolic and pyridinic nitrogen (Barbour & Petersen 1974; Moschopedis & Speight 1976; Ignasiak, Strausz & Montgomery 1977; Boduszynski, McKay & Latham 1980). A hypothetical structure of an asphaltene molecule is illustrated in Figure 2-2. The molecular weight of this compound is approximately 1244.

Chapter 2: Literature Review

hydrocarbon reservoirs, well bores, surface facilities, transportation systems and refineries (Schramm 1992; Langevin et al. 2004).

Many studies have been carried out in the last 40 years that have led to a better understanding of these complex systems. However, there are still many unanswered questions related to the peculiar behaviour of these emulsions. Langevin et al. (2004) reported that the complexity comes mostly from the oil composition, in particular from surfactants molecules contained in the crude. These molecules cover a large range of chemical structures and molecular weights; they can interact between themselves and/or reorganise at the water-oil interface. The same authors also reported that the presence of solids and gases make the system even more complex. Many studies have confirmed that asphaltenes are the most influential factor in emulsion forming and finally stability (Spiecker 2001; Aske, Kallevik & Sjoblom 2002; Havre 2002; Langevin et al. 2004). However, asphaltenes do not form emulsions by themselves. The asphaltene aggregates in heavy crudes are believed to be solvated by resins and other compounds. The polar functional groups in the asphaltenes are also capable of donating or accepting protons inter- and intra-molecularly. The most plausible mechanisms of asphaltene aggregation involve $\pi - \pi$ overlap between aromatic sheets, hydrogen bonding between functional groups, and other charge transfer (Spiecker 2001). After asphaltenes, resins are the most polar and aromatic species in crude oil and they contribute to the overall solubility of asphaltenes in crude oil by creating a strongly solvating layer on the polar and aromatic portions of the asphaltene aggregates (Miller 1982; Reynolds 1987; Ali, Bukhari & Hasan 1989). The solvation of asphaltenes by resin molecules is illustrated in Figure 2-4.

Once the resins have solvated the asphaltenes in crude oil as shown in Figure 2-4, they are susceptible to stabilising an emulsion system. That is, when the solvated asphaltene aggregates come into contact with water droplets, the asphaltenes likely shed a portion of the resins and adsorb to the interface. This process is depicted in Figure 2-5. The solubility of asphaltenes in crude oil is mediated largely by resin solvation and thus resins play a critical role in precipitation and emulsion stabilisation phenomena (McLean & Kilpatrick 1997a). However, the presence of resins in solution can destabilise emulsions via asphaltene solvation and replacement at the oil-water interface (McLean & Kilpatrick 1997b; Gafonova & Yarranton 2001; Langevin et al. 2004).

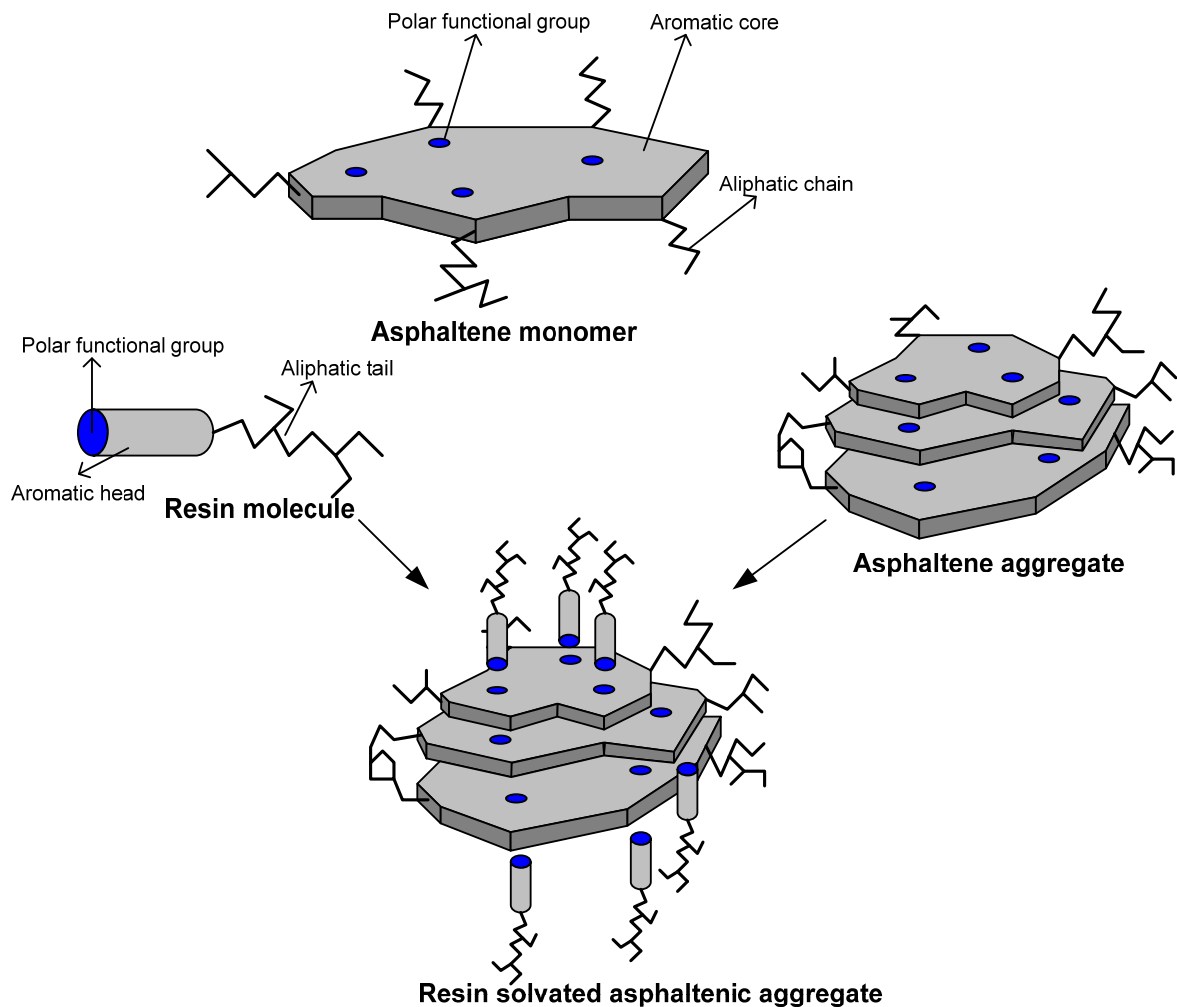


Figure 2-4: Schematic of the solvation of asphaltenes by resins, adapted from Spiecker (2001)

To understand the reasons for the relative stability of such systems, it is necessary to first determine the stability and the mechanisms of destabilisation. The stability of a disperse system is characterised by a constant behaviour in time of its basic parameters, namely the dispersity and uniform distribution of the dispersed phase in the medium. As a result of this, the dispersed phase should either settle out of the solution or coagulate to break the emulsion. Emulsion stability is a complicated matter, as many systems behave differently from one another. This section explains and summarises proposed mechanisms that lead to emulsion stability and breakdown. It is important to address the fact that emulsion stability still is a matter that needs further studies, as different emulsion systems will have different stability mechanisms. The mechanisms provided here are of prime importance to understand an emulsion system.

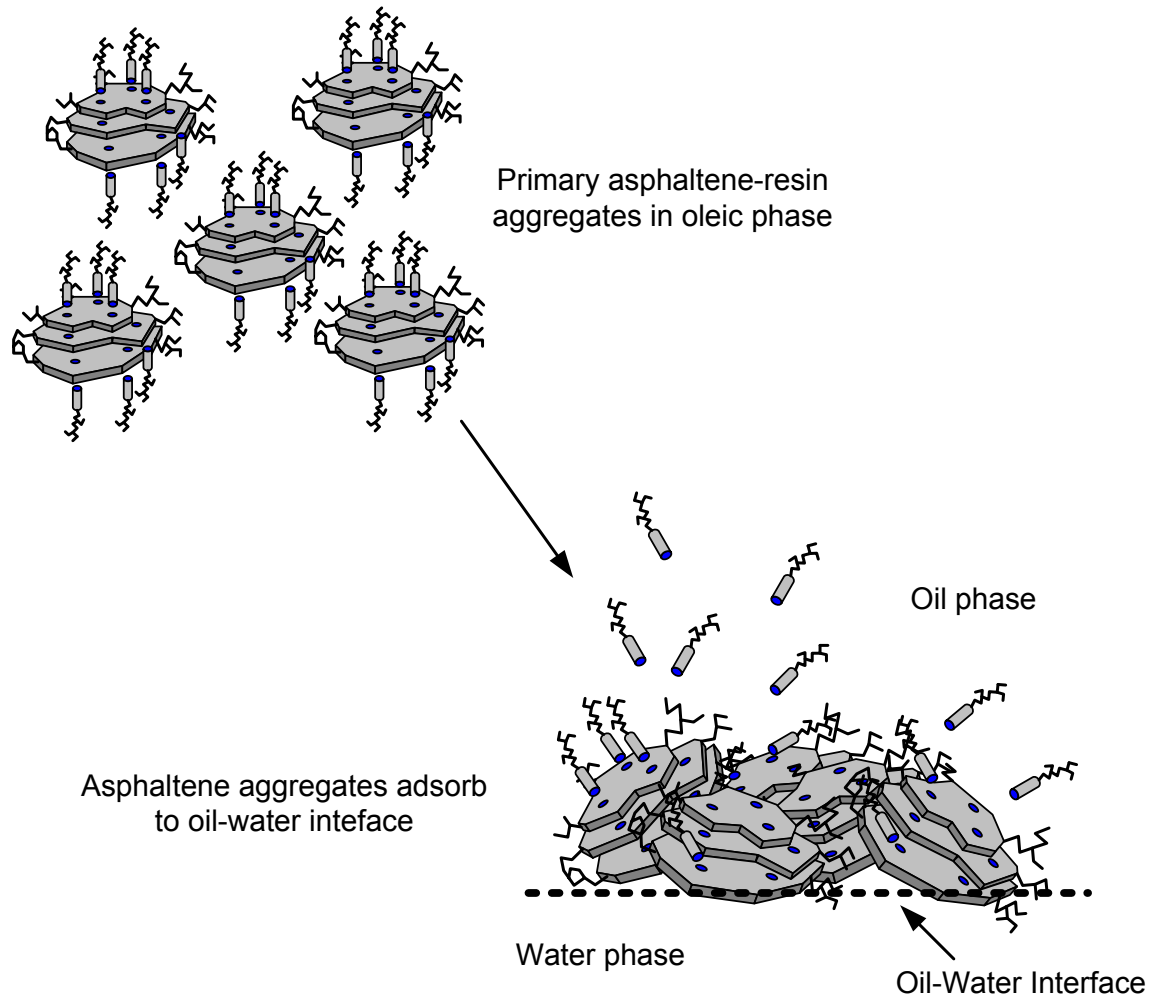


Figure 2-5: Adsorption of asphaltene aggregates on the oil water interface, adapted from Speieker (2001)

2.2.1 Stability mechanisms

Surfactants are referred to as amphiphilic molecules that have a hydrophilic and hydrophobic group; thus mixing immiscible liquids such as oil and water with a surface active agent will often lead to an emulsion of oil droplets in water (o/w) or water droplets in oil (w/o). The type of emulsion formed is determined from the hydrophobic lipophilic-balance (HLB) as stated in Bancroft's rule (Bancroft 1913): the liquid in which the surfactant is soluble becomes the continuous phase. Other factors, such as oil-to-water volume fractions and surfactant concentration, will influence the type of emulsion formed. After the droplets are completely

dispersed within the continuous phase, surfactants migrate to the oil-water interface and can inhibit droplet rupture by steric, Marangoni-Gibbs, or rigid-film-forming interactions. These stability mechanisms are outlined in Figures 2-6 and 2-7 respectively.

2.2.1.1 Steric stabilisation

Surfactants as a result of a hydrophilic, polar head group and hydrophobic tail group will typically orient themselves at oil-water interfaces. As a result of its polar characteristics and eventually hydrogen bonding, the head group has a natural affinity for water, while the tail group (normally hydrocarbon moiety) will preferentially remain in the oleic phase. Dispersed water droplets will thus be coated by surfactant material, with hydrophobic tails protruding into the oil phase. When droplets approach each other, their adsorbed surfactant tails prevent droplet contact and coalescence. See Figure 2-6 for a further illustration.

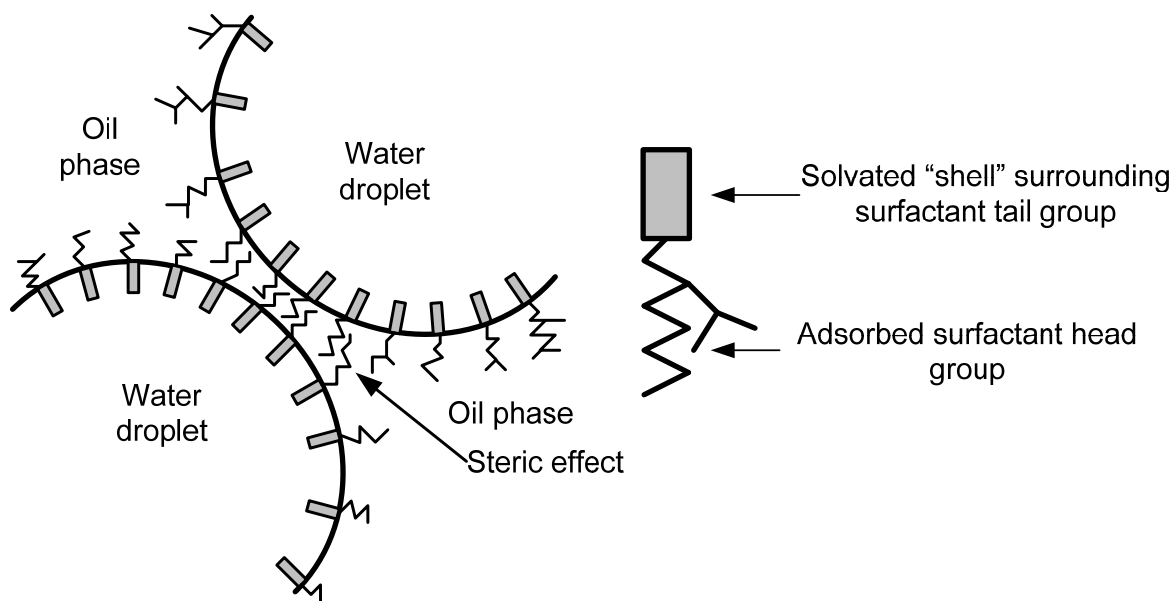


Figure 2-6: Emulsion stability by steric mechanism, adapted from Spiecker (2001)

2.2.1.2 Marangoni-Gibbs effect

The Marangoni-Gibbs effect can stabilise emulsions by preventing the drainage of the continuous phase from between two opposing droplets. As droplets approach each other, their surfaces eventually become plane parallel and the film layer attempts to drain (see Figure 2-7). This outward convection draws surfactants towards the droplet edges, leaving a region of low

surfactant concentration in the middle. This process sets up an unfavourable interfacial tension gradient along the interface. Surfactant diffusion thus proceeds in the direction opposing convection to eliminate the interfacial tension gradient. Stable emulsions can result from the balance of surface diffusion and film convection.

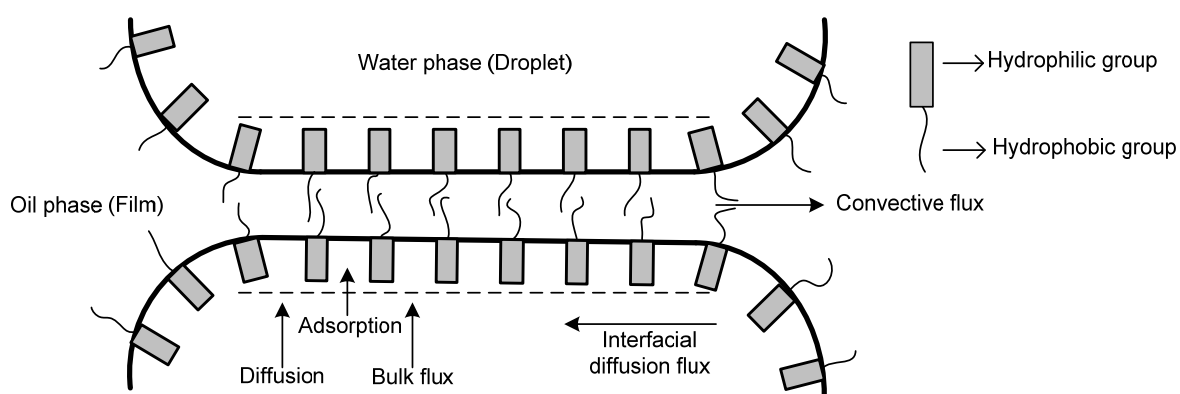


Figure 2-7: Emulsion stability in terms of the Marangoni-Gibbs effect (Spiecker 2001)

2.2.1.3 Rigid film formation

A third and most probable mechanism of petroleum emulsion stabilisation comes from an adsorbed layer of material with high rigidity and elasticity. Asphaltene aggregates in the oleic phase will adsorb to the oil-water interface and form a consolidated film or skin that resists droplet coalescence (Langevin et al. 2004). This process can be quite complex and depends on asphaltene chemistry, solvency and the kinetics of diffusion and adsorption (Spiecker 2001). This mechanism resembles the steric effect in that a surfactant prevents the water droplets from coalescing. In this mechanism, a rigid film surrounds the water droplets, which then hinders the separation of the drops. This mechanism has been proposed and/or reported by many authors (Lawrence & Killner 1948; Langevin et al. 2004).

2.2.2 Process of emulsion breaking

Emulsion stability is a matter that deserves a lot of attention, as the reason for the stability still has to be uncovered, although several studies are being carried out in order to understand and explain the mechanisms and/or causes that lead to emulsion stability. Previous experimental work carried out by Ese and Kilpatrick (2004) showed that the stability of a water-in-oil

emulsion depends on the type and structure of the surfactant. On the basis of experimental and theoretical work done so far, it is worthwhile to recall briefly the different hypothetical mechanisms leading to emulsion destabilisation.

2.2.2.1 Ostwald ripening

Ostwald ripening is the drop-growth process occurring when the disperse phase has a finite solubility into the continuous phase and can migrate between the drops of different sizes. The prediction of the drop radius $R(t)$ variation can be expressed as follows:

$$R(t) = \left(\frac{8\gamma D_e C_{eq} v}{9k_0 T} \right)^{\frac{1}{3}} t^{\frac{1}{3}} \quad (2.01)$$

where C_{eq} is the equilibrium concentration of the molecules of the dispersed phase in the continuous phase, D_e is the diffusion coefficient, v is the molecular volume, T is the absolute temperature, γ is the surface or interfacial tension, k_0 is the Boltzmann constant and t represents the time. The growth is faster at large drop-volume fractions, making exchanges between drops easier. In the case of heavy crude oils, the solubility of oil in water or of water in oil is low, and this process is likely to be very slow. No studies have been reported so far (Langevin et al. 2004).

2.2.2.2 Coalescence

Coalescence is the process by which two drops (also a drop and the bulk phase) merge to form one drop of bigger size. The coalescence between drops in an immiscible liquid medium, or between a drop and its own bulk phase occurs in three stages. In the first stage, the drops approach each other and are separated by a film of the continuous phase. The second stage involves the thinning of the film to reduce the interfacial area. The thinning rate is affected by the capillary pressure and the disjoining pressure, and it can be retarded due to the Marangoni-Gibbs effect if surfactant is present. In order for coalescence to occur, the film between the drops should rupture. The process of film thinning is quite often the controlling step toward coalescence. Parameters such as the viscosity of the continuous phase, the presence of surfactants, temperature and the size of the drops influence the coalescence rate of the drops. In petroleum processing, the presence of asphaltenes causes stable emulsions as a result of a rigid

film around the droplets, thus hindering the rupture of the film. Processes by which asphaltenes stabilise water-in-crude-oil emulsions are still under investigation. Many studies have reported that the interactions between the crude oil components may lead to stabilisation or destabilisation of the emulsion (McLean & Kilpatrick 1997b; Havre 2002; Langevin et al. 2004). Spontaneous coalescence can only occur before the formation of skins, and in any case, when small amounts of asphaltenes are adsorbed (Langevin et al. 2004).

2.2.2.3 Sedimentation or creaming

Emulsions with small drops (say 1 μm) are insensitive to the sedimentation or creaming Brownian motion dominating the effect of gravity; but when drop sizes are larger than a few microns, they sediment or rise. For more dilute dispersions, the sedimentation velocity of a drop of radius R and density ρ_i in a continuous phase of density ρ and viscosity μ is:

$$U = \frac{2R^2(\rho_i - \rho)g}{9\mu} \quad (2.02)$$

where g is the acceleration of gravity. If $\rho > \rho_i$, the drop rises, and the velocity is given by the same expression, provided the sign of the density difference is changed. The drop volume fraction increases with time, either at the bottom or at the top of the emulsion sample where drops concentrate locally. When 60% are in this region, the drops are no longer spherical; they distort into polyhedra, with the flattened regions between them being liquid films as in foams. The drop volume fraction continues to increase, although much more slowly than predicted by Equation 2.01. The liquid then flows through the interstitial spaces between the drops. With time, the films separating the drops thin and eventually break. This process is accelerated when flocculation occurs, simply because flocs have larger sizes.

Usually, electrocoalescence is considered to be the best method to enhance water and oil separation in the refinery environment (Eow, Sharif & Williams (2001). The sedimentation rate in this type of equipment is described by the Stokes equation (see Equation 2.02 for further illustration). From this equation it is evident that the sedimentation rate is strongly dependent on the droplet size, the density difference between the phases and on the viscosity of the continuous phase. The density differences and viscosity of the phases can be adjusted by diluents and

temperature, whereas the droplet size can be modified by an electric field, being applied so that efficient water removal is achieved (Eow, Sharif & Williams 2001).

2.3 NAPHTHENIC ACIDS

Problems are encountered in the production of acidic crudes where the acid creates production problems during crude oil processing in offshore or onshore facilities. The acids present in crude oil are referred to as naphthenic acids and they can cause corrosion and environmental problems either in the downstream or upstream facilities. This section summarises the origin and possible structure of these acids. The phase equilibrium that occurs in the reservoir is also explained, with more attention being paid to sodium chloride and calcium chloride. Finally, the influence of these acids on the interfacial tension is outlined.

2.3.1 Origin and structure

Naphthenic acids are defined as carboxylic monoacids with the generic formula RCOOH , where R is any cycloaliphatic structure. However, in general the term “naphthenic acid” is used to describe all carboxylic acids present in crude oil, including aromatic and acyclic acids.

Characterisation studies of these acids have been carried out by means of many different methods and analytical techniques (Fan 1991; Acevedo et al. 1999; Hsu et al. 2000; Jones et al. 2001). On the basis of these studies, naphthenic acids can be described mainly as C_{10} to C_{50} compounds with 0 to 6 fused rings, most of which are saturated, where the carboxylic acid group is attached to a ring through a short side chain (Robbins 1998). Examples of the structures of naphthenic acids are shown in Figure 2-8.

Naphthenic acids are believed to come from in-reservoir biodegradation of hydrocarbons in fossil deposits. They are considered to be a class of biological markers or traces (Behar & Albrecht 1984; Cranwell 1984; Brault, Marty and Sahot 1984; Fan 1991; Koik et al. 1992) and are related to the maturity and biodegradation level of the fields (Babaian-Kibala et al. 1993).

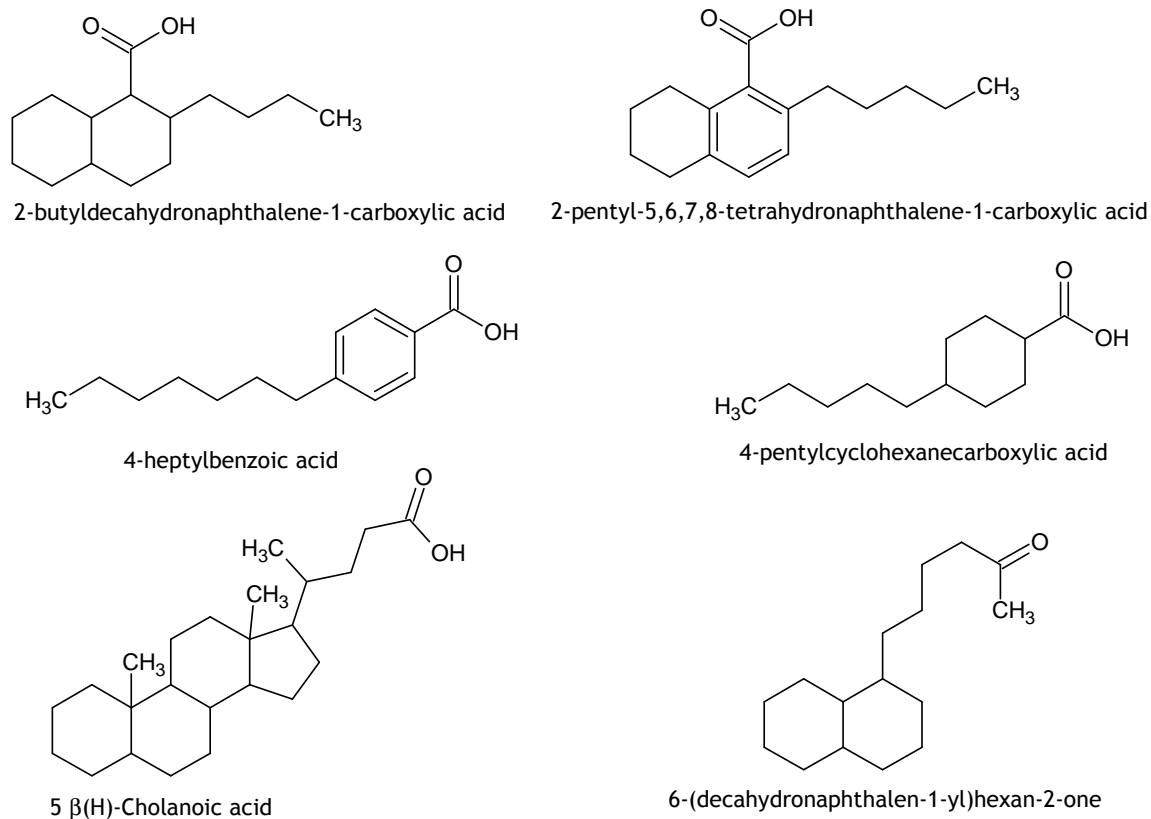


Figure 2-8: Types of naphthenic acids

2.3.2 Characterisation of naphthenic acids

The role naphthenic acids (NA) play in emulsion stability is still unknown but it is believed that naphthenic acids make crude oil more acidic or increase the total acid number (TAN). These acids act as surfactants, thus they are adsorbed at the oil-water interface. Depending on the contact angle created between the oil and the water, they may either prefer the oil phase or water phase. The presence of these acids in both the oil and the water phase is reported to cause corrosion problems in the refinery and/or allied industries. Therefore, the characterisation of such acids is of prime importance to at least predict the amount of these chemicals in the crude oil or water prior to processing them further.

There are many methods available to characterise these acids, although they lead to different results (Jones et al. 2001); the qualification and quantification of these acids in crude oil involves a sample preparation prior to using the sample in gas or liquid chromatography equipment. A

derivatisation technique is highlighted here. The carboxylic and/or naphthenic acid is converted to esters using a derivatising agent. St. John et al. (1998) used a tertiary-butyldimethylsilyl derivatisation method in which n-methyl-n-(tertiary-butyldimethylsilyl) trifluoroacetamide that contained 1% tertiary-butyldimethylsilyl chloride. The determination and/or characterisation of these acids still needs further research; the results achieved thus far differ from one technique to another and some require a long step (Jones et al. 2001).

2.4 FORMATION OF NAPHTHENATE SOAPS

Like any acid, naphthenic acid also shows the typical partitioning and dissociation characteristics in a multiphase system. The partitioning of naphthenic acids between the hydrocarbon phase and the aqueous phase is given by Equation 2.03.



with a partitioning coefficient expressed by Equation 2.04:

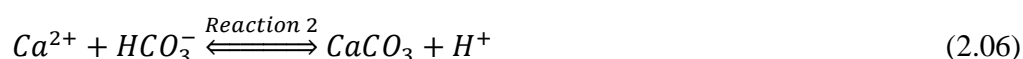
$$k = \frac{[R-COOH_{Water}]}{[R-COOH_{Oil}]} \quad (2.04)$$

Brandal (2005) reported that naphthenates are very surface active chemicals, and that they tend to stabilise oil-water emulsions by their affinity to form steric or electrostatic repulsion that prevents the oil or water droplets from uniting (see Figures 2-6, 2-7 and 2-8 for illustrations). The formation of naphthenates causes a significant drop in the surface tension. Therefore, the reduction in emulsion stability may be taken as a measure of the amount of naphthenate at the oil-water interface.

In order to explain the formation of naphthenates, the so-called calco-carbonic equilibrium reaction is used to demonstrate what may cause pH to increase in the reservoir water (Equations 2.05 and 2.06 illustrate the equilibrium). The increase in pH and subsequent formation and precipitation of calcium carbonate in the reservoir waters are caused by successive pressure drops (Hurtevent, Rousseau & Zhou 2001). The carbonates that are formed have very low

Chapter 2: Literature Review

solubility in water, thereby generating undesirable deposits that plug the chokes or fill the separators (Hurtevent, Rousseau & Zhou 2001).



The cations in reservoir waters can react with $RCOO^-$ naphthenate groups to form salts, commonly named soaps, essentially sodium and calcium naphthenates, which dissolve in either water or oil, depending upon their affinity for one phase or the other. Sodium naphthenates with a low molecular weight tend to dissolve in the water phase. Calcium, as divalent cations, is associated with two naphthenates groups, yielding lypophilic calcium naphthenates partition preferentially into the oil phase or adsorb at the oil-water interface (Hurtevent, Rousseau & Zhou 2001). When the soap concentration exceeds the solubility, the precipitation of a solid deposit is observed, or, in some cases, the formation of an intermediate third phase at the interface between the oil and the water phase (Hurtevent et al. 2006).

The release of CO_2 due to a shift in the calco-carbonic balance causes the pH value of the reservoir water to increase (Hurtevent et al. 2006). This is followed by competition between the formation of sodium or calcium naphthenate and the precipitation of calcium carbonate. The result is the potential formation of calcium carbonate deposit and/or emulsion stabilised by sodium/calcium naphthenates, with a decrease in the pH value, if the water is not buffered by bicarbonate. (See Figure 2-9 for further illustration).

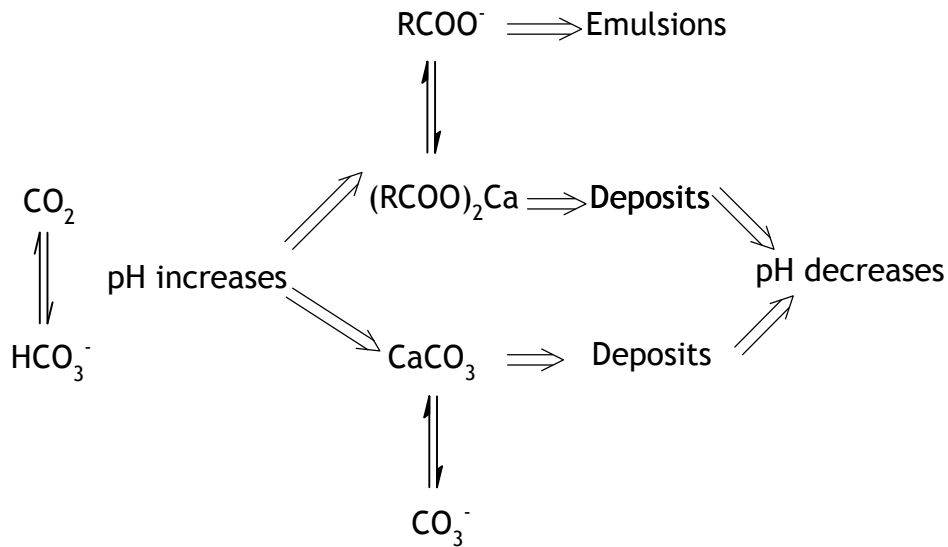


Figure 2-9: Equilibrium of naphthenate and the reservoir water

In the absence of bicarbonate, an increase in the pH value due to CO_2 degassing produces naphthenates and simultaneously, the dissociation of naphthenic acids releases protons, which act against the increase in pH, and thus hinder the formation of naphthenates. In the opposite case, naphthenates are produced as long as some bicarbonate is available to buffer the medium. Thus, the species that mainly contribute to naphthenate formation are $RCOO^-$, Na^+ , Ca^{2+} and HCO_3^- . From this it may be assumed that the following criteria should be considered when predicting the formation of stable emulsion and/or scale in the processing of acidic crude (Hurtevent et al. 2006): For water, its pH value at process conditions and the level of bicarbonate and calcium content, and for oil the amount of available naphthenic acids.

2.5 INTERFACIAL ACTIVITY OF NAPHTHENIC ACIDS

As a result of their amphiphilic properties, naphthenic acids are found in a complex mixture of crude oil, reservoir water and/or at the oil-water interface. The reservoir water contains a variety of salts. Brandal (2005) used Ca^{2+} , Mg^{2+} , Sr^{2+} and Br^{2+} for an experiment with different naphthenic acids and/or model compounds. The results showed that the interfacial tension

depended on the type or structure of the naphthenic acid, the divalent cations, the concentration of the compounds and the pH of the aqueous phase.

Introducing divalent cations to systems involving saturated naphthenic acids may cause a permanent lowering of the interfacial tension. The decline in the interfacial tension is explained by the electrostatic attraction forces across the interface, which in turn causes a higher interfacial density of the naphthenic acid monomers (Brandal 2005). The permanent lowering in interfacial tension is most likely due to the formation of positively charged monoacid complexes possessing high interfacial activity. However, the aromatic model compounds, the cations used by Brandal (2005), affected the interfacial tension differently, and this was explained to be caused by steric conditions.

When the pH of the co-produced water increases as a result of the release of CO₂ during fluid transportation from the reservoir to the topside, the acid monomers dissociate at the water-oil interface, making them even more interfacially active. Therefore, the combination of the naphthenic acids with the brine may cause the formation of metal soaps/naphthenates. Under certain conditions, these metal soaps can stabilise foams and emulsion (Ese & Kilpatrick 2004). In order to reduce the extent of naphthenate formation, chemical mixtures of various compositions are injected into the well stream (Brandal 2005). Naphthenate deposition is a problem only if the aqueous pH exceeds the pK_a of the naphthenic acids; this is why keeping the pH low may prevent naphthenate from forming.

2.6 THEORY OF ELECTROSTATIC

In dealing with electrostatic problems it soon becomes apparent that the boundaries of dielectrics have rather special properties, which have profound effects on the electric fields and potentials in the system. A concern is paid on charges located near the interfaces of a dielectric and a conductor, and between two dielectrics. However, before discussing specific cases, it is important to introduce some general rules that apply at all dielectric boundaries.

2.6.1 General rules at dielectric interfaces

2.6.1.1 Electric fields normal to the interface

An electric field is directed normally to the interface between two semi-infinite slabs of dielectrics, as illustrated in Figure 2-10. The relative permittivities of the dielectrics are ϵ_1 and ϵ_2 respectively. The flux density in material 1 is D_{N1} , while that in material 2 is D_{N2} , both being normal to the interface.

Since there are no charges enclosed within the pillbox, the flux approaching the interface must always equal the flux leaving, i.e. $D_{N1} = D_{N2}$, therefore the normal component of the flux density is continuous across a boundary. (See Figure 2-10, for further information).

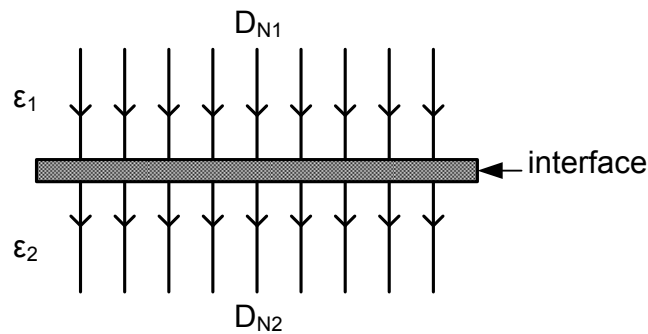


Figure 2-10: Electric fields normal to the interface, adapted by Crowley (1999)

$$D_{N1} = D_{N2} \quad (2.07)$$

$$E_{N1}\epsilon_1 = E_{N2}\epsilon_2 \quad (2.08)$$

Consequently, the electric field (E) and the dielectric constant (ϵ) can be expressed as follows:

$$\frac{E_{N1}}{E_{N2}} = \frac{\epsilon_2}{\epsilon_1} \quad (2.09)$$

A good conductor may be assumed to be a material that is infinitely polarisable, i.e. a material whose relative permittivity is infinitely large. If one assumes that material 2 is a conductor, then inserting $\epsilon_2 = \infty$ into the Equation 2.09 shows that, if E_{N1} is finite, then E_{N2} must be zero. In other words, a good conductor cannot support an electric field, and all flux lines must terminate

normally on charges located at the surface of the conductor, as shown in Figure 2-11. These surface charges on the conductor are said to have been induced by the electric field present in the adjacent insulating medium.

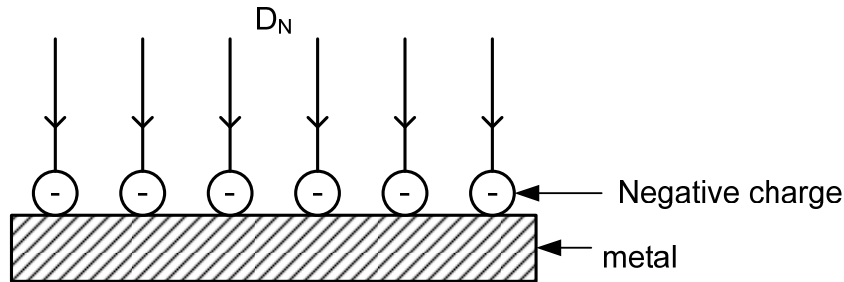


Figure 2-11: Electric fields normal to a metal surface, adapted by Crowley (1999)

2.6.1.2 Electric fields parallel to an interface

As shown in Figure 2-12, the electric field is directed parallel to the interface between two dielectrics. The magnitudes of the fields in the two materials are E_{T1} and E_{T2} respectively. If a small test charge is moved the two points, A and B located on the interface, then the change in its potential energy and therefore the potential difference between A and B should not depend on whether the path of the test charge takes it through material 1 or material 2.

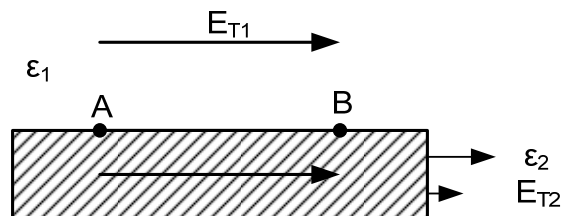


Figure 2-12: Electric fields parallel to an interface, adapted from Crowley (1999)

The potential at B relative to A is then given by

$$V_B - V_A = - \int_A^B E_{T1} dx = - \int_A^B E_{T2} dx \quad (2.10)$$

From which it is deduced that: $E_{T1} = E_{T2}$

Since the tangential components of electric field on either side of the boundary are identical, potential must be a continuous function across an interface. For the case where material 2 is a

conductor, E_{T2} must be zero. Therefore, the field E_{T2} in the dielectric close to the interface must also be zero. It follows then that flux lines must be incident normally on a conducting surface.

2.6.1.3 Interfacial charges

When charges are present at the interface between two dielectrics, as shown in Figure 2-13, an extra boundary condition is required, which is obtained by applying Gauss's theorem to a pillbox surrounding a small section of the charged interface.

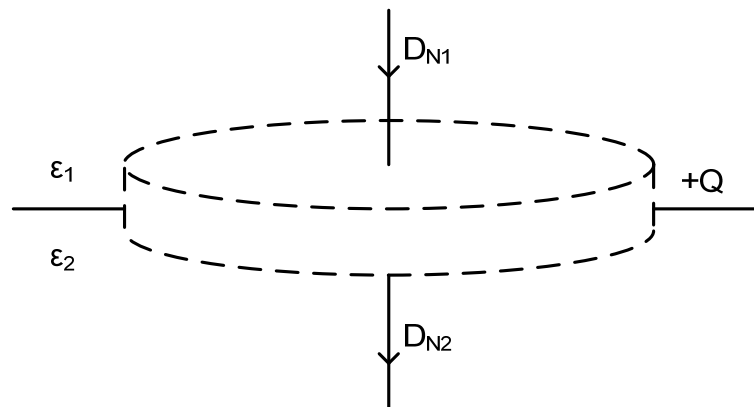


Figure 2-13: Interfacial charge between two media, adapted from Crowley (1999)

Thus, if Q is the charge per unit area of the interface then the following is applied:

$$D_{N2}A - D_{N1}A = QA \quad (2.11)$$

$$D_{N2} - D_{N1} = Q \quad (2.12)$$

On crossing a charged interface, the change in the normal component of flux density is equal to the charge density at the interface.

2.6.2 Spheres in external fields

A sphere of radius r_0 is immersed in an external field, as shown in Figure 2-14. Both the sphere and the external medium are conducting, with ohmic conductivities σ_a and σ_b (see Figure 2-14). The external field is oriented along the horizontal axis, which is also a polar axis of the spherical coordinate system. The voltage outside the sphere is expressed as follows:

$$V_b = -E_0 r \cos\theta + K_1 r^{-2} \cos\theta \quad (2.13)$$

In this case the bubble is not a conductor, so there may be an electric field inside the sphere. The process of selecting suitable terms for this region relies on the boundary conditions selected for the inside of the sphere. Assuming that there is no initial charge inside the sphere, the potential must be finite, and all terms with inverse powers of r can be discarded. Also since the potentials inside and outside must both satisfy the boundary conditions at the surface of the sphere, they will need to have the same θ dependence, so the potential inside the sphere must have the form:

$$V_a = K_2 r \cos\theta \quad (2.14)$$

In a relatively good insulator, however, double-layer effects are usually small, so the boundary condition for the tangential electric field becomes:

$$E_\theta(r = r^+) = E_\theta(r = r^-) \quad (2.15)$$

Charge relaxation at the interface must always be considered, however, since it is a dynamic process and occurs for at least part of the time after any change in the electric variables. It is described by the second boundary condition in terms of the current that flows to the surface charge, which builds up there as:

$$\sigma_a E_r(r = r^-) - \sigma_b E_r(r = r^+) = \frac{d}{dt} [\varepsilon_b E_r(r = r^+) - \varepsilon_a E_r(r = r^-)] \quad (2.16)$$

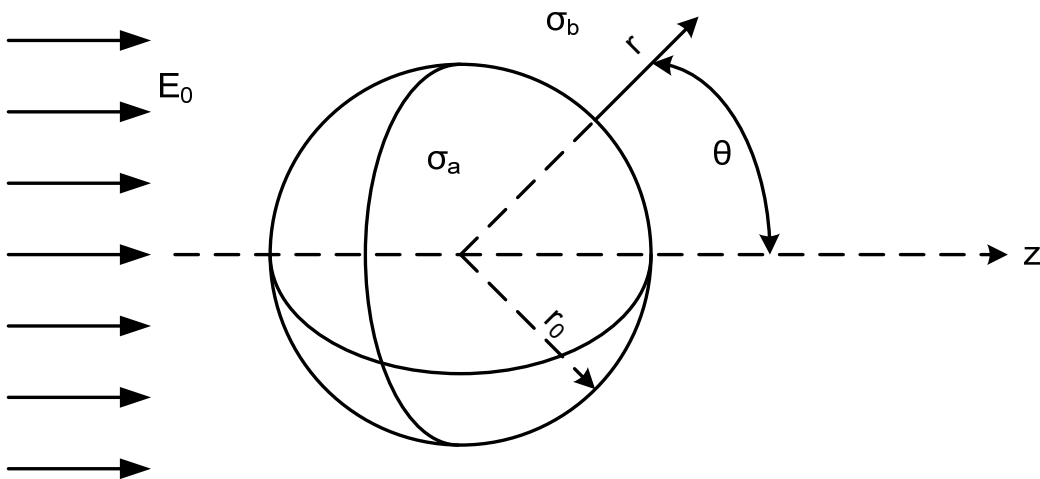


Figure 2-14: Spheres in external fields, adapted from Crowley (1999)

Chapter 2: Literature Review

Equation 2.17 is used for an ohmic conductor, where Gauss's law has been used to express the surface charge in terms of the electric fields. The effect of using direct current (d.c.) or alternating current (a.c.) is discussed here.

In the d.c. limit, variations, if any, in the surface charge are so slow that no net ohmic current through the liquid is needed to charge the interface. In terms of the boundary conditions, this amounts to neglecting the time derivatives in Equation 2.16, so that:

$$\sigma_a E_r(r = r^-) = \sigma_b E_r(r = r^+) \quad (2.17)$$

In this limit the radial (or normal) current must be continuous across the interface. since the conductivity is different in the two regions, the electric fields must also differ. Using the two boundary conditions, it becomes:

$$V_a = -E_0 \left(\frac{3\sigma_b}{\sigma_a + 2\sigma_b} \right) r \cos\theta \quad (2.18)$$

$$V_b = -E_0 \left[r - \frac{r_0^3}{r^2} \left(\frac{\sigma_a - \sigma_b}{\sigma_a + 2\sigma_b} \right) \right] \cos\theta \quad (2.19)$$

In the high frequency limit, the external field is varying too quickly to allow the conduction process to change the charge at the surface of the sphere, so that:

$$\frac{d}{dt} [\varepsilon_b E_b(r = r^+) - \varepsilon_a E_a(r = r^-)] = 0 \quad (2.20)$$

This condition requires only that the charge at the interface remain constant. With a simple interface, however, it is also true that the net charge vanishes, so that the constant value may be set equal to zero. Similar equations are obtained for the a.c. limit.

$$V_a = -E_0 \left(\frac{3\varepsilon_b}{\varepsilon_a + 2\varepsilon_b} \right) r \cos\theta \quad (2.21)$$

$$V_b = -E_0 \left[r - \frac{r_0^3}{r^2} \left(\frac{\varepsilon_a - \varepsilon_b}{\varepsilon_a + 2\varepsilon_b} \right) \right] \cos\theta \quad (2.22)$$

2.7 ELECTRIC SEPARATORS

An electric separator is nothing more than a vessel and or tank equipped with electrodes, at least one of them is earthed and at least other electrode is suspended by an insulator, to which an electrical potential is applied (Eow & Ghadiri 2002b). The conventional electric separators are huge, as large residence times are required for the electrocoalescence regions and settling zones to separate the enlarged water droplets from the crude-oil. However, this could cause complications for offshore platforms as they have limited space (Waterman 1965; Thompson, Taylor & Graham 1985; Tsouris, Shin & Yiacomou 1998; Urdahl, et al. 2001). Several types of electric fields have been demonstrated to be effective for electrocoalescence, such as alternating current (a.c.) fields, pulsed a.c. fields, direct current (d.c.) fields and pulse d.c. fields. The a.c. electric field has been used since 1911 up to the present time.

There are many ways in which an electrical separation technology can be used (Eow & Ghadiri 2002b), such as in combination with centrifugation, heating, chemical treatment, filtration, pressure and mixing; sometimes it can be used alone as electrical treatment only (Eow & Ghadiri 2002b). As a result of this, electrical separators will differ according to which combination is used. Figure 2-15 illustrates a typical separator that uses heat, electrical and mechanical methods. The emulsion or dispersion enters the separator and is heated; this will reduce the viscosity of the continuous phase, which is then exposed to an electric field that eventually increases the droplet sizes. The droplets are then separated in the mechanical separation section, as illustrated in Figure 2-15.

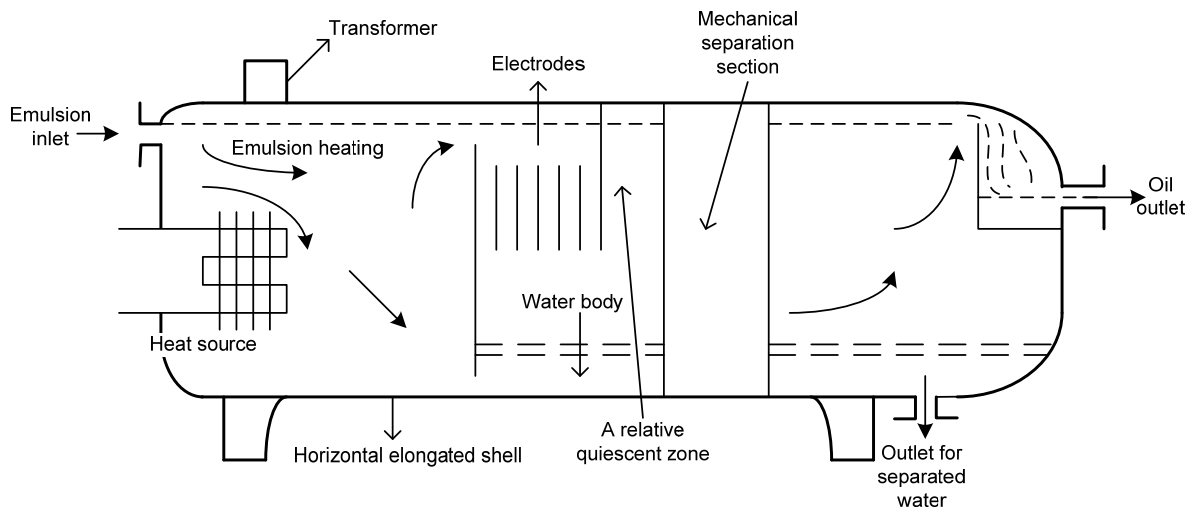


Figure 2-15: Sectional drawing of a horizontal separator that combines heat, electrical and mechanical separating methods adapted from Eow and Ghadiri (2002b)

2.8 FACTORS AFFECTING ELECTROCOALESCENCE

Electric-separators are used to enhance the coalescence rate of water droplets in a water-in-oil emulsion so that these droplets can grow to a certain size in order to be separated from the continuous phase either by gravitational or centrifugal methods. Several important features of a typical electrostatic separator are therefore worthy of discussion.

2.8.1 The electric field

An electric field is efficiently applied to enhance the coalescence rate of dispersed phase in an emulsion when the continuous phase has a much lower permittivity than the dispersed phase or when the continuous phase has a low conductivity and acts as an insulator between the two electrodes. The means of applying a high electric field include at least a pair of electrodes, one at a relatively high voltage and the other at low voltage (earthed). In addition, this high voltage may be pulsed alternating current (a.c.), direct current (d.c.), or pulsed d.c. or a combination of them can be utilised in the separation of water-in-oil dispersions or emulsions. Each field type acts according to different mechanisms in enhancing phase separation by droplet-droplet coalescence

(Waterman 1965). The a.c. field predominantly has a polarising effect, whilst some electrophoresis effects may also be present for the d.c. field.

2.8.2 The electrode

The characteristics and geometry of an electrode (generally cylindrical or plate) determine the performance of the electrostatic coalescer. The type of electric field and the emulsion will influence the choice of the electrode geometry. The maximum distance between the electrodes is limited by electrode edge effects (fringing fields) and the potential that must be applied to create sufficiently high electric field strength (Waterman 1965). In the former, as the electrode spacing is increased, the fringing electric field becomes more significant. In the latter, the transformer design and electrical circuitry are influential. The electrodes are commonly arranged as either closely-spaced long electrodes or widely-separated short electrodes. The choice of electrode geometry is another aspect that should be considered. Safety and practical considerations usually dictate the design of a coalescer to be a cylindrical pressure vessel when the emulsion is at a high pressure and temperature. A cylindrical electrode mounted co-axially in a vertical coalescer turns out to be a simple and yet effective arrangement. Generally, an insulated electrode may be used efficiently when the content of the dispersed phase is less than or about 15% of the emulsion; short-circuiting may occur above this limit (Harris 1918; McKibben 1919; Bailes 1996; Bailes, Freestone & Sams 1997). However, in some operations, the use of centrifugal force may eliminate the need for an insulated electrode (Edmondson 1998).

3 WATER-IN-CRUDE-OIL EMULSION STUDIES

Emulsions in the petroleum industry are created by a reduction in the reservoir pressure, friction losses, and the presence of surfactants (Schramm 1992; Langevin et al. 2004). Many studies have been carried out on emulsions over the last 40 years and although people have a good understanding of these complex systems today, there still remain many unanswered questions related to the peculiar behaviour of these emulsions. The demand for quality crude-oil involves removing the water content and/or solids. The presence of asphaltenes, resins, wax, naphthenic acids, solids and other chemicals in crude oil have been reported to influence the stability of water-in-crude-oil emulsions (Aske, Kallevik & Sjoblom 2002; Langevin et al. 2004). The presence of these indigenous crude oil components contributes to the formation of a viscoelastic film on the crude oil/water interface which may contribute to a stable emulsion (Havre 2002; Langevin et al. 2004). Among the indigenous crude oil components, asphaltene is the heaviest and most polar component and is one of the main contributors to emulsion stability (McLean & Kilpatrick 1997a; McLean & Kilpatrick 1997b; Havre 2002; Langevin et al. 2004). It is believed that asphaltenes are kept in solution by resins (McLean & Kilpatrick 1997a; McLean & Kilpatrick 1997b; Spiecker 2001; Spiecker et al. 2003) and possibly by naphthenic acids (Havre 2002). The emulsion stability also depends on the type and structure of a surfactant. Therefore, it is important to isolate and characterise the crude oil components so that valuable conclusions regarding factors contributing to the emulsion stability can be made.

There are many methods available for determining the stability of water-in-crude-oil emulsions, including near-infrared spectroscopy, the critical-electric-field (CEF) method, the Langmuir technique, the pendant drop technique, and centrifuging. A study of water-in-crude-oil emulsions is described here. The main objective of this study was to investigate the stability of water-in-crude-oil emulsions, focusing on the effects of different crude oil blends on the emulsion

stability. Three methods were used to determine the stability of the emulsions, namely gravity-settling, the CEF method and the centrifuge method. The asphaltenes, resins, wax content and the total acid number (TAN) were obtained from the suppliers.

3.1 EXPERIMENTS

3.1.1 Chemicals and materials

All chemicals were used as supplied without any further purification. Seven crude oil samples from different wells, namely A, C, H, M, P, U and V, were used for this research work. Distilled water was used to prepare the synthetic water; NaCl (99.5%, Merck) and CaCl₂ (99%, Sigma-Aldrich) were added to the distilled water to achieve the ionic strength of the brine solution. NaOH (99%, BDH) and HCl (99%, Sigma-Aldrich) were added to the distilled water to adjust the pH of the brine solution to the desired values. A CEF cell similar to the one used by Aske, Kallevik and Sjoblom (2002), Eow and Ghadiri (2003b) and Sjoblom et al. 2006) was constructed and used. The CEF was assisted by a d.c. (direct current) power supply (Agilent 6634B), which could deliver a voltage of 100 V and a current of 1 A. The cell had a square injection hole of 1 cm x 1 cm. A centrifuge (mrc) was used to separate the emulsion that formed. An IKA RW 16 basic mixer stirrer (IKA-WERKE), operating at 1 200 rpm maximum, was used to create the emulsion. The specific gravity and the viscosity of the crude oil samples were measured in the laboratory using a hydrometer and a Rheoplus rheometer, respectively. The physical properties of crude oil from different wells are tabulated in Table 3-1. Some other important physical properties of the crude oil samples are shown in Figure 3-1.

Table 3-1: Physical properties of crude oil from the different wells, as measured in the laboratory

	A	H	U	C	M	P	V
Gravity, ($\times 10^{-2}$)	86.5	87.8	90.4	88.5	91.0	86.0	87.5
Gravity, API	32.1	29.7	25.0	28.4	24.0	33.0	30.2
Viscosity, Pas-25°C ($\times 10^{-3}$)	52.0	94.0	216.0	76.0	206.0	14.0	28.0
Viscosity, Pas-40°C ($\times 10^{-3}$)	40.0	62.0	142.0	54.0	120.0	09.0	17.0

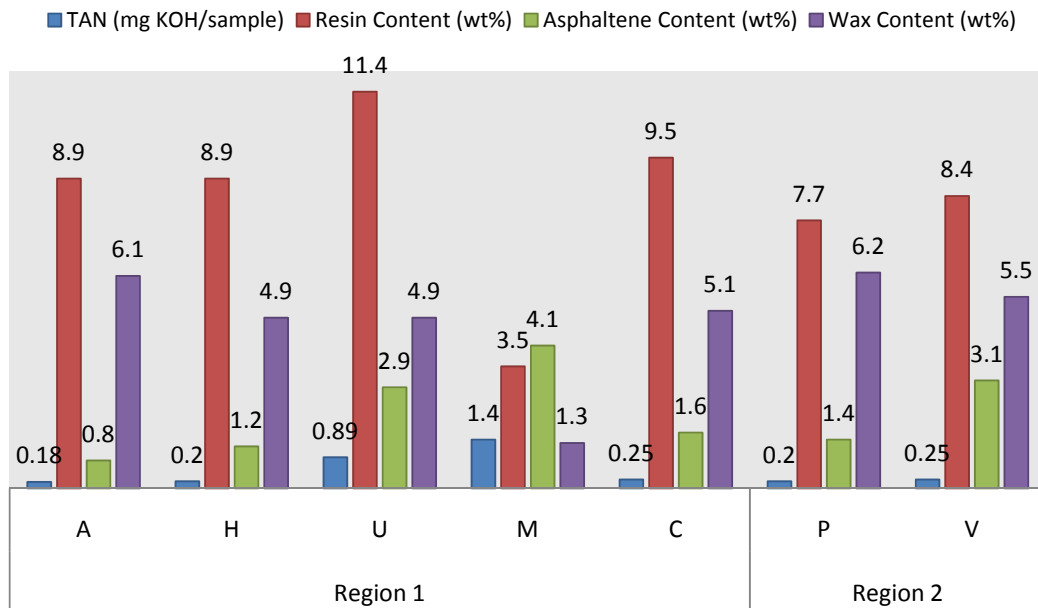


Figure 3-1: Other important properties of crude oil from the different wells, as supplied by the source

3.1.2 Experimental design

For the experimental design it is important to select the appropriate variables that will enable an engineer to investigate the relevant effects on a particular process (Montgomery 2005). Before the experimental method was addressed here, it was important to become familiarised with the number of runs required for the subsequent experiments. For the gravity-settling experiment the following were set as the main factors influencing the emulsion stability: pH of the brine, the water-cut, temperature of the emulsion, mixing time and the speed of stirring. Figure 3-2 provides a model of the experimental approach used. Here the volume of water that separated under gravity was taken as the response, in the gravity test method. The operating parameters of the gravity test method are shown in Table 3-2. The experiments were replicated once and Statistica 7.0 was used to evaluate the effects. The operating parameters for the CEF and the centrifuge test methods were subsequently selected, based on the results obtained from the gravity test method. The operating parameters for the CEF and the centrifuge test methods were set as follows: water cut at four levels (20, 35, 50 and 60% respectively); stirring speed at 1 200 rpm; stirring time at 1 minute; and the pH at 7. The operating conditions were selected to create

water-in-crude-oil emulsions. The experiments were replicated once. These operating parameters were also used for the blends.

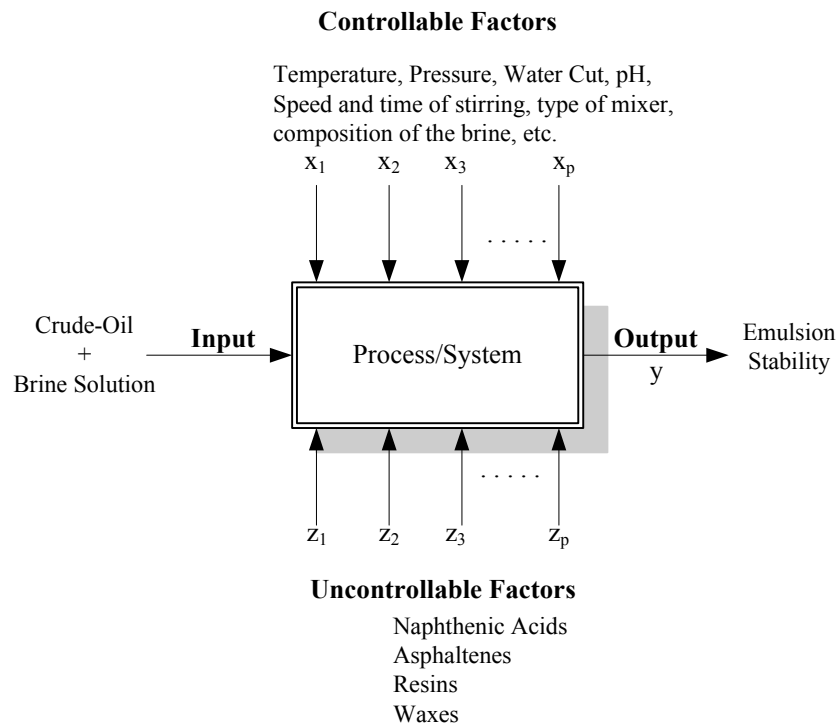


Figure 3-2: Model of the experimental approach used (adapted from Montgomery 2005).

Table 3-2: Operating parameters used for the gravity test method.

Factors	Low level	High level
Water cut	20%	50%
pH	4.00	8.00
Speed of stirring	685 rpm	1 200 rpm
Time of mixing	1 minute	4 minute

3.1.3 Methods

A brine solution (4 wt% NaCl and 1 wt% CaCl₂) and crude oil (200 mL in total) were preheated to approximately 60°C and then mixed according to the design matrix selected. The resulting emulsion was then used for the gravity-settling, CEF and centrifuge test method respectively. In the gravity-settling test the sample was allowed to settle for 10 minutes at 60°C, and the volume of water separated was recorded. In the case of the CEF and the centrifuge tests, however, no sooner was the emulsion created than a small quantity was used for the CEF cell or centrifuged.

The CEF and the centrifuge tests were done separately, although the same process variables were used. In the CEF test the voltage was increased stepwise and the voltage at which the first increase in the current was noted was recorded; this was noted as the CEF. In the centrifuge test, the samples were centrifuged at 30 000 rpm for a period of 10 minutes and the volume of water centrifuged was recorded. The same procedures were followed for the blends.

3.2 RESULTS AND DISCUSSION

3.2.1 Gravity test method

The changes in the pH of the brine solution upon contact with the crude oil samples under acidic and basic conditions, after several runs, are illustrated in Figure 3-3 and 3-4 respectively (see Appendix A for the data). However, the change in the pH of the brine might have been caused by the absence of a buffer, which frequently occurs during the extraction of crude oil from the reservoir to the surface. This behaviour was also observed during previous work done on some crude oil samples (data not shown here). The change in the pH under acidic conditions may be due to the strength of the indigenous naphthenic acids present in the crude oil samples. Figure 3-3 shows that, in the case of crude oil samples H, A and U, the pH of the brine decreased upon contact with the brine, whilst in the case of crude oil samples P, C, V and M the pH of the brine increased. The decrease in the pH might have been caused by the partitioning of hydronium ions to the water phase, leading to an increase in the concentration of the hydronium ions, and thus decreasing the brine pH; whereas the increase in the pH is suspected to be caused by the presence of salts in the crude oil, which eventually consume the hydronium ions in the brine. Data on the change in the brine pH showed that sample H contained the strongest acid, followed by samples A and U (in that order). The weakest acids might be present in sample C, and possibly samples P and M, as their values were above the horizontal dashed line in Figure 3-3. The horizontal dashed line indicates the initial pH of the brine: in this case the pH was 4.04. The crude oil samples H, A and U may have a high capacity for the formation of naphthenate under favourable conditions, as the pH of the acidic brine solutions decreased in these cases.

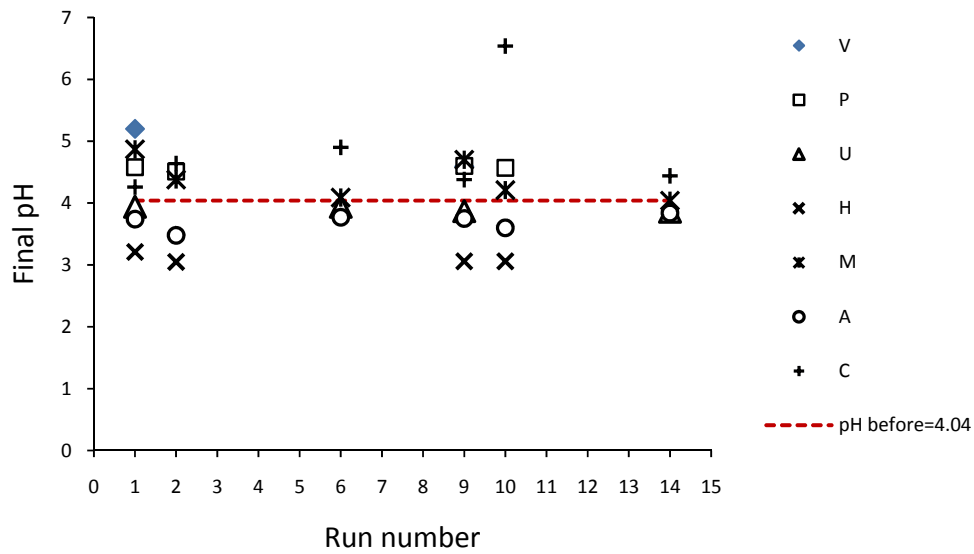


Figure 3-3: Change in the pH of the brine under acidic conditions, after the separation of the emulsion

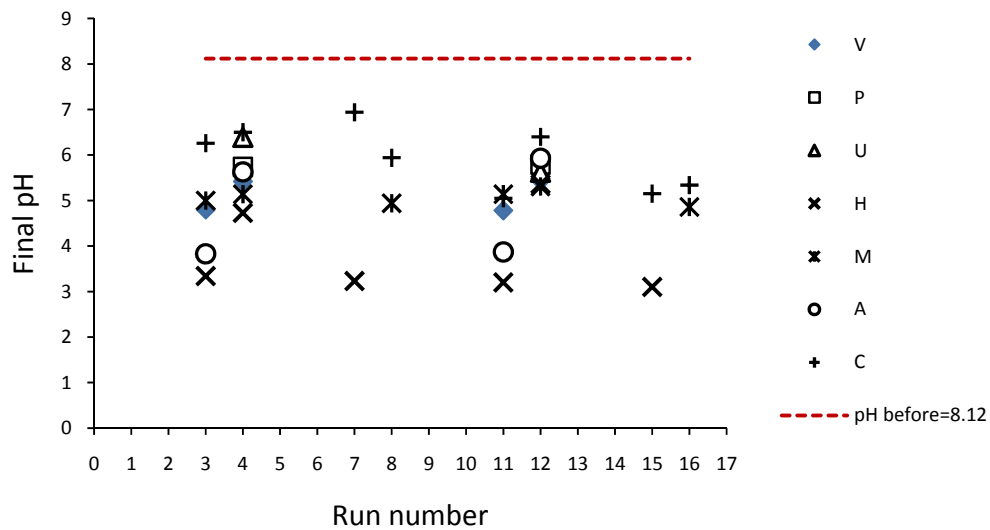


Figure 3-4: Change in the pH of the brine under basic conditions, after the separation of the emulsion

The results presented in Figure 3-4 confirmed the strength of the acids present in samples H and A in terms of reducing the brine pH, however, opposite behavior was seen for sample U as shown in Figure 3-4. The latter could be explained by a lower concentration of acids in sample U, but this contradicts the higher TAN values provided in the experimental section. It was also

confirmed that the acids present in sample C were the weakest, as illustrated in Figure 3-4. The viscosity and density of the samples did not correlate with the shift in the brine pH. The viscosity seemed to be one of the possible limiting factors as it presents internal resistance to mixing. The TAN values provided did not correlate with the pH shift. In order to rank the crude oil samples in terms of creating stable emulsion, the intercepts (β_0) obtained from the equations for each crude oil tested (see Equation 3.01) were compared. Table 3-3 tabulates the ranking of the crude oil samples.

Equation 3.01 was used to model the response in the gravity test when the factors were varied. Where y is the response (the volume of water separated under gravity), β_0 is the intercept, β_i and x_i (the subscript $i = 1, 2, 3$ and 4) are the regression coefficients and the factors respectively, and ε is the random error. Here x_1 stands for water-cut, x_2 stands for pH, x_3 stands for stirring speed, x_4 stands for stirring time and the interactions stand for x_{12} , x_{13} and x_{14} (also referred to as 1 by 2; 1 by 3 and 1 by 4, respectively). The model equations for all the samples explained more than 98% of the actual data.

$$y = \beta_0 + \beta_1x_1 + \beta_2x_2 + \beta_3x_3 + \beta_4x_4 + \beta_{12}x_{12} + \beta_{13}x_{13} + \beta_{14}x_{14} + \varepsilon \quad (3.01)$$

In this section, the results for sample V crude oil are explained (see Appendix C for the other samples). The experiments with sample V crude oil showed that all factors and their respective interactions had a significant effect on the response, in which the stirring speed (x_3) had the major effect on the response. The water-cut-pH interaction (x_1x_2) also had an impact on the response. The x_4 effect comes after the x_1x_2 interaction, as illustrated in Figure 3-5. This figure ranks the effects and their interaction in terms of creating emulsion.

In order to understand the operating range of the factors and their interactions, the normal probability plot, as illustrated in Figure 3-6, was used. It is clear that the stirring speed (x_3), stirring time (x_4) and water-cut (x_1) lay on the left-hand side of the normal probability plot, thus inferring a negative effect on the response, that is, the response was decreased when these factors were operated at their higher level. However, the brine pH had a positive effect on the response, meaning that the response was increased when the process was operated at higher brine pH.

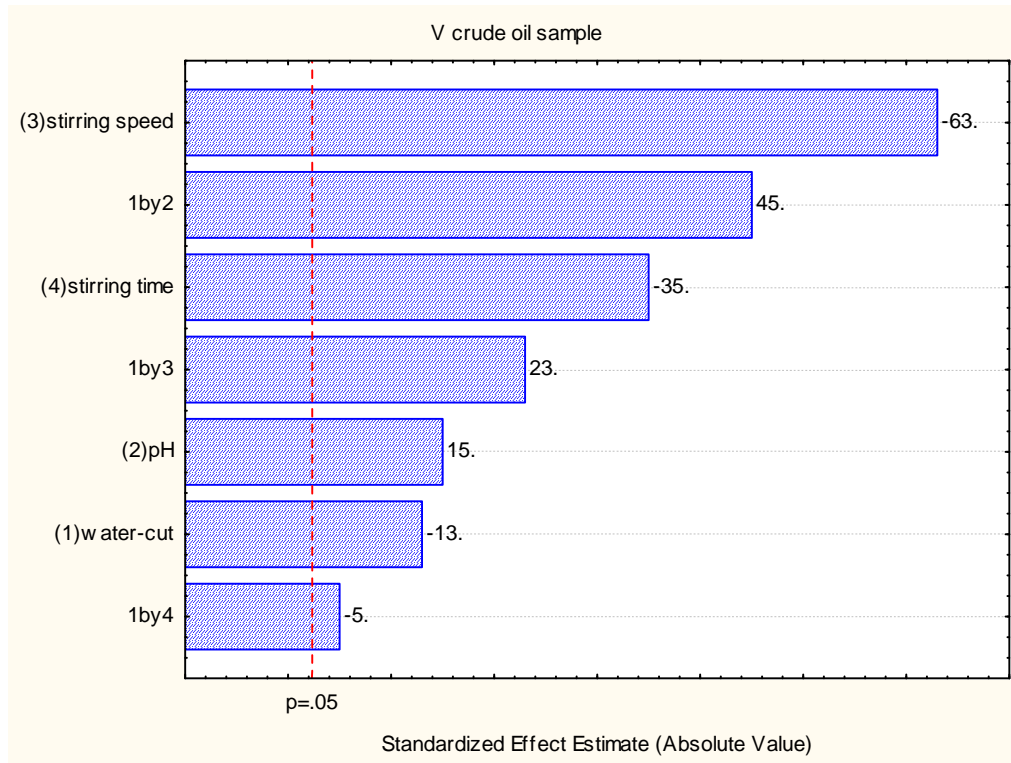


Figure 3-5: Pareto chart for the sample V crude oil experiments

The interactions in this experiment had quite a significant effect compared to some of the factors. It can be seen from Figure 3-6 that the water-cut-pH interaction (x_1x_2) lay on the right-hand side, implying that operating the process at both higher water-cut and brine pH increased the response when the other two factors were operated at lower level. Furthermore, there is also a positive effect of the water-cut-stirring speed (x_1x_3) interaction, which implies that operating the process at higher water-cut and stirring speed respectively increases the response when the stirring time is set at the lower level and the brine pH at the higher level. However, the water-cut-stirring time interaction (x_1x_4) had a negative effect on the response, though it is the least effect of all of the factors, but in a confidence level of 95% it was considered; the negative effect implied that operating the process at higher water-cut and stirring speed respectively decreased the response, provided that the stirring speed was run at the higher level and the brine pH at the lower level.

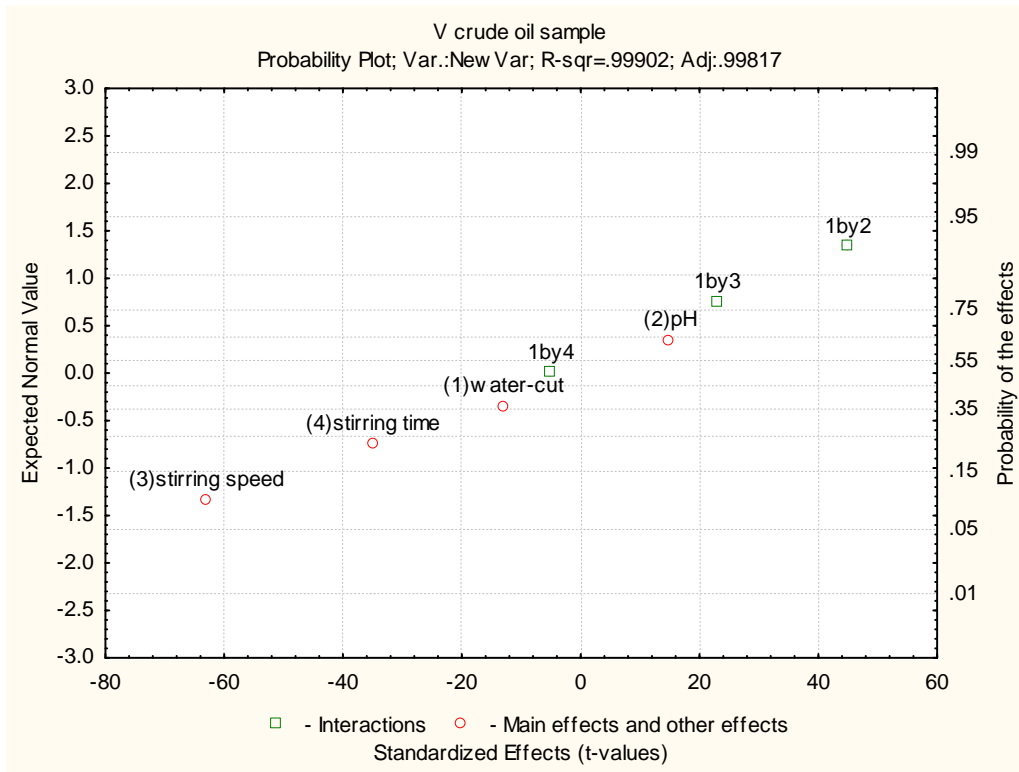


Figure 3-6: Normal probability plot for the experiments with sample V crude oil

From the analyses done so far, the conclusions were as follows: In order to increase the response (the volume of water separated), the process should be run at a higher water-cut and brine pH respectively, with the stirring time and stirring speed set at a lower level respectively. The response for this experiment is represented mathematically as follows (see Equation 3.01):

$$y = 22.81 - 4.06x_1 + 4.69x_2 - 19.69x_3 - 10.94x_4 + 14.06x_1x_2 + 7.19x_1x_3 - 1.56x_1x_4$$

The model explained 99.906% of the actual data. The same procedure was done with the other crude oil samples. The results of the 2^{IV-1} fractional factorial design are summarised in Table 3-3; the crude oil samples are given in terms of decreasing emulsion stability.

The ranking of the crude oil sample correlated well with the quantity of asphaltenes contained by the crude oil samples from Region 2. Similar correlations have been reported by Spiecker (2001), Aske, Kallevik and Sjoblom (2002), Havre (2002), Spiecker et al. (2003), Langevin et al. (2004) and Sjoblom et al. (2006). However, in the case of samples from Region 1, the asphaltene content did not correlate with the emulsion stability: the asphaltene content of crude oil sample

M was higher than that of sample U. This implies that another reason is required to explain the causes of the stable emulsions created by these crude oil samples. Havre (2002) found that the ratio of asphaltenes to resin could explain the emulsion stability. The resins will help to disperse the asphaltenes under favourable condition (Spiecker 2001; Havre 2002), thus reducing the emulsion stability. However, if conditions are not favourable, the asphaltenes will precipitate, and enhance the emulsion stability. Asphaltenes may also be dispersed by naphthenic acids to some extent (Havre 2002), which may lead to competition between resins and naphthenic acids. Further studies are required here.

Table 3-3: Ranking of the crude oil samples in terms of creating emulsion

Crude samples	Coefficients and intercepts							
	β_0	x_1	x_2	x_3	x_4	x_1x_2	x_1x_3	x_1x_4
V	22.81	-4.06	4.69	-19.69	-10.94	14.06	7.19	-1.56
U	31.72	18.91	-6.72	-9.97	-27.84	6.09	2.84	-15.03
P	35.59	4.03	5.34	-25.03	-15.59	5.03	-11.59	2.22
H	40.16	-6.41	9.22	-25.16	-9.53	-5.47	-8.59	5.78
A	43.84	3.53	5.91	-30.34	-10.22	-0.03	-5.03	-1.16
M	54.14	22.58	4.13	-3.89	-15.05	8.17	19.55	-3.48
C	56.00	14.75	-3.75	-26.50	-12.50	-10.00	-2.75	-1.25

The regression coefficients of the equations used for each crude oil sample (excluding the interactions) were plotted in order to determine the general effects that each crude oil sample had on the emulsion stability. The results are shown in Figure 3-7.

A positive regression coefficient implies less emulsion stability, whereas a negative regression coefficient implies higher emulsion stability. Increasing the water-cut led to destabilisation of the emulsion stability of samples A, C, M, P and U; however, an abnormal behaviour was noticed for samples H and V, where the emulsion stability increased when the water-cut was increased. The stability of the emulsion decreased when samples A, M, H, P and V were mixed with basic brine solution, as illustrated in Figure 3-7. Ese and Kilpatrick (2004) and Langevin et al. (2004) also noticed this behaviour. They observed lamellar crystalline films under acidic conditions, and it was subsequently claimed that they covered the water droplets, which then led to an increase in the stability of the emulsions. However, crude oil samples C and U behaved differently and contradicted the mechanism proposed by Ese and Kilpatrick (2004) and Langevin et al. (2004). The emulsion stability of these samples increased when in contact with basic brine. The

following explanation for this is offered: naphthenates might have been formed, which, together with the indigenous molecules, stabilised the emulsions.

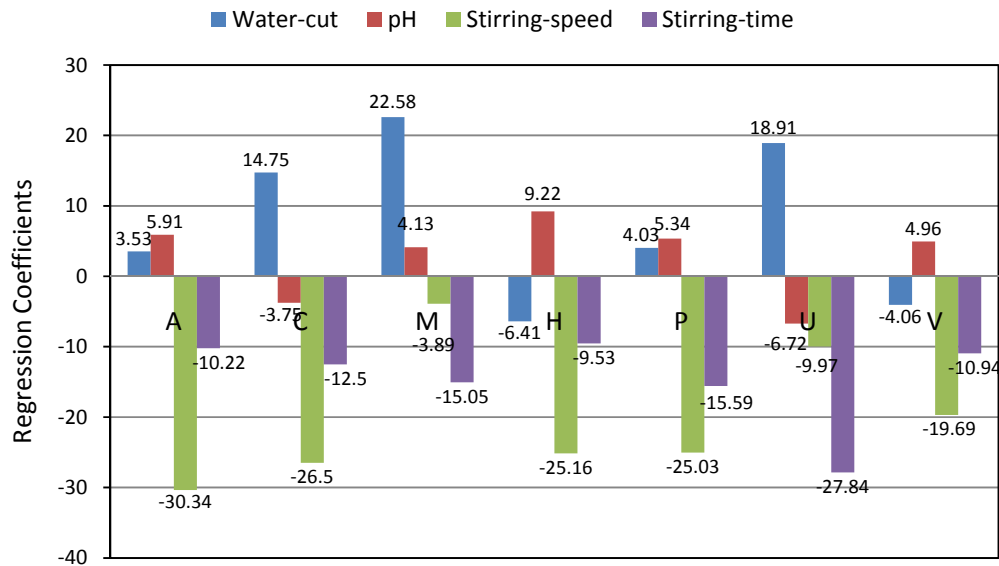


Figure 3-7: Overall effects for the gravity test method for different crude oil samples

The difference in behaviour of the different crude oil samples towards the emulsion stability arises from the difference in the nature of the acids, asphaltenes and resins. Characterisation of naphthenic acids is needed to predict the associated emulsion stability and eventually naphthenate risks. Another issues that was not included was the percentage of water for each crude oil sample, this might have helped to explain the unusual behavior observed during the experiments.

3.2.2 The critical-electric-field and centrifuge methods

The results obtained from the gravity test method were used to rank the crude oil samples in terms of entraining water droplets. Previous work performed on some of the crude oil samples demonstrated that some crude oil samples dehydrated easily in the initial stage and had poor dehydration characteristics at the end. Here the CEF and the centrifuge test methods were used to determine the emulsion stability. The crude oil samples V, C and H, and two blends (Blend 1 and Blend 2), were used. Blend 1 comprised crude oil from Region 1, whereas Blend 2 comprised crude oil from Region 2.

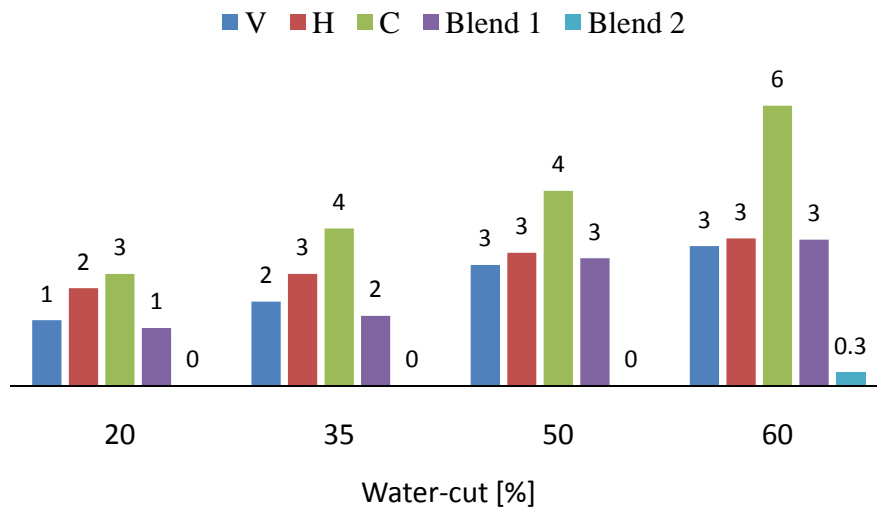


Figure 3-8: Volume [mL] of water centrifuged from a sample of 10 mL emulsion created by different crude oil samples

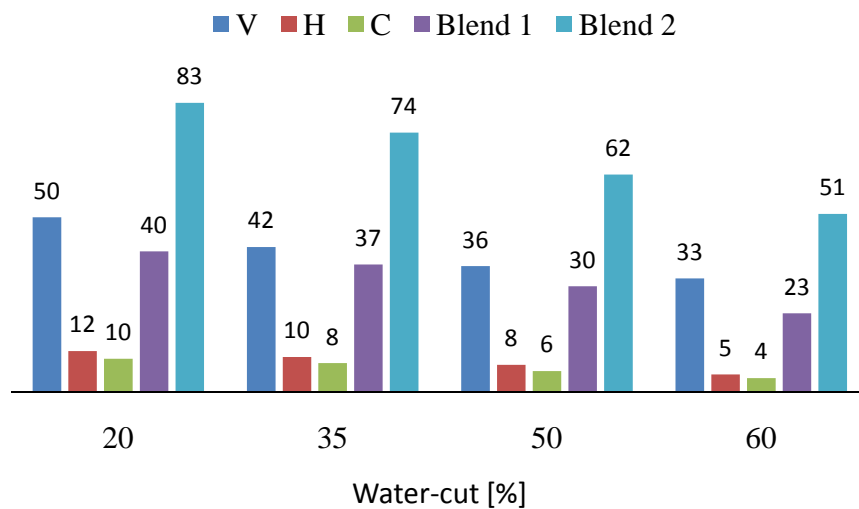


Figure 3-9: Critical electric field (V/cm) values needed to break the emulsion formed by different crude oil samples

The results of these two test methods confirmed the ranking order that emerged from the gravity test method. The volume of water centrifuged was found to be inversely proportional to the CEF, as illustrated in Figures 3-8 and 3-9 (see Appendix A for the data). Blend 2 afforded the most stable emulsions compared to the other samples tested. Furthermore, the blends afforded more stable emulsions than their respective constituents. This could be accounted for by the fact that,

Chapter 3: Water-in-Crude-Oil Emulsion Studies

when different crude oil samples are blended, the system becomes even more complex because there may be different chemical and thermodynamic equilibria.

In Figures 3-8 and 3-9 the increase in the water-cut destabilised the emulsion in both methods (CEF and centrifuge). This confirms that the increase in water-cut decreased the amount of water that centrifuged. This is explained in the following way. According to the centrifuge concept, the centrifugal force pushes heavier components (water) away from and lighter components (crude oil) towards the centre of the centrifuge tube; the water drops coalesce and are attracted by gravity. Increasing the water content, increases the volume fraction of water in the emulsion, and eventually more water drops are in contact with the its bulk phase, therefore an increase in the volume of water centrifuged was noted. The CEF values were plotted on the x-axis from left to right on this axis, represent a water-cut of 60, 50, 35 and 30%. Here again the increase in the water-cut decreased the emulsion stability. The increase in the water-cut increased the volume of water in the emulsion, which then increased the conductivity of the medium. This explains the low voltage measured when the water-cut was increased.

The physical parameters presented in the experimental section (Table 3-1 and Figure 3-1) do not correlate with the emulsion forming of these samples. Similar justification was observed in the samples in the gravity test method. The presence of many indigenous components in the crude oil may explain the unanswered behaviour in emulsion stability.

4 THE ROLE OF ORGANIC ACIDS IN EMULSION STABILITY

An understanding of the equilibria involved in a water/oil/naphthenic acid system is important in order to understand the different problems naphthenic acids cause in crude oil production. Previous work on naphthenic acids has been reported by Havre (2002), Ese and Kilpatrick (2004) and Brandal (2005). The presence of an electrolyte in the system prevents the formation of water continuous emulsion (Ese and Kilpatrick 2004), thus in a crude oil reservoir the predominant emulsion is the water-in-crude-oil emulsion. The amphiphilic characteristic of naphthenic acids and their salts means that they are preferentially attracted to the interface. However, some naphthenic acids and their salts are more soluble in one of the phases. The partitioning of naphthenic acids is an important parameter for evaluating the equilibria involved when the reservoir brine contacts the crude oil. Havre (2002) found that naphthenic acids with three rings are apparently more hydrophilic than acids with one or two rings. Experiments carried out by Ese and Kilpatrick (2004) showed that water-in-oil emulsions are stabilised at a high acid/soap ratio. They also demonstrated that, under optimal conditions, naphthenic acid or naphthenates alone are well suited as stabilisers for water-in-oil emulsions. Previous work on crude oil samples reported on in Chapter 3 showed that the emulsion stability depended on the type of crude oil and that it did not correlate with the parameters provided in Table 3-1 and Figure 3-1. It was also found that the change in the brine pH upon contact with crude oil samples indicated the strength of the naphthenic acids present in the crude oil samples. It is believed that the type and/or structure of naphthenic acids are of prime importance in the formation of stable emulsions or the formation of naphthenates. Here the role of different organic acids in the emulsion stability was evaluated, and different types of organic acids were used. Heptane and toluene were used as the model compounds for crude oil.

4.1 EXPERIMENTS

Before a theory or a concept is suggested, an experimental method is carried out. This section deals with the experimental work carried out on some of the organic acids. It is believed that organic acids resembling carboxylic acids are causing serious problems in the petroleum industries, in that they are preferentially soluble in the oil phase, which enhances the water-in-crude-oil emulsion stability together with other surfactants (Havre 2002; Ese and Kilpatrick 2004; Hurtevent et al 2006). However, they are also attracted to the aqueous phase, which causes problems in processing the water as corrosion problems and environmental threats arise. The main objective is to assess the behaviour of these acids when they are exposed to different conditions. The materials and equipment used are described below, as well as the approach used to investigate the behaviour of the acids.

4.1.1 Materials

All chemicals were used without any further purification. Heptane (99%, Fluka) and toluene (99.5%, Riedel-de Haën) were used as the model for the crude oil phase. Heptanoic acid (97%, Sigma), undecanoic acid (99%, Aldrich), tridecanoic acid (98%, Sigma), 4-heptylbenzoic acid (97%, Aldrich), 5 β -cholanic acid (Sigma) and naphthenic acid (a mixture of alkylated cyclopentane carboxylic acids from Aldrich) were used as the carboxylic acids. Distilled water, sodium chloride (99.5%, Merck) and calcium chloride were used to make up the brine solution. Sodium hydroxide and hydrochloric acid were used to adjust the brine pH to the desired values. A RW 16 basic mixer (IKA-WERKE) was used to create the emulsion and/or to mix. A liquid chromatograph (Waters API Quattro Micro) and a gas chromatograph (Agilent 6890N GC with CTC CombiPAL autosamples and Agilent 5975B MS) were attached to their respective mass spectrometers.

4.1.2 Preliminary experiments

Before examining an optimal procedure, preliminary experiments were performed. These experiments involved mixing all the acids in the mixture of heptane-toluene (50% v/v) and then mixing them with the brine solution at 1 200 rpm for a period of 10 minutes. The resulting mixture was separated using a separating flask, by which the amount of water and separated organic phase were taken for further analysis for the contents of the acids in the oil and the water phase. A GC-MS was used to analyse the samples. The column used was the DB-FFAP (60 m, 0.25 mm ID, and 0.5 μ m film thickness). The instrument settings were as follows: the injector temperature was 250°C; the injection volume was 1 μ L; and the split ratio was 1:25 for the organic samples and 1:5 for the water samples. The flow rate was set at a constant 1.5 mL/min. Helium was used as the carrier gas. The MS transfer was performed at 240°C, with a positive ionisation and electron energy of 70eV; the scanning mass range was set from 35 to 250 m/z and the solvent delay was 10 minutes. The organic samples were injected as they were; however, for the water samples, NaCl and 1 mL dichloromethane were added, which were vortexed and sonicated. After the removal of the dichloromethane, the water solution was injected.

The results obtained from these experiments were as follows: The 5 β -cholanic acid in the organic samples was not detected in this column; the heptanoic, undecanoic, tridecanoic and 4-heptylbenzoic acids in the organic samples were detected with residence times (RT) of 18.86, 29.09, 35.60 and 36.90 minutes respectively. In the case of the naphthenic acids, the main peak had an RT of 18.71 minutes, whereas the other peaks were detected between 18.86 and 29.09 minutes. (See Figure 4-1 for an illustration). The RT of the tridecanoic and the 4-heptylbenzoic acid are not shown in Figure 4-1.

Chapter 4: The role of organic acids in emulsion stability

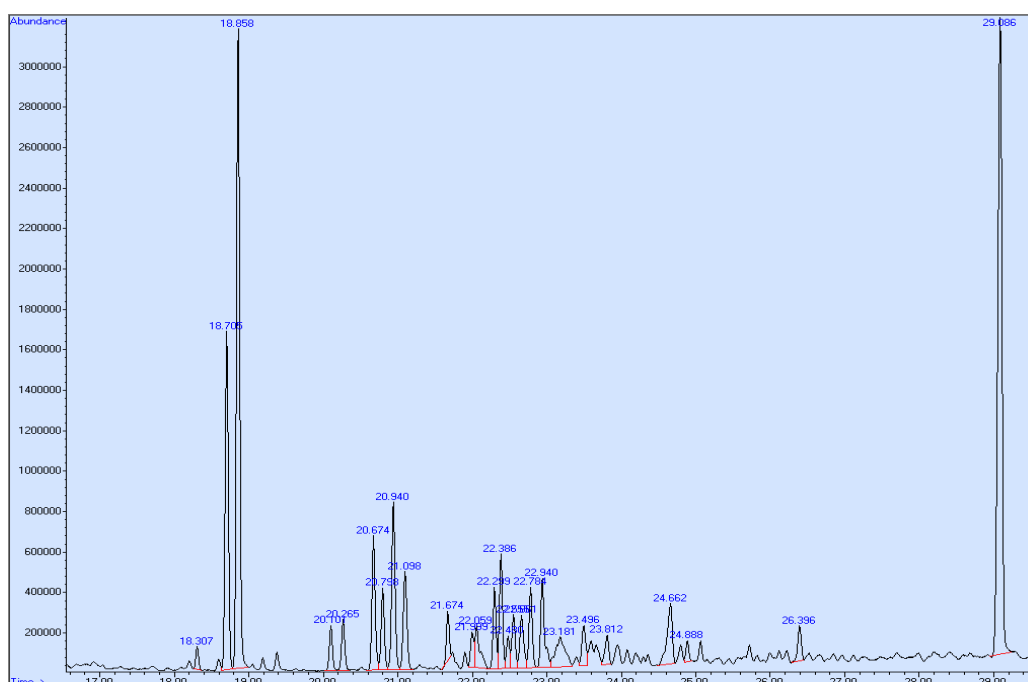


Figure 4-1: Chromatogram of the mixture of all the acids

The 4-heptylbenzoic acid caused problems in detecting it because it was not completely eluted from the column, and this was noticed when a blank oil sample (heptane-toluene mixture) was injected. This is illustrated in Figure 4-2. The water samples gave poor results for all the samples tested. As a result of this and related problems the following experimental procedures were used: The naphthenic acid and a cocktail (comprised of heptanoic, undecanoic and tridecanoic acid) were analysed separately using the GC-MS, whereas the 5 β -cholanic acid and the 4-heptylbenzoic acid were analysed using LC-MS. Another reason why naphthenic acid was not used in the mixture of the other acids was due to a possible existence of heptanoic, undecanoic and tridecanoic acid in the naphthenic acid sample.

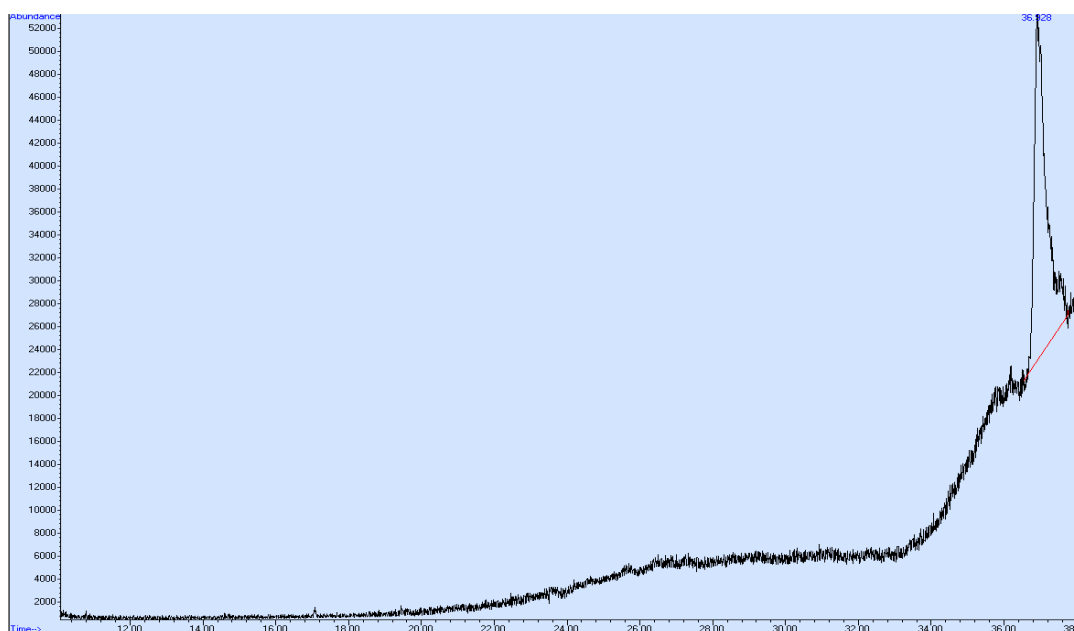


Figure 4-2: Confirmation of the 4-heptylbenzoic acid after elution with blank heptol sample

4.1.3 Experimental procedure

4.1.3.1 Naphthenic acids

A mixture of equal volume (100 mL in total) of heptane and toluene (heptol) was prepared and stirred. Naphthenic acid (hereafter referred to as NA) was added to the heptol and then stirred until it was homogeneous. The brine was prepared by adding NaCl (4 wt%) and CaCl₂ (1 wt%) to distilled water. NaOH and HCl were diluted in distilled water and then used to adjust the brine pH to the desired values. No sooner were the organic samples and brine solution prepared than 100 mL of brine solution was poured into the organic phase, and stirred at 1 200 rpm for a period of 10 minutes. The mixture was then separated in a separating flask. The organic phase that was obtained was taken to a GC-MS to determine the concentration of the acids in the sample. The pH of the separated brine solution (the final brine pH) was also measured. The compositions of the organic samples are tabulated in Table 4-1. The brine pH used was as follows: 3, 5, 7, 9 and 11. The GC-MS setting was the same as used in the preliminary experiments.

Table 4-1: Standard composition of the NA samples

COMPONENTS	ρ [g/cm^3]	m [g]	% m	V [mL]	C_0 [ppm]
NAPHTHENIC ACID	0.920	1.0	1.20	1.087	9892.47
HEPTANE-TOLUENE	0.821	82.1	98.80	100.000	
TOTAL		83.1	100.00	101.087	

The density (ρ) of naphthenic acid was obtained from the supplier, whilst that of the mixture of heptane and toluene (hereafter referred to as heptol) was obtained as follows: equal volumes of both fluids were mixed and weighed; therefore the density was calculated using the basic formula:

$$\rho = \frac{m}{V} \quad (4.01)$$

The concentration of the acid was calculated as follows:

$$C_0 = \frac{m}{V_T} \times 10^6 \quad (4.02)$$

where, m is the mass in grams of the acid and V_T is the total volume of the organic phase (including the acid). A standard sample was prepared and diluted twice in order to obtain a calibration curve (see Table 4-1). The experiments were replicated once.

4.1.3.2 Mixture of acids

A similar procedure was followed with the mixture of acids, which comprised of heptanoic (HA), undecanoic (UDA) and tridecanoic acid (TDA). The acids were added in equal quantities, as illustrated in Table 4-2. Here the organic samples were also analysed in a GC-MS, following the same procedure as the one used in the preliminary experiments. The concentrations of the acids were calculated using Equation 4.02. A brine solution with the same concentration as the one used for the naphthenic acid experiments was used. The volume of the brine was the same as the volume of the heptol, which was 50 mL. The brine pH was the same as described in the naphthenic acid experiments. The final brine pH was also measured. Here the experiments were replicated once and a standard sample was prepared separate from the other samples; it was diluted to obtain a calibration curve (see Appendix A). Dodecanoic acid (DDA) was used as the internal standard in order to control the loss of the acids (HA, UDA and TDA) during elution.

Table 4-2: Standard composition of the cocktail of acids

COMPONENTS	ρ [g/cm^3]	m [g]	% m	V [mL]	C_0 [ppm]
HEPTANOIC ACID	*0.938	0.20	0.48	0.213	3948.28
UNDECANOIC ACID	*0.909	0.20	0.48	0.220	3948.28
TRIDECANOIC ACID	*0.901	0.20	0.48	0.222	3948.28
HEPTANE-TOLUENE	0.821	41.05	98.56	50.000	
TOTAL		41.65	100.00	50.655	

*Densities obtained from The Good Scents Company. (<http://www.thegoodscentscompany.com/data/rw>).

4.1.3.3 5 β -Cholanic and 4-heptylbenzoic acid

The 5 β -cholanic (hereafter referred to as CA) and 4-heptylbenzoic acid (HBA) were added to the heptol phase. The concentration of the brine and the pH remained unchanged (the same values as in the experiments with naphthenic acids and the cocktail of acids). The procedure used for the naphthenic acid was followed for the experiments with CA and HBA. The organic phase was analysed using an LC-MS for the samples containing HBA and the brine phase was analysed in a LC-MS, for the samples that contained CA. The brine samples containing CA were injected as supplied, whilst the organic samples with HBA were diluted 1 000 times in methanol before injecting them into the LC-MS. The standard curves were created by using different injection volumes of the standard samples (heptol + the acids). The mass used for the acids was 1 g, which resulted in an initial concentration of 19 574.45 ppm for the sample containing HBA, and 9 892.47 ppm for the sample containing CA. The final pH of the brine was also measured. Tables 4-3 and 4-4 illustrate the organic phase compositions for the CA and HBA samples. The density value of NA was used for HBA and CA to facilitate the calculations.

Table 4-3: Standard composition of the organic phase for CA samples

COMPONENTS	ρ [g/cm^3]	m [g]	% m	V [mL]	C_0 [ppm]
5 β -CHOLANIC ACID	0.920	1.0	1.20	1.087	9, 892.47
HEPTANE-TOLUENE	0.821	82.1	98.80	100.000	
TOTAL		83.1	100.00	101.087	

Table 4-4: Standard composition of the organic phase for HBA samples

COMPONENTS	ρ [g/cm^3]	m [g]	% m	V [mL]	C_0 [ppm]
4-HEPTYLBENZOIC ACID	0.920	1.00	2.38	1.087	19, 574.45
HEPTANE-TOLUENE	0.821	41.05	97.62	100.000	
TOTAL		42.05	100.00	101.087	

4.1.4 Determination of the partitioning coefficient

The partitioning coefficient of the acids was calculated using Equation 2.04, as follows:

$$k = \frac{[Acid]_w}{[Acid]_o}$$

where k is the partitioning coefficient and the subscripts **w** and **o** represent the concentration of the acid in the water and organic sample, respectively. The partitioning coefficient determine whether an acid is more soluble in one of the phases (organic or water). For values of $k > 1$, the acid is more soluble in the water phase and for $k < 1$, the acid is more soluble in the organic phase. Finally, for $k = 1$, the acid is adsorbed preferentially at the interface of the water organic phase.

4.2 RESULTS AND DISCUSSION

4.2.1 Influence of naphthenic acids on emulsion stability

The result of the experiment with naphthenic acid is shown in Figure 4-3. More than 18 organic species were identified in the naphthenic acid chromatogram; thus 18 species were considered, as illustrated in Figures 4-3 and 4-4. The peak area percentage of each of the components was generated, and this was correlated with the mass percentage for each component in the naphthenic acid. The red lines in Figures 4-3 and 4-4 represent the integration results. Some of the peaks could not be integrated. Figure 4-4 shows an enlarged part of Figure 4-3. From these figures it can be shown that naphthenic acid is indeed a mixture of various acids and/or species. The determination of the structure of each component is of prime importance in predicting the abnormal behaviour presented by crude oil emulsion. Here specific acids were selected and a literature review was carried out in order to estimate a possible chemical structure. The structures of the acids are illustrated in Figure 4-5. See Appendix A for the data of the experiment with naphthenic acid.

Chapter 4: The role of organic acids in emulsion stability

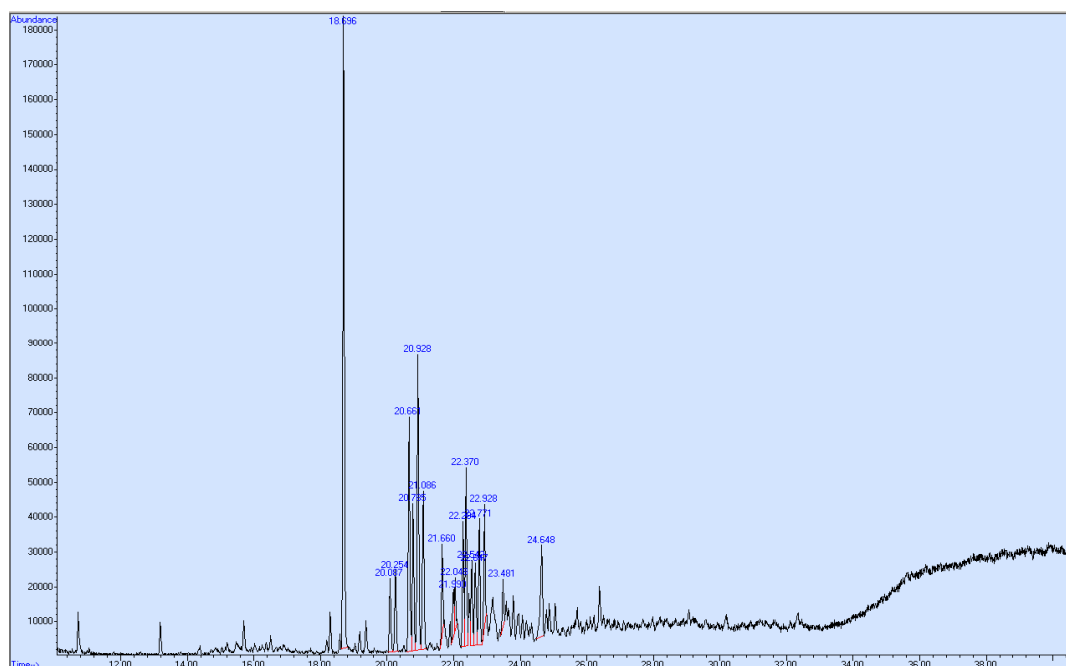


Figure 4-3: Chromatogram of the standard naphthenic acid with all the peaks

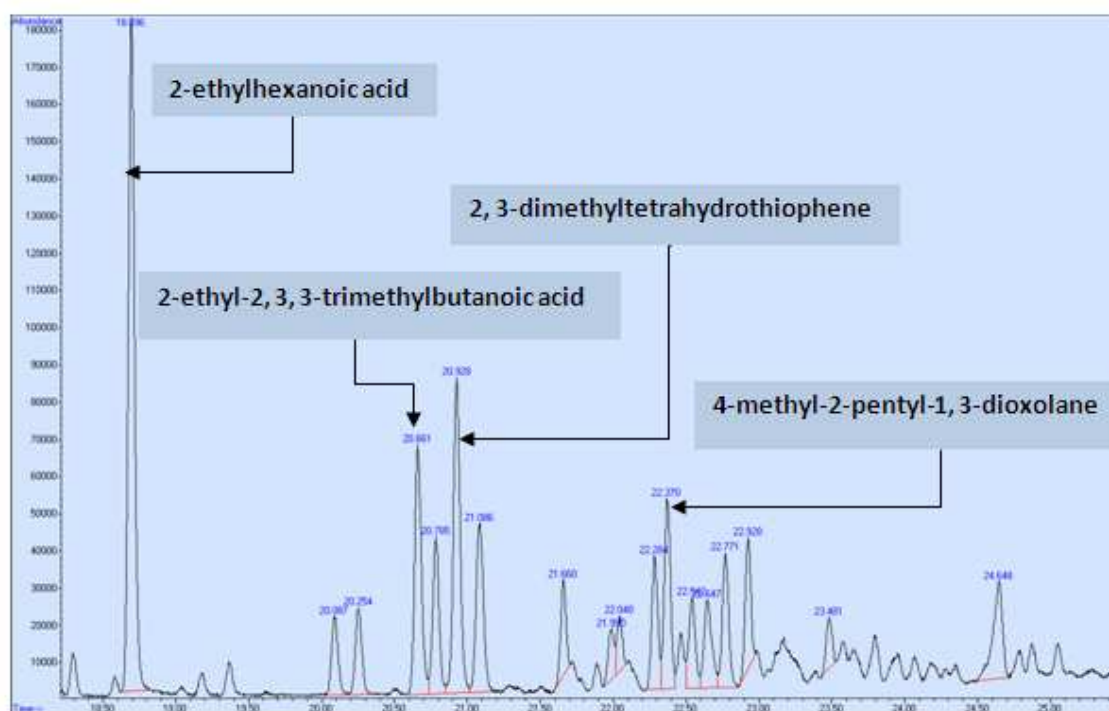


Figure 4-4: Amplified chromatogram of the standard naphthenic acid

Chapter 4: The role of organic acids in emulsion stability

The acids and/or species were identified as 2-ethyl-hexanoic acid, 2-ethyl-2,3,3-trimethylbutanoic acid, 2,3-dimethyltetrahydrothiophene and 4-methyl-2-pentyl-1,3-dioxolane, for the residence times of 18.7, 20.7, 20.9 and 22.4 minutes (in that order) from the chromatogram (see Figure 4-4). As can be seen, most of the species available in the naphthenic acids are carboxylic acids, oxygenated compounds and compounds containing sulphur (see Figure 4-5 for an illustration). The functional group for all the components has at least two lone pair electrons, which favours a possible compatibility with the other polar substance. The hydrophilic part and a hydrocarbon moiety, allow the steric effect to be present.

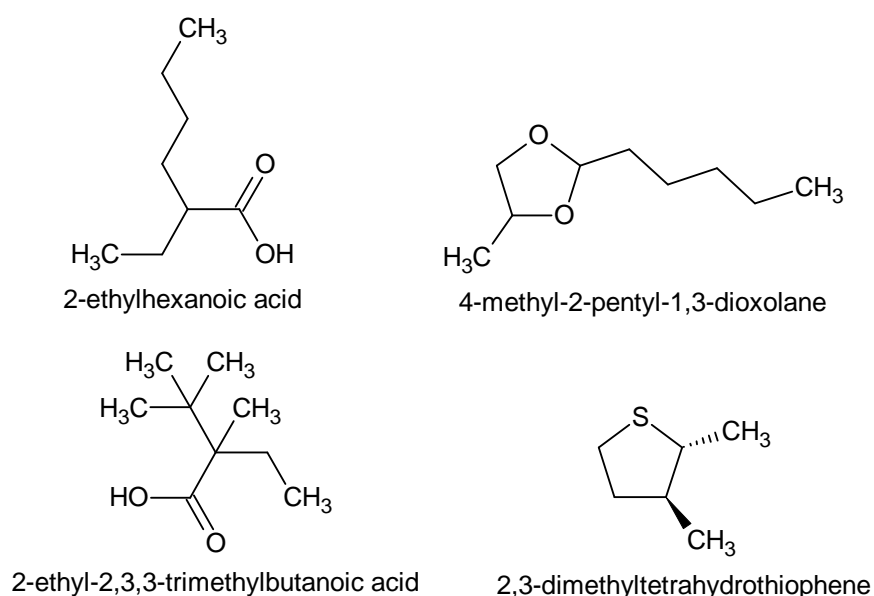


Figure 4-5: Some of the hypothetical carboxylic acids identified in the naphthenic acid sample

The mass percentages of the components in NA are tabulated in Table 4-5. The concentration of each component was determined by multiplying the mass percentage of each of the components with the initial concentration of NA sample.

Table 4-5: Mass percentage and the concentration of the components in the NA sample

Naphthenic acid details			
Components	Molecular weight	% area of the peak	C_0 [ppm]
NA_18.7	144	22.54	2230
NA_20.7	158	9.02	892
NA_20.9	116	11.50	1138
NA_22.4	158	6.47	640

The results of the change in the brine pH are shown in Figure 4-6. The naphthenic acids decreased the brine pH for samples with a pH of 5.43, 7.21, 9.14 and 11.26. However, the brine pH was increased from 3.07 to 3.43.

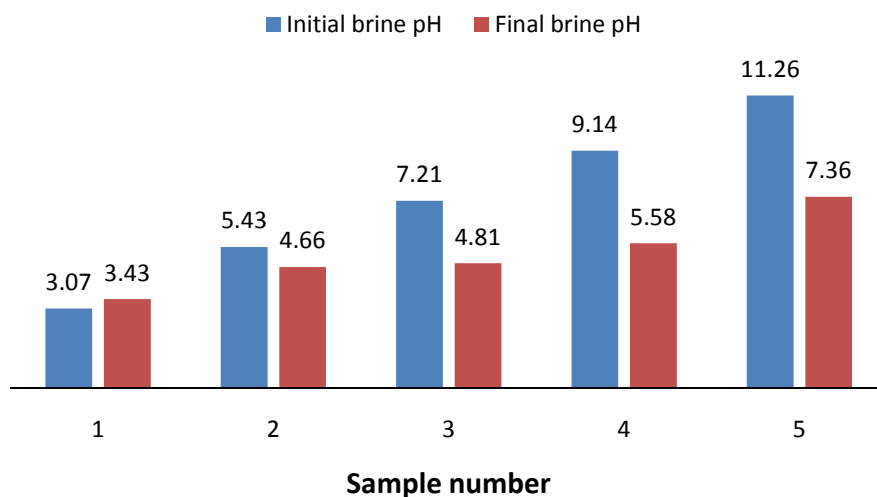
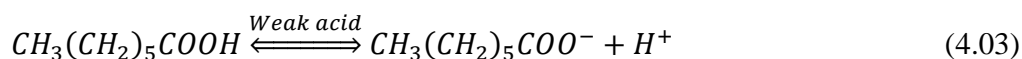


Figure 4-6: The shift of brine pH with NA

The change in the brine pH can be explained using Equation 1. Heptanoic acid is used to illustrate.



Since the brine solution contains hydronium ions (H^+), Le Chatelier's principle may apply here. Remember that the higher the pH, the smaller is the concentration of H^+ . When the organic phase and the brine are mixed, the hydrophilic group of the acid will be in contact with the water and the hydrophobic group will be in contact with the organic phase. The hydrophilic group enables the dissociation of the acids into the water phase. The dissociation of the acids into the water phase is affected by the steric effect of the hydrocarbon moiety; the type and concentration of the metal cations; and the pH of the brine solution. In this case, when the acid dissociates in water that contains H^+ , the reaction in Equation 4.03 is shifted to the left, thus forming more acid than the respective ions. However, this can be counterbalanced by the formation of metal soap (reaction of the acid conjugate with the metal cations), which shifts the reaction to the right. At a higher pH the concentration of the H^+ is small and it will shift the reaction to the right; this

may result in the formation of soap, which then decreases the final brine pH and eventually increases the solubility of the acid in the aqueous solution. This happened in the experiments when the brine pH decreased. However, the increase in brine pH may be justified as follows: the concentration of the H^+ in the water is high enough to shift the reaction in Equation 4.03 to the left, which reduces the concentration of H^+ in the aqueous solution. This decreases the solubility of the acids in the aqueous phase.

The solubility of the acids in the aqueous phase can also be confirmed from the final concentrations in the different tests conditions, as illustrated in Figure 4-7. Here, the concentration of the acids in the organic phase decreased with increasing brine pH.

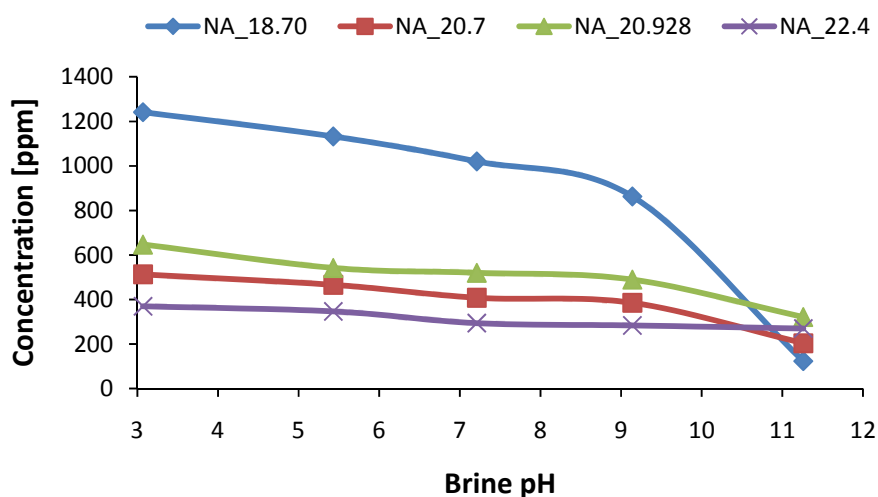


Figure 4-7: Graph of concentration vs. brine pH of the four acids from the naphthenic acid sample

In order to evaluate the solubility of the acids, the partitioning coefficients of the acids at varying brine pH were plotted, as shown in Figure 4-8. It is clear from this figure that the partitioning coefficient increased with increasing brine pH. When the brine pH was increased from 3 to 9, the partitioning remained between 0.73 and 1.58, which indicates that the acids are rather adsorbed at the interface between the two phases, with more tendencies to the organic phase. Here the steric effect of the hydrocarbon moiety had a significant effect on the partitioning of each acid in both phases. However, at a pH of 11 the steric was negligible. The partitioning of the acids is higher than with the other samples. Since the structures of the acids were predicted from the literature, one can not explain the influence of the structure of the acids. Regardless of the

concentration differences among the acids, the most polar acid is the NA_{18.7}, followed by NA_{20.7}, NA_{20.9} and NA_{22.4}. This indicates that the polarity of the acids depends on the structure of the acids, for acids with different structure. Here the acids were preferentially soluble in the brine.

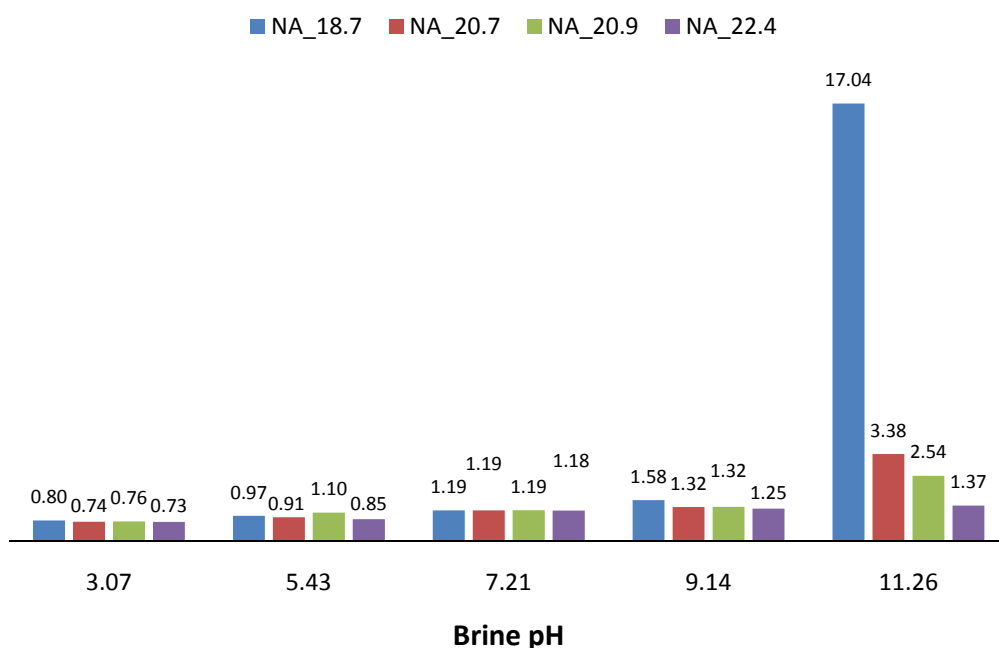


Figure 4-8: The partition coefficient of the NA samples at different brine pH

4.2.2 Influence of cocktail acids on the emulsion stability

In order to assess the effect of molecular weight, straight chain carboxylic acids were used such as heptanoic (HA), undecanoic (UDA) and tridecanoic acid (TDA). Here the effect of the change in the pH was similar to that shown for the NA, and the change in the brine pH is illustrated in Figure 4-9. The shift in the brine pH upon contact with the organic phase is used to estimate the strength of the acids in the organic phase.

The concentration of the acids in the organic phase was expressed by the ratio of the acids to internal standard (IS), which was dodecanoic acid (DDA). Figure 4-10 illustrates the change in the concentration of the acids under different pH conditions. The concentration of the acids decreased when the brine pH was changed from 3 to 5. It was expected to note a decrease in the

Chapter 4: The role of organic acids in emulsion stability

concentration as the brine pH was increased; however fluctuation occurred at some points, as shown in Figure 4-10.

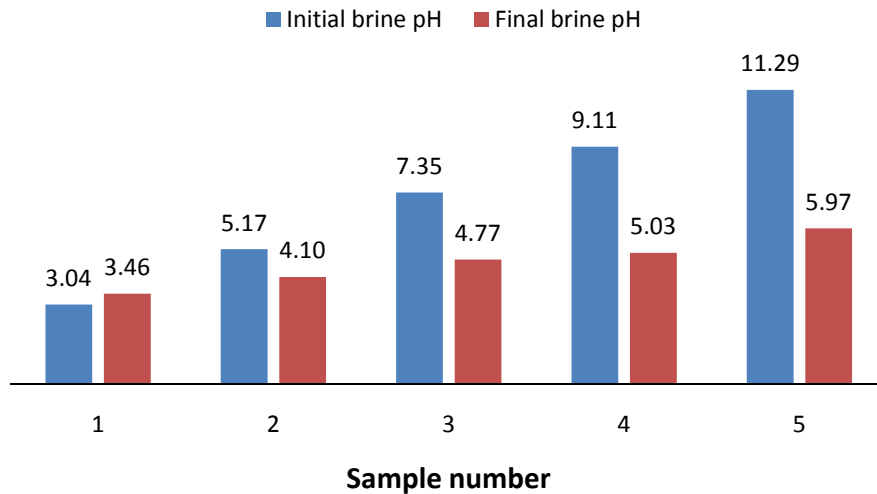


Figure 4-9: The shift of the brine pH with cocktail acid

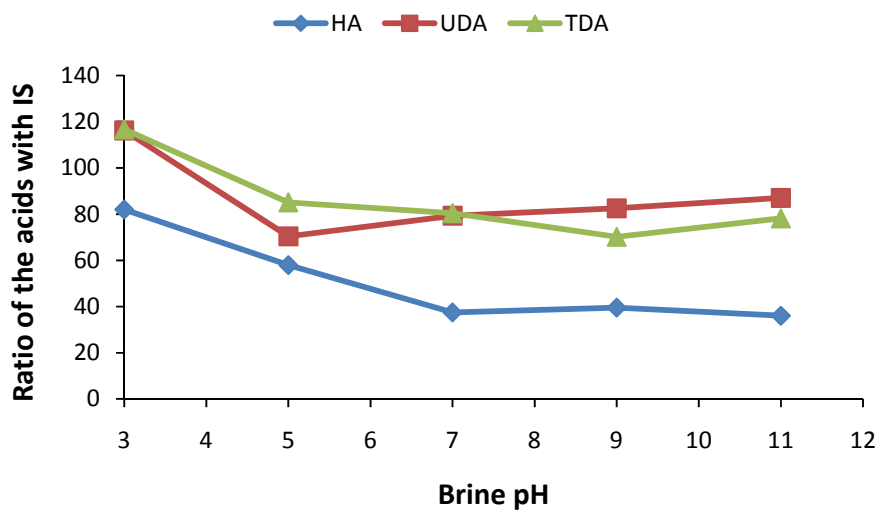


Figure 4-10: Ratio of the acids with IS vs. brine pH

The reason for the fluctuation is as follows: it is suspected that there is a competition between the acids, in which the steric effect of the hydrocarbon moiety might have influenced the acids to be preferentially attracted to the water phase. In order to assess the solubility of the acids under different pH conditions the partitioning coefficient was plotted at different pH conditions, as

illustrated in Figure 4-11. It is apparent that HA is preferentially soluble in the brine at a pH of 7, 9 and 11 because of the higher partitioning coefficient values ($k > 1$), as shown in Figure 4-11. On the other hand, the UDA and TDA are not soluble in the brine solution because of their small partitioning coefficient ($k < 1$), as shown in Figure 4-11. This is explained by the higher molecular weight of UDA and TDA compared to HA for the straight-chain hydrocarbon moiety; this increases the hydrophobic behaviour of the acids. Therefore, for acids with straight-chain hydrocarbons, their solubility decreases with increasing molecular weight.

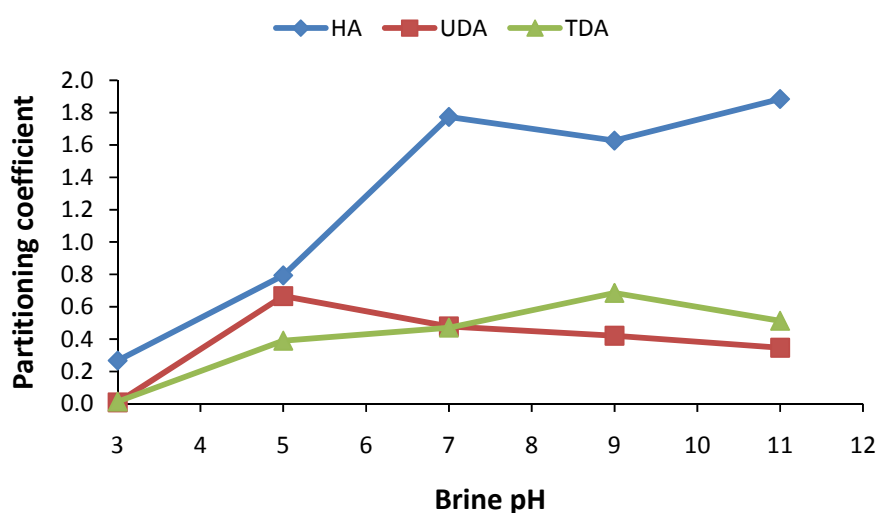


Figure 4-11: Partitioning coefficient vs. brine pH with the cocktail of acids

The results of these experiments assessed the effect of increasing the molecular weight for acids with straight chains. However, in order to extend the knowledge to the partitioning coefficient of naphthenic acids in the oil reservoir or elsewhere in the process industries, other types of acids were used namely 5 β -cholanic acid (CA) and 4-heptylbenzoic acid (HBA). These acids have been used by different authors (Havre 2002; Ese & Kilpatrick 2004) as they resemble the hypothetical structure of the naphthenic acids found in crude oil.

4.2.3 Influence of 5 β -cholanic acid on the emulsion stability

The result of chromatography for the 5 β -cholanic acid (CA) with a pH of 3 is illustrated in Figure 4-12.

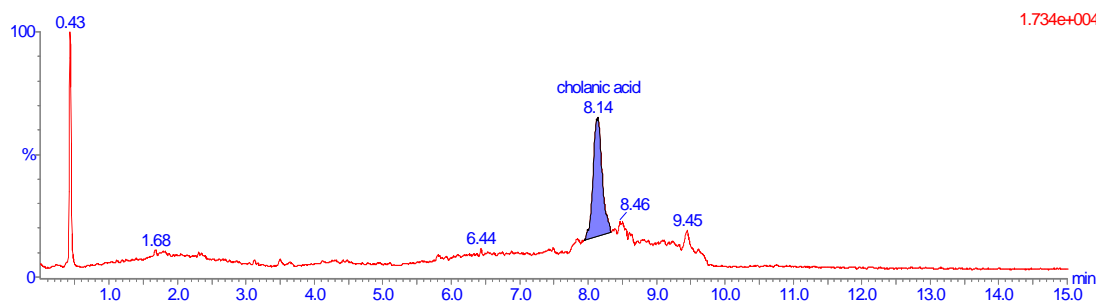


Figure 4-12: Chromatogram of CA in aqueous pH at pH of 3.2

The results of the change in the brine pH with 5 β -cholanic acid (CA) are illustrated in Figure 4-13. Here the brine pH increased when a brine pH of 3 and 5 was used and the brine pH decreased for a brine pH of 7, 9 and 11, as illustrated in Figure 4-13. This indicates that CA has a higher pK_a value than the cocktail of acids and NA.

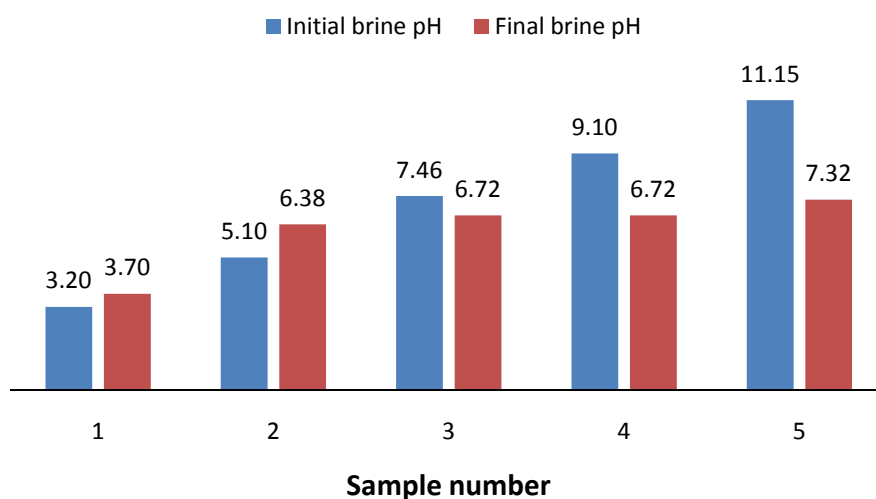


Figure 4-13: Shift of the brine pH with CA

The results in Figure 4-13 prove that CA is less soluble in the water phase. In order to confirm the solubility of this acid in the water phase, the final concentration of CA under different pH conditions was determined. The results are plotted in Figure 4-14.

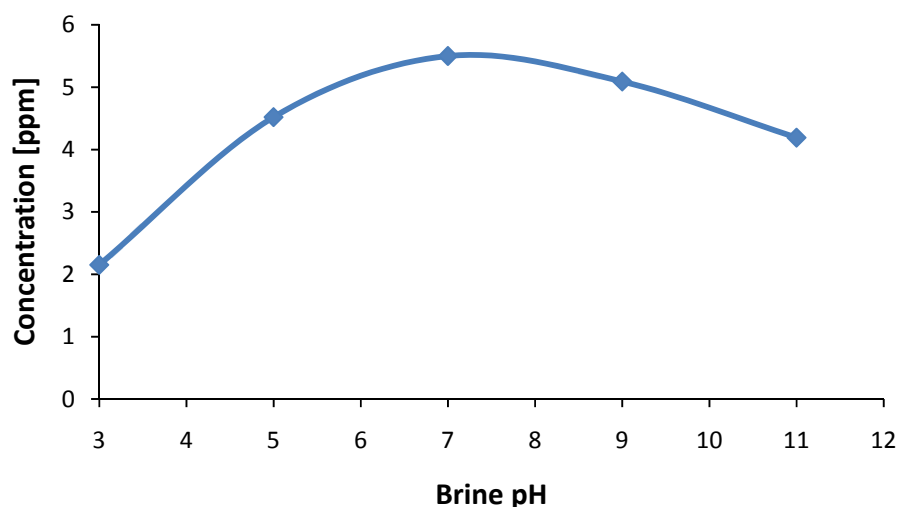


Figure 4-14: Final concentration of CA vs. brine pH

The concentration of CA in the aqueous phase increased with increasing brine pH for a brine pH of 3, 5 and 7, as illustrated in Figure 4-14. The concentration of CA in the aqueous phase decreased for a brine pH of 7, 9 and 11, as illustrated in Figure 4-14. The reasons for the decrease in the concentration of CA may be explained by the formation of a soap-like structure at the interface between the two phases, as illustrated in Figure 4-15. This structure formed when brine solution at a pH of 7, 9 and 11 was in contact with the organic phase containing CA. This influenced the concentration of CA in the aqueous phase, and therefore a small concentration of CA was detected in the water samples. It is believed that the soap-like layer adsorbed part of the water. This behaviour may be one of the causes of stable emulsion in the petroleum industries. It is believed that the CA reacted with the metal cations present in the aqueous phase and then formed a stable soap, which is preferentially attracted to the interface. The soap is believed to be preferentially soluble in the organic phase as a result of its high molecular weight (see Appendix B).

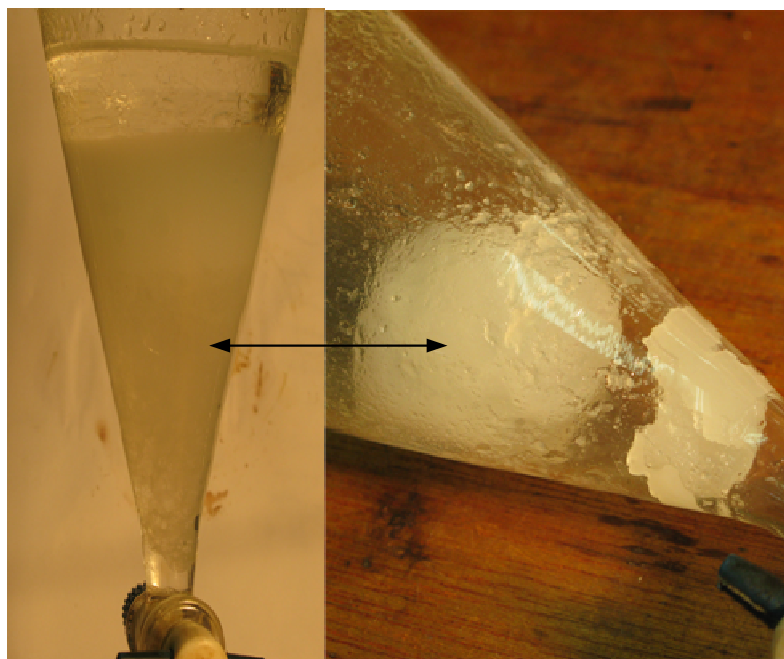


Figure 4-15: Formation of “scale” at pH of 11 when CA was used

In order to assess the solubility of CA and the so-called soap-like compound, the partitioning coefficient at different brine pH was plotted, as illustrated in Figure 4-16.

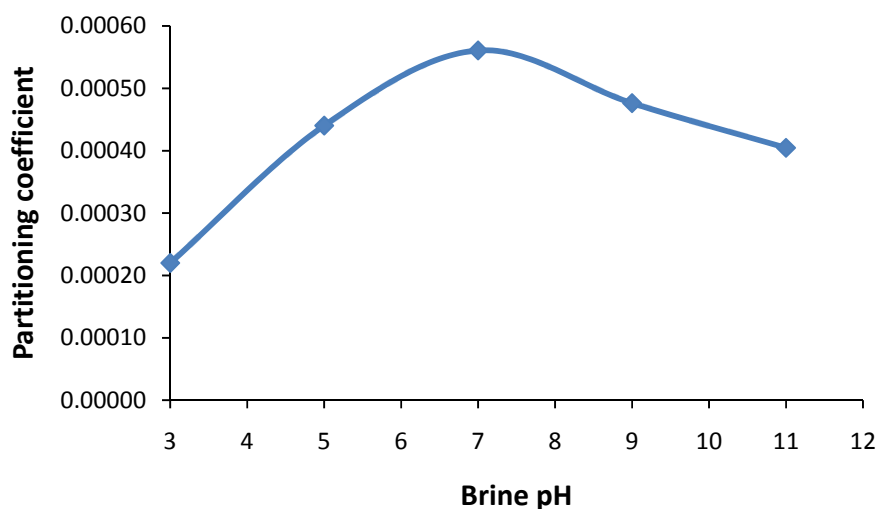


Figure 4-16: Partitioning coefficient of CA vs. brine pH

It is clear that the partitioning coefficient is below 0.0006, which means that a small amount of CA goes into the aqueous phase. The intermediate layer formed seems to be attracted to the

organic phase. The soap formed explains the presence of naphthenates (naphthenic acid soaps) in some of the crude oil deposits in the world. This actually enhances the emulsion stability at small water fractions (water-cuts). As a result of the tendency of the soap-like layer to prefer the organic phase, a water-in-oil emulsion may result because the intermediate layer adsorbs part of the water.

4.2.4 Influence of 4-heptylbenzoic acid on the emulsion

The organic samples that contained 4-heptylbenzoic acid (HBA) were analysed by liquid chromatography, and the result of the chromatogram for the experiment with brine solution at a pH of 3 is illustrated in Figure 4-17. The effect of a benzene ring was evaluated here.

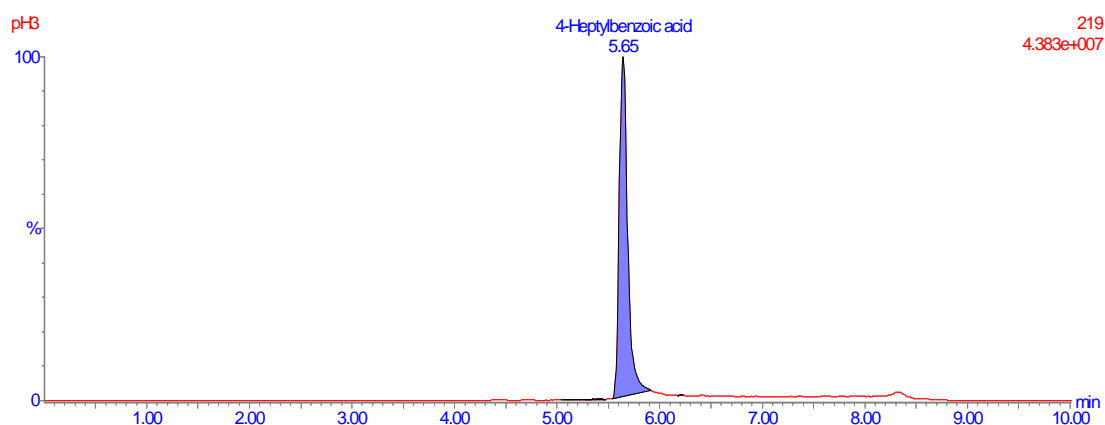


Figure 4-17: Chromatogram of organic phase that contained HBA

The change in brine pH with HBA is quite similar to the one with CA, as illustrated in Figure 4-18. Here the brine pH was increased for the brine with a pH of 3 and 5, whereas the brine pH was decreased when a pH of 7, 9 and 11 was used.

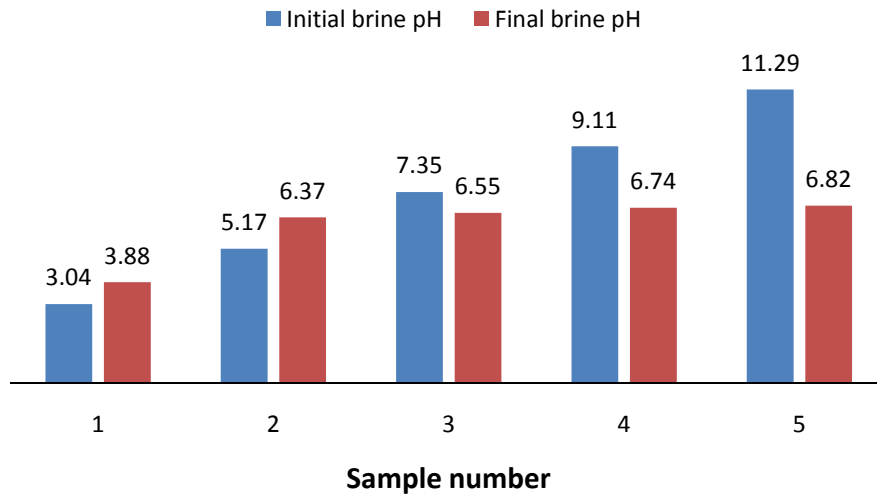


Figure 4-18: Shift of the brine pH with HBA

The concentration of HBA in the organic phase decreased with increasing brine pH, from a pH of 3 to 7, as illustrated in Figure 4-19. However, the concentration of HBA increased slightly from a pH of 9 to 11, as shown in Figure 4-19. The samples with a pH of 7, 9 and 11 showed precipitate at the bottom of the sample, as illustrated in Figure 4-20. This might have led to the unexpected concentration of the samples of pH 9 and 11, as shown in Figure 4-19. The formation of precipitate in the organic phase is believed to be linked to the formation of dimers.

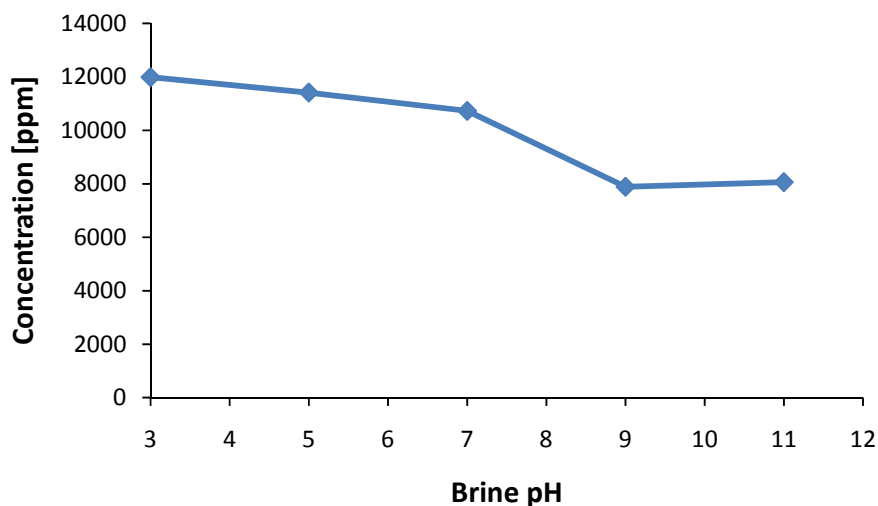


Figure 4-19: Graph of the final concentration vs. brine pH for the HBA samples

Chapter 4: The role of organic acids in emulsion stability

The formation of dimers or micelles makes the HBA or its soap preferentially soluble in the water phase. The influence of this behaviour is illustrated in Figure 4-21, in which the partitioning coefficients for the samples with a pH of 9 and 11 lie well above 1.



Figure 4-20: Effect of brine pH on the samples containing HBA

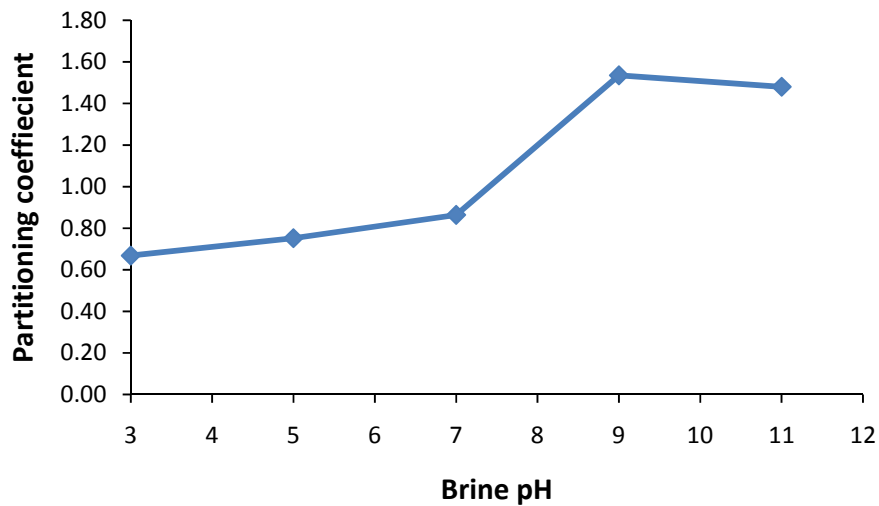


Figure 4-21: Graph of the partitioning coefficient vs. brine pH for the HBA samples

4.2.5 Comparison of the partitioning coefficients of different acids

The results obtained from previous runs on the model naphthenic acids were grouped to compare the partitioning coefficients. The result of the partitioning coefficient of NA_18.7 at a pH of 11 was not included here because its value was higher than the rest. (See Figure 4-22 for an illustration).

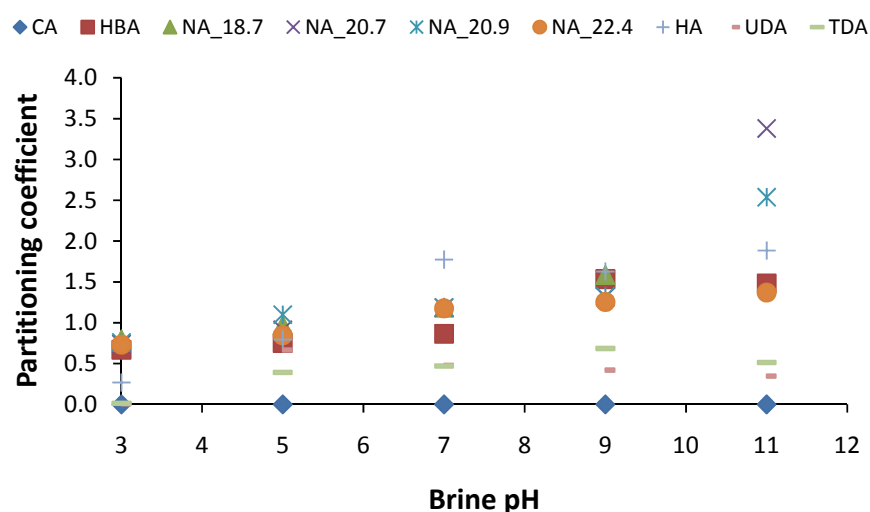


Figure 4-22: Comparison of the partitioning coefficient of different carboxylic acids

The partitioning coefficients of CA, TDA and UDA were below 1 for all the brine pH levels used. The partitioning coefficient of the other acids increased when the brine pH increased, as seen in Figure 4-22. At a pH of 3, the partitioning coefficient of HA was lower than that of HBA; at a pH of 5 the partitioning coefficients of the two acids were quite similar. At a pH of 7, the partitioning coefficient of HA is higher than that of HBA; at a pH of 9 the values were quite similar; and at a pH of 11 the partitioning coefficient of HA was higher than that of HBA. The partitioning coefficient values of HBA, at pH levels of 7, 9 and 11, was affected by the formation of a precipitate, as already explained in Section 4.2.4 (also see Figure 4-20 for an illustration). It is believed that the partitioning coefficient of HBA is lower than that of HA. The similarity in the partitioning coefficient between HA and HBA shows the influence of a benzene ring in the acid. The HBA has a higher molecular weight than UDA and TDA (see Appendix B), but as a result of the benzene ring it has a higher partitioning coefficient than these acids.

Chapter 4: The role of organic acids in emulsion stability

The CA samples had the smallest partitioning coefficient when compared to the acids tested here. This may be explained by their molecular weight (see Appendix B) to some extent. It was seen that carboxylic acids with a ring attached formed an extra layer; this was noted for HBA and CA. It is believed that naphthenic acids that enhance emulsion stability have similar structures to CA and/or HBA. CA and HBA should be considered to assess the formation of solid precipitate and/or lamellar crystalline liquids in the emulsion systems.

5 DETERMINATION OF THE EFFICIENCY OF AN ELECTRIC SEPARATOR

In many chemical processes, the efficient removal of a disperse water phase from a continuous oil phase is of prime importance. There currently are several methods currently available for this, such as chemical demulsification, gravity or centrifugal settling, pH adjustment, filtration, heat treatment, membrane separation and electrostatic demulsification (Lissant 1993; Sun et al., 1998). The use of chemical demulsifiers can modify the water oil interfacial properties, thus allowing water droplets to coalesce more easily into larger ones. However, problems can arise with respect to the removal of the demulsifiers from the respective aqueous and oil phases. The pH effect can be utilised to separate oil-in-water emulsions, but it generally is not applicable in breaking water-in-oil emulsions. Centrifugation, an effective method for separating a colloidal dispersion, has a high operating cost. Heat treatment can reduce the viscosity of the continuous phase (oil), thus enabling any water droplet to fall more rapidly through the oil phase and therefore helping in the separation of any entrained gas in the crude oil. However, heat and chemical treatments are rather expensive and heating results in high fuel consumption. Some cost savings have been achieved with the application of electrostatic technology (Eow & Ghadiri 2002c). This technology has a low power requirement, requires no addition of chemicals, and the method is free from any mechanical break-down because no moving parts are involved (Eow & Ghadiri 2002b). The exact way in which the electrical separation occurs is not yet fully understood (Eow, Ghadiri & Williams 2001), thus a disadvantage may arise in designing a separation process suits to different emulsions scenarios. The slow rate at which liquids are naturally separated in many water-in-oil dispersions has important consequences in many commercial operations (Taylor 1996; Tsouris, Shin & Yiaccoumi 1998). For example, water-in-oil emulsions are readily formed in the production of crude oil, causing problems at different

stages of the production and finally downgrading the quality of the crude oil. Hence, there are many reasons for removing and/or reducing the water content in the crude oil. Furthermore, the separation of the fine water drops dispersed in crude oil is done in large tanks and it takes a long time. There is therefore good reason for reducing the settling time of the water droplets in the separating tanks.

Eow and Ghadiri (2002a, 2002b) have developed a novel electric separator that combines an electric field with centrifugal and/or gravity force (hereafter referred to as a centrifugal electric separator) to remove dispersed water droplets in a flowing liquid. Here, the research focused on determining the efficiency of a centrifugal electric separator in removing water droplets in flowing organic phases, namely crown oil, crude oil blend and heptane.

5.1 EXPERIMENTAL SET-UP AND PROCEDURE

5.1.1 The electric separator

The novel centrifugal electric separator (approximately 1.5 L) was adapted from the one used by Eow and Ghadiri (2002a; 2002b). The separator combines centrifugal force with an electric field to separate the dispersed water droplets. Figure 5-1 depicts the separator used in this study. The design and development of this separator were based on theoretical and experimental studies carried out by Eow, Ghadiri and Sharif (2000), Eow, Ghadiri and Williams (2001), and Eow and Ghadiri (2002b; 2003a; 2003b), who showed that the fundamental mechanisms in this system are drop charging and drop-drop coalescence, followed by drop-interface coalescence. The separator consists of a brass cone that forms the positive-voltage electrode, and a brass strip and shaft, which form the negative-voltage electrode. The feed enters in a tangential way. The water droplets are charged and they exhibit different behaviour inside the separator, as illustrated in Figure 5-1. In region A, some of the droplets are charged by contact with the positive-voltage brass cone, while others are polarised, and it is probable that drop-drop coalescence may occur in this region. In region B, the electric field is higher than in region A. Drop break-up may occur in this section and the coalescence of the fine droplets may be enhanced. In region B the droplets may either be influenced by gravity or by the drag force of the continuous liquid. In region C, the

Chapter 5: Determination of the Efficiency of an Electric Separator

droplets are large enough, thus gravity pulls them downward. Drop-drop coalescence and drop-interface coalescence occurs in this region. In region D the droplets are carried out by the continuous liquid. As one moves upward from this region the electric field increases, thus drop charge, drop-drop coalescence and drop break-up may occur. In region E, the droplets may be much bigger than the droplets entering at the bottom of the cone, and these droplets then escape from the separator.

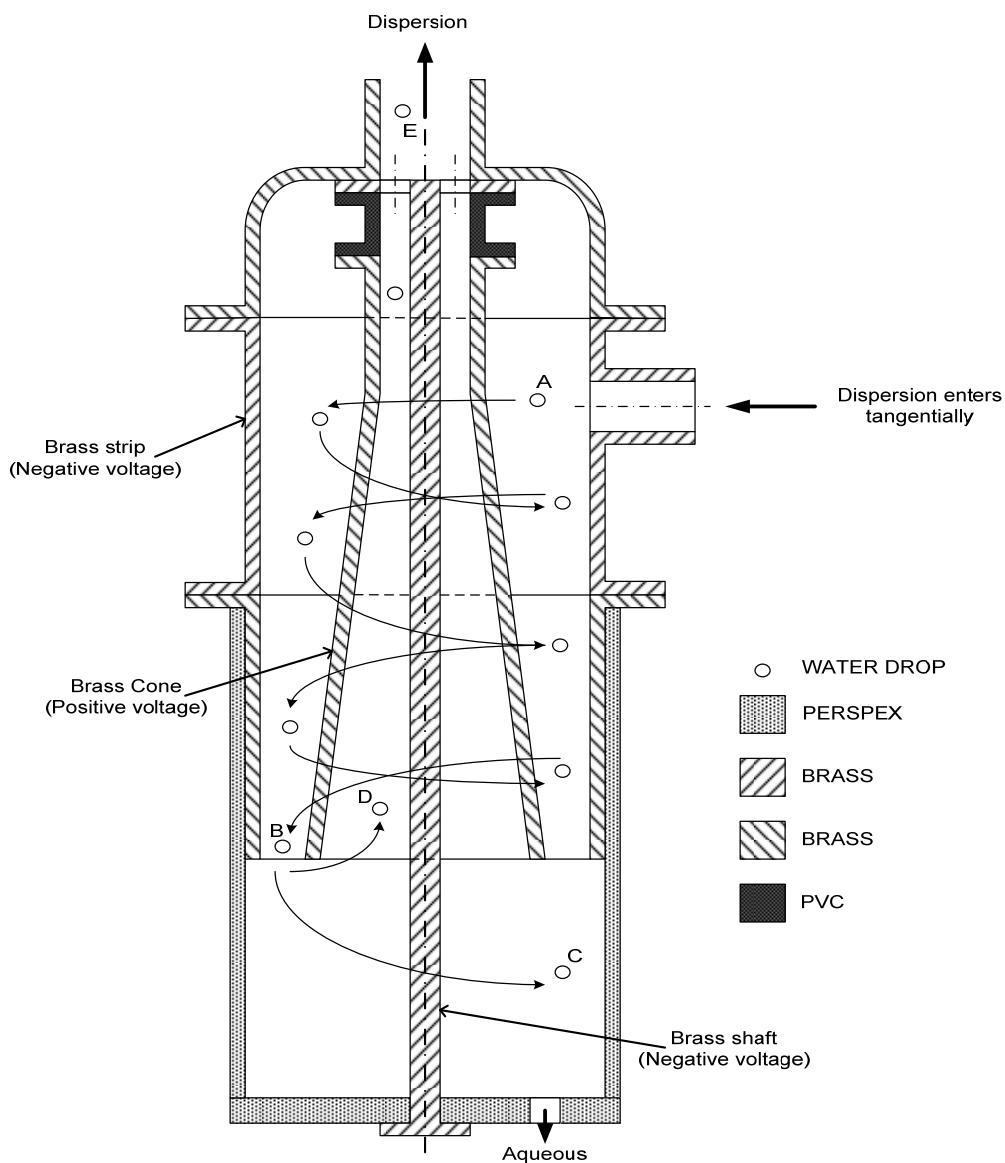


Figure 5-1: Sectional drawing of the separator and flow pattern

5.1.2 The separating plant and operation

A plant was designed in order to determine the efficiency of the separator in removing the water droplets. The plant consisted of a mixing tank (made of clear Perspex); a heating tank (made of clear Perspex) incorporating a Kwikheat Spiral element and a Kwiktherm Thermostat (both from Kwikot); a centrifugal electric separator; a d.c. power supply (Agilent 6634B); a mixer RW 16 basic (IKA-WERKE); and a diaphragm pump (Versamatic Tool Inc.). Silicone pipes of 10 mm ID were used. Four ball valves (1, 2, 3 and 4) and a needle valve (5) were used. See Figure 5-2 for further information on the plant layout and the components. For the high-temperature experiments, a heating element similar to the one used in the heating tank, was incorporated into the mixing tank. See Appendix D for more illustrations of the equipment used.

For this research, heptane (99%, Fluka), vegetable oil (Crown) and crude oil blend (blend of seven crude oils from different sources) were used as the continuous phases. Tap water was used as the dispersed phase for the heptane experiments, whereas distilled water was used in the vegetable oil and the crude oil experiments to avoid the formation of complex soap. After one experiment with the crude oil, the equipment and pipes were flushed with heptane and cleaned thoroughly to avoid contamination. The viscosity of the vegetable oil and crude-oil blends was measured with a Rheoplus rheometer. The viscosity of the heptane was obtained from the supplier. The specific gravities of the vegetable oil and crude oil blends were measured with a hydrometer. The specific gravity of the heptane was obtained from the supplier. The properties of the water were obtained from the literature. The surface tension and the dielectric properties of the liquid used were also obtained from the literature. All the physical properties are referenced adequately. The diaphragm pump was attached, with a monometer, a ball valve and a needle valve. The ball valve was positioned before the needle valve; the needle valve was set to open to a fixed position and the ball valve was fully opened. The pump was calibrated with water, set to deliver 6.32 L/min. This was maintained by controlling the pressure using the manometer. The average velocity of the fluid was 1.34 m/s. The flow rate was kept constant throughout this study.

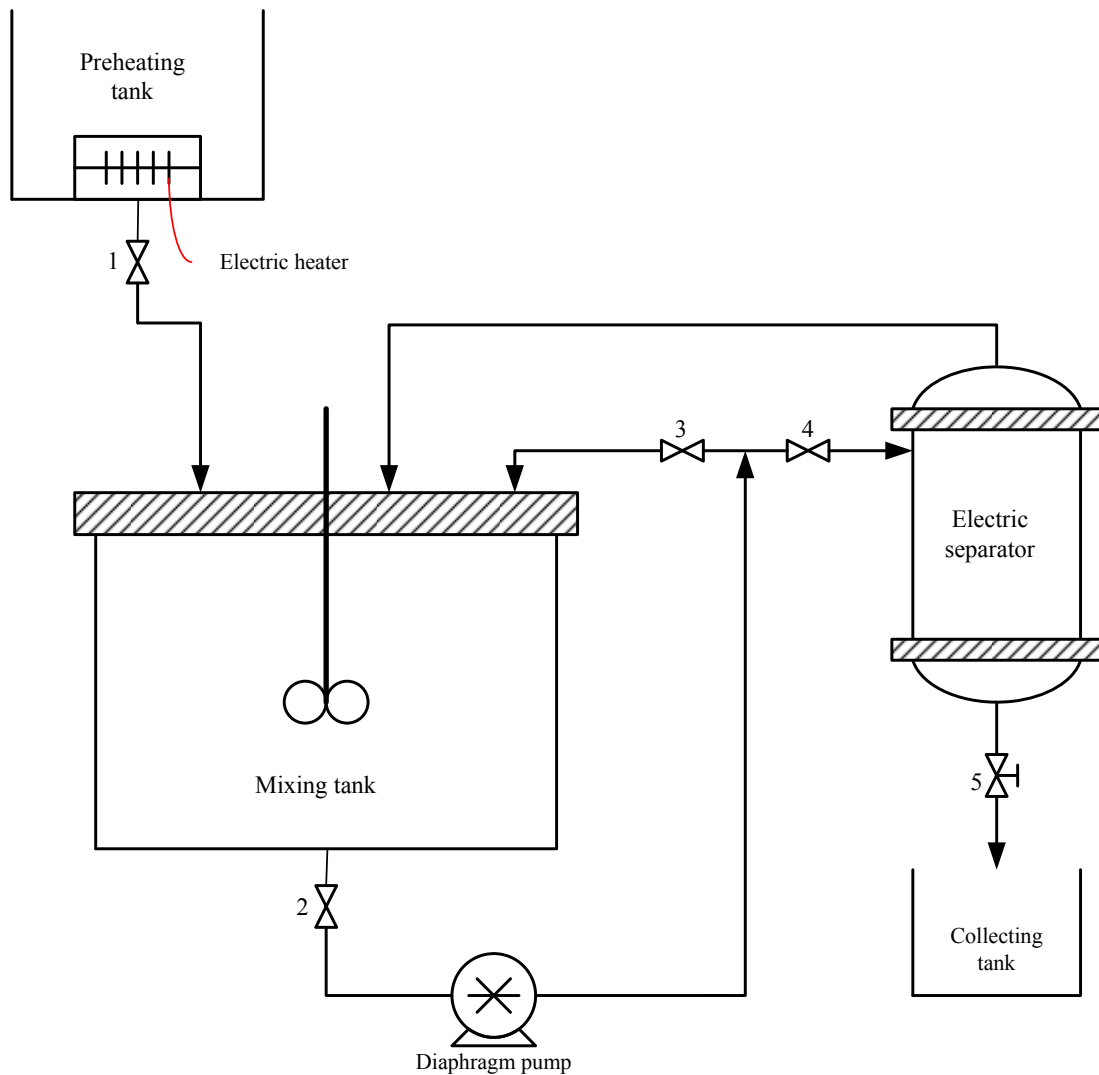


Figure 5-2: Process flow diagram

5.1.3 Physical properties of the liquid used

The physical properties of the liquids used in this experiment are tabulated in Table 5-1. Where specific gravity is represented by SG, dielectric constant is represented by ϵ , surface tension is represented by γ and viscosity by μ . It is apparent that the densities of crude oil and vegetable oil are very close to that of water, but their viscosities are higher than that of water, which poses a challenge when using gravity separation. Although the density of heptane is quite low compared with that of water, it was used to carry out a preliminary assessment of the separator efficiency in removing water droplets from a flowing organic phase. Furthermore, water has a high dielectric

constant compared to vegetable oil, crude oil and heptane, which enables the use of electric separation.

Table 5-1: Physical properties of the liquids used

Components	SG	ϵ	γ [mN/m]	μ [mPa.s]
Crude oil blend	0.908 ^{20°C}	*2.10 ^{20°C}	**34.37 ^{70°C}	65.43 ^{70°C}
Vegetable oil	0.925 ^{20°C}	*3.96 ^{38°C}	34.00	44 ^{25°C} , 13.6 ^{70°C}
Heptane	0.684 ^{20°C}	*1.90 ^{20°C}	20.14 ^{20°C}	0.386
Water	1.000	*80.00 ^{20°C}	72.80 ^{20°C}	1 ^{20°C}

*Values obtained from: <http://www.orioninstruments.com/html/tools/dielectric.aspx>

** (Abdul-Majeed & Al-Soof 2000)

Electric separation exploits the difference in electrical conductivity or dielectric properties of a liquid in which the more dielectric liquid will be charged or polarised; in the case of water droplets dispersed in an oil phase, the electric field will enhance the contact between the droplets, thus enhancing their coalescence.

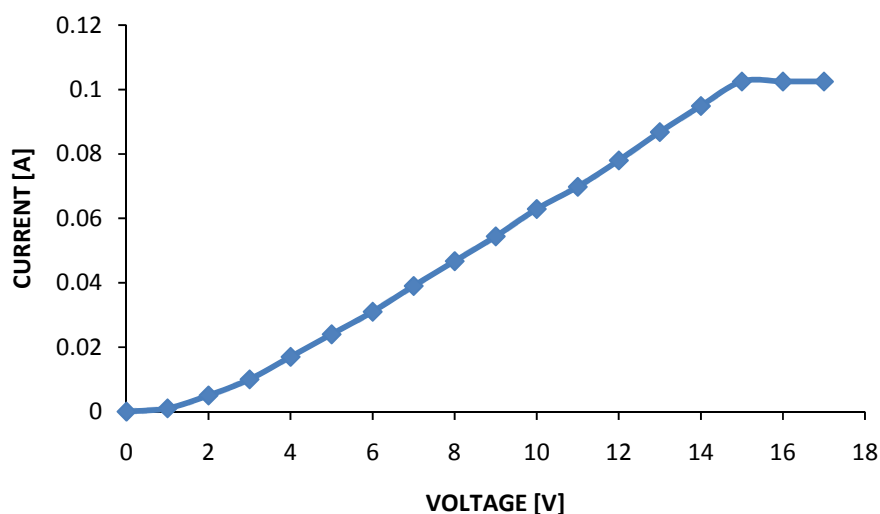


Figure 5-3: Graph of current vs. voltage for the tap water

The electrical conductivity of the fluids was confirmed by pumping the pure liquids into the separator, increasing the voltage, and then measuring the current. The organic samples did not conduct electricity but the water phase conducted electricity easily. (See Figure 5-3 for an illustration of the current vs. voltage of the tap water). The conductivity difference gave a good insight for proceeding with the research.

5.1.4 Experiments with heptane

The experiments with heptane were performed at room temperature. The volume percentage of water in the continuous phase (water-cut) was set to 5, 2.5, 1.25 and 0.625%, and for each water-cut, the voltages applied to the separator were as follows: 0, 10, 20, 40, 80 and 100 V. Tap water was added to the continuous phase (heptane). It was dispersed for approximately 4 minutes at a mixing speed of 942 rpm and then the mixer was switched off. The mixture was then pumped to the separator over a period of approximately 4 minutes. The needle valve at the bottom of the separator was adjusted to collect the volume of water separated during this period; the valve was slightly opened when the layer of water was seen. The efficiency of the separator was determined as follows:

$$\eta = \frac{[V_{H_2O}]_f}{[V_{H_2O}]_i} \times 100\% \quad (5.01)$$

where the subscripts f and i stand for the final and initial volumes of water, respectively. The experiments with vegetable oil and crude oil were performed differently to the experiment with heptane.

5.1.5 Experiments with vegetable oil at room temperature

Before proceeding with the experiments with the vegetable oil and crude oil samples, the flow rate at different percentages of the needle valve opening at the bottom of the separator was measured. The measurement was done using tap water; the tap water was pumped and the valve was turned through 360° from its initial position. The outlet flow rate measured is shown in Figure 5-4. This was done in order to eliminate error caused by opening the valve differently in each of the subsequent runs. As can be seen in Figure 5-4, the valve was opened at different percentages (the percentages were taken with reference to 360°) in this study approximately 29% opening was used for the experiments with vegetable oil and crude oil.

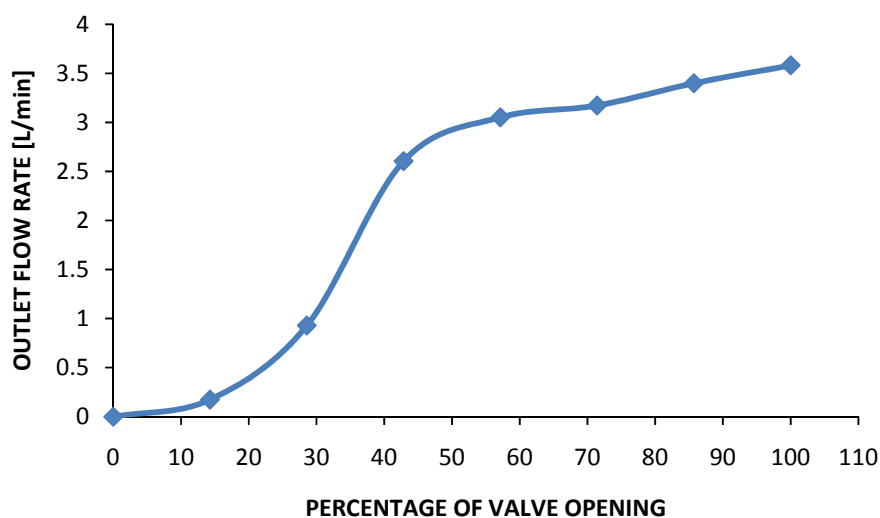


Figure 5-4: Outlet flow rate at different percentages of the needle valve opening in separator

In the experiments at room temperature, the vegetable oil samples were mixed with the distilled water at 298 rpm for a period of 1 minute, and the mixture was pumped into the separator. The needle valve at the bottom of the separator was opened after 1 minute of the steady state. The steady state was commenced when the fluid reached the recycle line. In this experiment, 20% and 35% water-cut were used, and for each water-cut the voltage was varied from 0, 20, 60 and 100 V. Here the water-cut values were higher than that used for the heptane experiments; this was to avoid very stable emulsions. The valve was opened with 2-turn and the liquid was allowed to flow until it had reached the initial volume of the water added. The collected liquid was then allowed to settle under gravity at room temperature for a period of 1 hour, after which the volume of water separated was measured. The efficiency was taken as the volume of water separated with reference to the initial volume.

5.1.6 Experiments at higher temperature

The crude oil blends could not be used in the experiments at room temperature as a result of the wax appearance temperature. The crude oil blend experiments were run with 20% water-cut. The experiment with vegetable oil was also done at a temperature of $\pm 70^{\circ}\text{C}$, as were the experiments with the crude oil blends. Here the mixing of the liquids was done by circulating the liquid for a period of approximately 1 minute (valves 2 and 3 open, and valve 4 closed: see Figure 5-2). Then valve 3 was closed and valve 4 was fully opened, to enable the fluid to flow into the

separator. The same procedure was then followed as in the experiment carried out with vegetable oil at room temperature.

In the experiment with the vegetable oil, two layers were seen after 1 hour: the oil phase at the top and a whitish liquid at the bottom. In order to confirm that this whitish liquid was water, the specific gravity was measured (see Figure 5-5 for an illustration). The specific gravity of the top layer was 0.925 (the same as measured for the vegetable oil) and that of the bottom layer was close to 1 (approximately that of water).

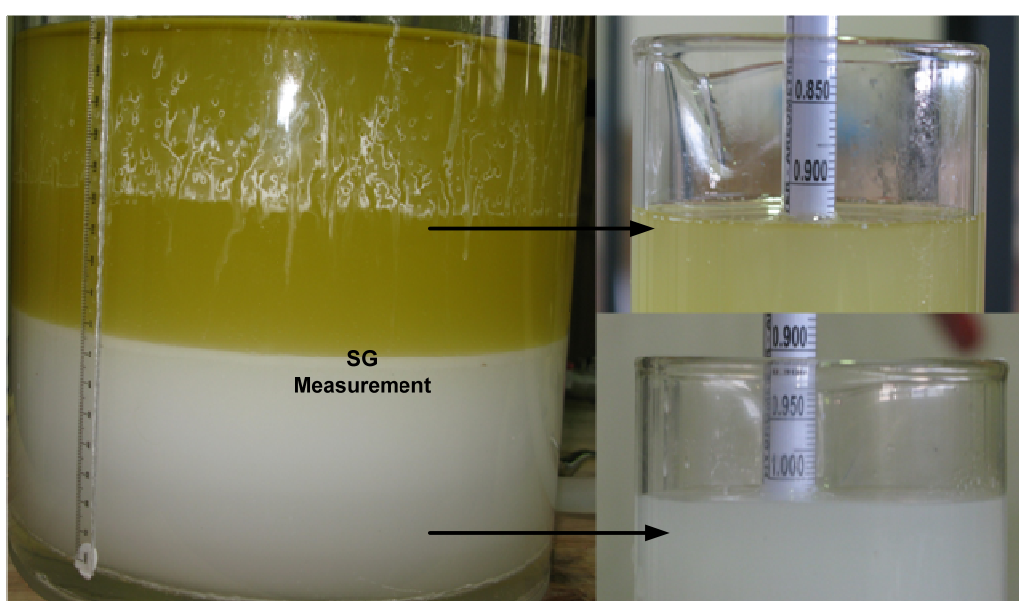


Figure 5-5: Specific gravity determination of the two layers in the vegetable oil experiments

5.2 RESULTS AND DISCUSSION

5.2.1 Experiments with heptane

The results of the heptane experiments showed that the efficiency of the separator increased with increasing water-cut when a water-cut of 0.732, 1.25 and 2.5% was used, as illustrated in Figure 5-6 (see Appendix A for the data). However, from 0 to 40 V the efficiency of the separator decreased when the water-cut was increased from 2.5 to 5%. The reason for this was that the

time at which the liquid was collected from the 5% run was not long enough to remove the dispersed water droplets, which then resulted in a decrease in the separator efficiency. On the other hand, on further increasing the voltage from 40 to 100 V the efficiency of the separator increased with increasing voltage for all the water-cut values tested, as seen in Figure 5-6.

The effect of the voltage on the separator efficiency was also investigated. When the separator was operated with a 0.732% water-cut, the efficiency increased from 46 to 58% when the voltage was increased from 0 to 10 V, and decreased to 38% when the voltage was increased from 10 to 100 V (Figure 5-6).

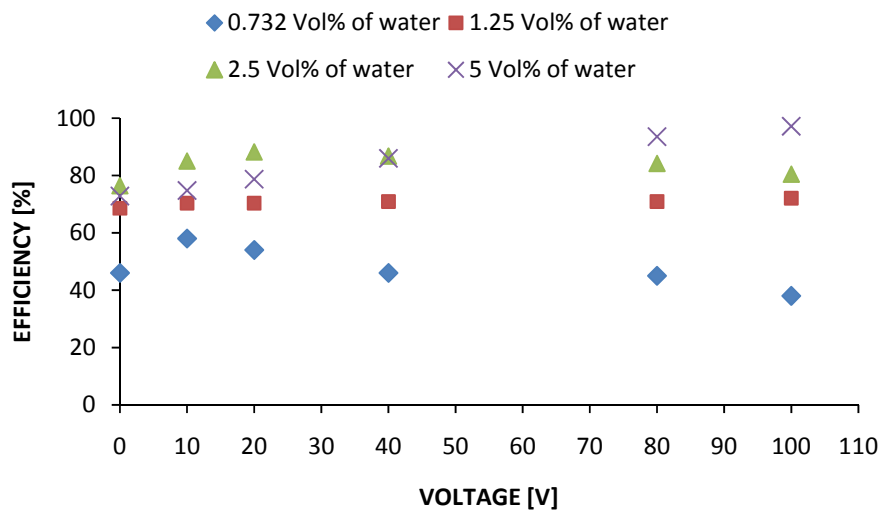


Figure 5-6: Performance of the separator in removing tap water from heptane at room temperature

A similar result was observed when the separator was operated with a 2.5% water-cut: the efficiency increased from 76 to 88% when the voltage was increased from 0 to 20 V, and then decreased to 80% when the voltage was increased from 20 to 100 V (Figure 5-6). The decrease in the efficiency might have resulted from droplet break-up, which would decrease the droplet size. The smaller the size of the droplet, the greater the tendency for droplets to be removed by the continuous phase, which acts on the droplets by its drag force, and thus the amount of water droplets at the bottom of the separator decreased. This phenomenon was also observed by Eow and Ghadiri (2002a; 2002b; 2003a; 2003b) when using d.c. and pulsed d.c. electric fields. The voltage did not show a significant improvement when the separator was operated with a 1.25%

water-cut as the efficiency increased only slightly, from 69 to 72%, when the voltage was increased from 0 to 100 V, and eventually no droplet break-up occurred. A significant improvement in the efficiency from 73 to 97% was observed when the separator was operated with a 5% water-cut.

5.2.2 Experiments with vegetable oil

The research was then expanded to vegetable oil, where the effect of changing a less viscous continuous phase to a more viscous one was determined. The vegetable oil is heavier than heptane and its specific gravity is close to that of water. Vegetable oil contains free fatty acids, which may also be considered as surfactants. Preliminary experiments with vegetable oil showed that two layers were obtained: the top layer was the vegetable oil and the bottom layer was a whitish liquid (later confirmed to be water). The whitish liquid seemed to be contaminated with surfactants. The efficiency of the separator in removing distilled water droplets from flowing crown oil at room temperature and $\pm 70^{\circ}\text{C}$ is illustrated in Figure 5-7 (see Appendix A for the data).

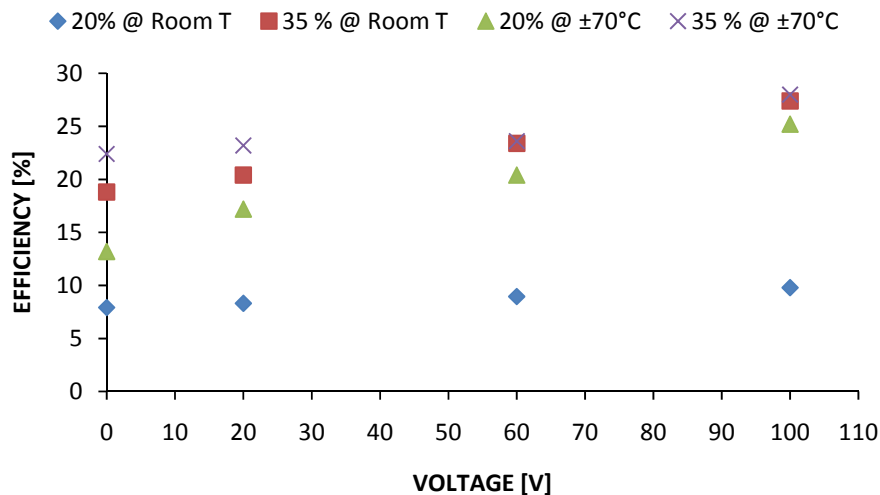


Figure 5-7: Performance of the separator in removing distilled water from vegetable oil at room temperature

The separation efficiency increased with an increased water-cut under all test conditions. The temperature effect was also investigated. The temperature had a significant effect on the

efficiency when the separator was operated at 20%, but when it was operated at 30% water-cut there was a slight increase in the efficiency, as illustrated in Figure 5-7. The increase in temperature resulted in a decrease in the viscosity of the vegetable oil, which then increased the settling velocity. It also increased the contact between the water droplets. The increase in the settling velocity and the contact of the water droplets enhanced the efficiency of the separator. The influence of the voltage was also investigated. An increase in voltage enhanced the separation efficiency in all the experiments performed, as illustrated in Figure 5-7.

5.2.3 Influence of the crude oil blend on the efficiency

The final part of this research involved testing the separator with a crude oil blend. The experiment was performed with distilled water at 20% water-cut at $\pm 70^{\circ}\text{C}$. The experiment was run at a temperature higher than 60°C to avoid the appearance of wax. The results from this experiment were compared to the one from the crown oil experiments at 20% water-cut (carried out at room and $\pm 70^{\circ}\text{C}$) (see Figure 5-8). The separation efficiency of the separator with the blend increased with increasing voltage. The maximum efficiency of the separator with the blend was approximately 5% lower compared to the efficiency achieved with vegetable oil. Crude oil is indeed more viscous than crown oil and has more surfactant molecules, which influenced the efficiency. See Appendix A for the data.

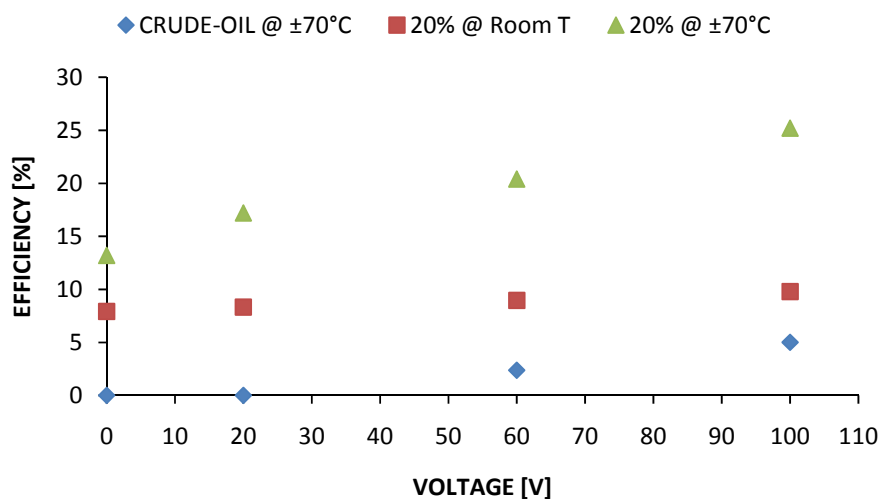


Figure 5-8: The efficiency of the separator with crude oil and vegetable oil at 20% water-cut

6 CONCLUSIONS

An investigation of water-in-oil emulsion stability and separation was undertaken in this thesis. The stabilisation/destabilisation of water-in-crude-oil emulsions is a complex field that has great implications for petroleum processing. In spite of the huge economical and environmental consequences caused by the failure to properly resolve such emulsions, the mechanisms and factors controlling the process are still far from fully understood. Here the ability of different crude oil and crude oil blends to create emulsions has been studied by gravity settling, critical electric field and centrifuge test methods. The results from these tests showed that the parameters such as asphaltenes, resins, wax, TAN, viscosity and density do not correlate with the emulsion stability created by different crude oil samples. It is believed that the structure of the naphthenic acids and/or other surfactants plays a significant role in the emulsion stability.

An investigation of the role of different organic acids in emulsion stability was carried out. The partitioning coefficient is a parameter that can be used to determine the solubility of an acid in one of the phases. The partitioning coefficients decreased with increasing molecular weight when acids with a straight-chain hydrocarbon moiety were used. However, the structures of the acids influenced the partitioning coefficient to some extent; for acids with similar molecular weight the presence of a benzene ring increased the partitioning coefficient. It was also seen that acids with rings created an intermediate layer when the organic phase samples were mixed with brine at a higher pH. This can be used to estimate the formation of ultra stable emulsion created when the pH of reservoir water increases during the extraction of crude oil. It is believed that the naphthenic acids that cause stable emulsions in the petroleum industries have high molecular weights and that they have rings attached to their polar group. To take this study further, high molecular acids with and without rings should be tested at different levels of brine pH. Another impact that should be considered is the concentration of the ionic strength in the brine solution, that is, different ionic solutions should be tested in the creation of a stable emulsion. Thermodynamic properties such as temperature and pressure should also be considered.

Chapter 5: Conclusions

Emulsion remains a complex issue to deal with. The development of more techniques to characterize the structure of the components in crude oil is needed.

Another aspect that is needed in petroleum extraction is the removal of the fine water droplets from crude oil. Here a novel electric separator using a d.c. electric field was used to enhance the coalescence of the fine droplets dispersed in a flowing organic liquid. This separator removes water droplets from a flowing organic liquid. The use of a d.c. electric field enhanced the removal of water droplets in a flowing organic liquid. However, droplet break-up with a high electric field decreases the separation efficiency. The separator can easily be installed into existing process lines and does not require much space. Its use may save time in the removal of water drops in offshore and related industries. However, further improvements in the design of this separator are needed. More experiments should be performed at voltages higher than 100 V, and the effect of different electric fields should be investigated, and compared.

7 REFERENCES

- Abdul-Majeed, G.H. & Al-Soof, N.B.A. 2000, 'Estimation of gas-oil surface tension', *Journal of Petroleum Science and Engineering*, vol. 27, pp. 197-200.
- Acevedo, S., Escobar, G., Ranaudo, M.A., Khazen, J. & Borges, B. 1999, 'Isolation and characterization of low and high molecular weight acidic compounds from Cerro Negro extraheavy crude oil: role of these acids in the interfacial properties of the crude oil emulsions', *Energy and Fuel*, vol. 13, pp. 333-335.
- Ali, M.F., Bukhari, A. & Hasan, M.U. 1989, 'Structural characterization of Arabian heavy crude oil residue', *Fuel Science and Technology International*, vol. 7, no. 8, pp. 1179-1208.
- Aske, N., Kallevik, H. & Sjöblom, J. 2002, 'Water-in-crude oil emulsion stability studied by critical electric field measurements. Correlation to physico-chemical parameters and near-infrared spectroscopy', *Journal of Petroleum Science and Engineering*, vol. 36, pp. 1-17.
- Babaian-Kibala, E., Craig, H.L., Rusk, G.L., Blanchard, K.V. Rose, T.J., Uehlein, B.L., Quinter, R.C. & Summers, M.A. 1993, 'Naphthenic acid corrosion in refinery settings', *Material Performance*, vol. 32, no. 4, pp. 50-55.
- Bailes, P.J. 1996, *Resolution of emulsions*, US Patent 5580464.
- Bailes, P.J., Freestone, D. & Sams G.W. 1997, 'Pulsed d.c. fields for electrostatic coalescence of water-in-oil emulsions', *The Chem. Eng.*, vol. 644, pp. 34-39.
- Bancroft, W.D. 1913, 'Theory of emulsification', *Journal of Physical Chemistry*, vol. 17, pp. 501.
- Barbour, R.V. & Petersen, J.C. 1974, 'Molecular interactions of asphalt: an infrared study of the hydrogen-bonding basicity of asphalt', *Analytical Chemistry*, vol. 46, no. 2, pp. 273-277.

References

- Behar, F.H. & Albrecht, P. 1984, 'Correlation between carboxylic acids and hydrocarbons in several crude oils alteration by biodegradation', *Organic Geochemistry*, vol. 6, pp. 597.
- Bland, W.F. & Davidson, R.L. 1967, *Petroleum processing handbook*, McGraw-Hill, USA.
- Boduszynski, M.M., McKay, J.F. & Latham, D.R. 1980, 'Asphaltenes, where are you?', *Proceedings of the Association of Asphalt Paving Technologists*, pp. 123-143.
- Brandal, O. 2005, 'Interfacial (o/w) properties of naphthenic acids and metal naphthenates, naphthenic acid characterization and metal naphthenate inhibition', Doctor of Engineering dissertation, Norwegian University of Science and technology, Trondheim.
- Brault, M., Marty, J.C. & Sahot, A. 1984, 'Fatty acids from particulate matter and sediment in hydrothermal environments from the East Pacific Rise, near 13 degree N', *Organic Geochemistry*, vol. 6, pp. 217.
- Cranwell, P.A. 1984, 'Alkyl esters, mid chain ketones and fatty acids in late glacial and postglacial lacustrine sediments', *Organic Geochemistry*, vol. 6, pp. 115.
- Crowley, J.M. 1999, *Fundamentals of applied electrostatics*, Laplacian Press, California, USA.
- Edmondson, J.M. 1998, *Method and apparatus of oil/water demulsification*, US Patent 5714048.
- Eow, J.S., Ghadiri, M. & Sharif, A.O. 2000, 'The separation of particles/drops in a flowing viscous liquid by electrostatic and hydrodynamic effects', *Proceedings of the First Asian Particle Technology Symposium*, Bangkok, pp. 13-15.
- Eow, J.S., Ghadiri, M. & Williams, T.J. 2001, 'Electrostatic enhancement of the coalescence of water droplets in oil: a review of the current understanding', *Chemical Engineering Journal*, vol. 84, no. 3, pp. 173-192.
- Eow, J.S. & Ghadiri, M. 2002a, 'Electrocoalesce-separators for the separation of aqueous drops from a flowing dielectric viscous liquid', *Separation and Purification Technology*, vol. 29, pp. 63-77.

References

- Eow, J.S. & Ghadiri, M. 2002b, 'Electrostatic enhancement of coalescence of water droplets in oil: a review of the technology', *Chemical Engineering Journal*, vol. 85, pp. 375-368.
- Eow, J.S. & Ghadiri, M. 2002c, 'Electrostatic and hydrodynamic separation of aqueous drops in flowing viscous oil', *Chemical Engineering and Processing*, vol. 41, pp. 649-657.
- Eow, J.S. & Ghadiri, M. 2003a, 'Drop-drop coalescence in an electric field: the effects of applied electric field and electrode geometry', *Colloids and Surfaces A*, vol. 219, pp. 253-279.
- Eow, J.S. & Ghadiri, M. 2003b, 'Motion, deformation and break-up of aqueous drops in oils under high electric field strengths', *Chemical Engineering and Processing*, vol. 42, pp. 259-272.
- Ese, M-H. & Kilpatrick, P.K. 2004, 'Stabilization of water-in-oil emulsions by naphthenic acids and their salts: model compounds, role of pH, and soap:acid ratio', *Journal of Dispersion Science and Technology*, vol. 25, pp. 253-261.
- Fan, T.P. 1991, 'Characterization of naphthenic acids in petroleum by fast atomic bombardment mass spectrometer', *Energy and Fuel*, vol. 5, pp. 371-375.
- Gafonova, O.V. & Yarranton, H.W. 2001, 'The stabilization of water-in-hydrocarbon emulsions by asphaltenes and resins', *Journal of Colloid and Interface Science*, vol. 241, no. 2, pp. 469-478.
- Harris, F.W. 1918, *Process and apparatus for dehydrating emulsions*, US Patent 1281952.
- Havre, T.E. 2002, 'Formation of calcium naphthenate in water/oil system, naphthenic acid chemistry and emulsion stability', Doctor of Engineering dissertation, Norwegian University of Science and Technology, Trondheim.
- Hobson, G.D. 1973, *Modern petroleum technology*, 4th edition, Applied Science and the Institute of Petroleum, UK.
- Hsu, C.S., Dechert, G.J. Robbins, W.K. & Fukuda, E.K. 2000, 'Naphthenic acids in crude oils characterization by mass spectrometer', *Energy and Fuel*, vol. 14, pp. 217-223.

References

- Hurtevent, C., Rousseau, G. & Zhou, H.G. 2001, 'Calcium carbonate and naphthenate mixed scale in deep-offshore fields', *Paper presented at the Third International Symposium on Oilfield Scale*, SPE 63307
- Hurtevent, C., Rousseau, G., Bourrel, M. & Bracart, B. 2006, 'Production issues of acidic petroleum crude oils', In J. Sjöblom (ed.), *Emulsions and emulsion stability*, 2nd edition, , Surfactant Science Series vol. 132.CRC Press, USA.
- Ignasiak, T., Strausz, O.P. & Montgomery, D.S. 1977, 'Oxygen distribution and hydrogen bonding in Athabasca asphaltene', *Fuel*, vol. 56, pp. 359-365.
- Jones, D.M., Watson, J.S., Meredith, W., Chen, M. & Bennett, B. 2001, 'Determination of naphthenic acids in crude oils using nonaqueous ion exchange solid-phase extraction', *Analytical Chemistry*, vol. 73, pp. 703-707.
- Koik, L., Reboucas, L. Marsaioli, A. Richnow, H. & Michaelis, W. 1992, 'Naphthenic acids from crude oils of Campo Basin', *Organic Geochemistry*, vol. 18, no. 6, pp. 851-860.
- Langevin, D., Poteau, S. Henaut, I. & Argillier, J.F. 2004, 'Crude oil emulsion properties and their application to heavy oil transportation', *Oil & Gas Science and Technology*, vol. 59, pp. 511-521.
- Lawrence, A.S.C. & Killner, W. 1948, 'Emulsions of seawater in Admiralty fuel oil with special reference to their demulsification', *Journal of the Institute of Petroleum*, vol. 34, pp. 281.
- Lissant, K.J. 1993, *Demulsification*, in Surfactant Science Series 13, Marcel Dekker, New York.
- McKibben, C.W. 1919, *Method of separating associated liquids*, US Patent 1299589.
- McLean, J.D. & Kilpatrick, P.K. 1997a, 'Effects of asphaltene aggregation in model heptane-toluene mixtures on stability of water-in-oil emulsions', *Journal of Colloid and Interface Science*, vol. 196, no. 1, pp. 23-34.
- McLean, J.D. & Kilpatrick, P.K. 1997b, 'Effects of asphaltene solvency on stability of water-in-crude oil emulsions', *Journal of Colloid and Interface Science*, vol. 189, pp. 242-253.

References

- Miller, A.M. & Neogi, P. 2008, *Interfacial phenomena: equilibrium and dynamic effects*, 2nd edition., vol. 139, CRC Press Taylor & Francis Group, New York.
- Miller, R. 1982, 'Hydrocarbon class fractionation with bonded-phase liquid chromatography', *Analytical Chemistry*, vol. 54, no. 11, pp. 1742-1746.
- Mitchell, D.L. & Speight, J.G. 1973, 'The solubility of asphaltenes in hydrocarbon solvents', *Fuel*, vol. 52, no. 4, pp. 149-152.
- Montgomery, D.C. 2005, *Design and analysis of experiments*, 6th edition, John Wiley & Sons, USA.
- Moschopedis, S.E. & Speight, J.G. 1976, 'Investigation of hydrogen bonding by oxygen functions in Athabasca bitumen', *Fuel*, vol. 55, pp. 187-192.
- Reynolds, J.G. 1987, 'Characterization of heavy residua by application of a modified D 2007 and asphaltene separation: effect of solvents on physical and chemical properties of fractions derived from Hondo 850F residuum', *Fuel Science and Technology International*, vol. 5, no. 5, pp. 593-620.
- Robbins, W.K. 1998, 'Challenges in the characterization of naphthenic acids in petroleum', *American Chemical Society Petroleum Chemistry Division Pre-print*, vol. 43, no. 1, pp. 137-140.
- Schramm, L.L. 1992, *Emulsions, fundamentals and applications in the petroleum industry*, Advances in Chemistry Series., Washington D.C.
- Sjöblom, J., Øye, G., Glomm, W.R., Hannisdal, A., Knag, M., Brandal, Ø., Ese, M-H., Hemmingsen, P.V., Havre, T.E., Oschmann, H-J. & Kallevik, H. 2006, 'Modern characterization techniques for crude oils, their emulsions, and functionalized surfaces', In J. Sjöblom (ed.) *Emulsions and emulsion stability*, 2nd edition, Surfactant Science Series vol. 132, CRC Press, New York.

References

- Spiecker, P.M. 2001, 'The impact of asphaltene chemistry and solvation on emulsion and interfacial film formation', PhD dissertation, North Carolina State University, North Carolina.
- Spiecker, P.M., Gawrys, K.L., Trail, C.B. & Kilpatrick, P.K. 2003, 'Effects of petroleum resins on asphaltene aggregation and water-in-oil emulsion formation', *Colloids and Surfaces A-Physicochemical and Engineering Aspects*, vol. 220, pp. 9-27.
- St. John., W.P., Rughani, J., Green, S.A. & McGinnis G.D. 1998, 'Analysis and characterization of naphthenic acids by gas chromatography-electron impact mass spectrometry of tert-butyltrimethylsilyl derivatives', *Journal of Chromatography A*, vol. 807, pp. 241-251.
- Sun, D., Duan, X. Li, W. & Zhou, D. 1998, 'Demulsification of water-in-oil emulsion by using glass membrane', *Journal of Membrane Science*, vol. 146, pp. 65-72.
- Taylor, S.E. 1996, 'Theory and practice of electrically-enhanced phase separation of water-in-oil emulsion', *Trans. IChemE A*, vol. 74, pp. 526-540.
- Thompson, D.G., Taylor, A.S. & Graham, D.E. 1985, 'Emulsification and demulsification related to crude oil production', *Colloid Surface*, vol. 15, pp. 175-189.
- Tsouris, C., Shin, W.T. & Yiacoymi, S. 1998, 'Pumping, spraying, and mixing of fluids by electric fields', *Canadian Journal of Chemical Engineering*, vol. 76, pp. 589-599.
- Urdahl, O., Wayth, N.J., Fordedal, H. Williams, T.J. & Bailey A.G. 2001, 'compact electrostatic coalescer technology', In , J. Sjöblom (ed.), *Encyclopedic handbook of emulsion technology*, Marcel Dekker, New York.
- Vindstad, J.E., Bye, A.S., Grande, K.V., Hustad, B.M., Hustvedt, E. & Nergard, B. 2003, 'Fighting naphthenate deposition at the Heidrum field', presented at 2003 Society of Petroleum Engineers, 5th International Symposium on Oilfield Scale in Aberdeen, SPE80375, UK.
- Waterman, L C. 1965, 'Electric coalescers', *Chemical Eng. Progr.*, vol. 61, no. 10, pp. 51-57.

References

Yen, T.F., Erdman, J.G. & Pollack. S.S. 1961, 'Investigation of structure of petroleum asphaltenes by X-ray diffraction', *Analytical Chemistry*, vol. 33, no. 11, pp. 1587-&.

8 NOMENCLATURE

A	Interfacial area	m^2
C_e	Equilibrium concentration	mol/L
C_0	Initial concentration of an acid	ppm
D_e	Diffusion coefficient	$mol.m^2/s$
D_N	Flux density	C/m^2
E_N, E_T, E_0, E_a, E_b	Electric field	V/m
g	Acceleration of gravity	m/s^2
K_1	Integration constant	V/m^2
K_2	Integration constant	V/m
k	Partitioning coefficient	
k_0	Boltzmann constant (1.380658×10^{-23})	J/K
m	Mass of the components	g
Q	Charge per unit area	C/m^2
R	Drop size	mm
r_0	Internal radius of a bubble	m
SG	Specific gravity	
T	Temperature	K
t	Time	s
U	Sedimentation velocity	m/s
V_A, V_B, V_a, V_b	Voltage	V
V_T, V	Volume of the mixture and volume for each component	mL
V_{H_2O}	Volume of water	mL
x	Distance between two points	m
γ	Surface tension	mN/m
$\varepsilon_1, \varepsilon_2, \varepsilon_a, \varepsilon_b$	Dielectric constant	
η	Separator efficiency	$\%$
θ	Phase angle	
μ	Viscosity	$Pa.s$
v	Molar volume	m^3/mol
ρ	Density of a component	g/cm^3
σ_a, σ_b	Ohmic conductivity	S/m

9 APPENDIX A: EXPERIMENTAL DATA

9.1 WATER-IN-CRUDE-OIL EMULSION STUDIES

9.1.1 Gravity test method

Table 9-1: Data of the experiments with sample A during the gravity test.

RUNS	FACTORS				AQUEOUS pH		RESPONSE	
	x_1	x_2	x_3	x_4	Before	After	V (mL)	% Water
1	-1	-1	-1	-1	4.04	3.74	29.00	72.50
2	1	-1	-1	1	4.04	3.48	57.00	57.00
3	-1	1	-1	1	8.12	3.83	25.00	62.50
4	1	1	-1	-1	8.12	5.63	100.00	100.00
5	-1	-1	1	1	4.04		0.00	0.00
6	1	-1	1	-1	4.04	3.77	19.00	19.00
7	-1	1	1	-1	8.12		11.00	27.50
8	1	1	1	1	8.12		5.00	5.00
9	-1	-1	-1	-1	4.04	3.75	26.00	65.00
10	1	-1	-1	1	4.04	3.60	74.00	74.00
11	-1	1	-1	1	8.12	3.87	25.00	62.50
12	1	1	-1	-1	8.12	5.93	100.00	100.00
13	-1	-1	1	1	4.04		0.00	0.00
14	1	-1	1	-1	4.04	3.84	16.00	16.00
15	-1	1	1	-1	8.12		13.00	32.50
16	1	1	1	1	8.12		8.00	8.00

Appendix A – Experimental Data

Table 9-2: Data of the experiments with sample M during the gravity test.

RUNS	FACTORS				AQUEOUS pH		RESPONSE	
	x_1	x_2	x_3	x_4	Before	After	V(mL)	% Water
1	-1	-1	-1	-1	4.06	4.87	26.00	65.00
2	1	-1	-1	1	4.06	4.38	31.25	31.25
3	-1	1	-1	1	8.12	5.00	16.00	40.00
4	1	1	-1	-1	8.12	5.14	94.00	94.00
5	-1	-1	1	1	4.06		0.00	0.00
6	1	-1	1	-1	4.04	4.09	98.00	98.00
7	-1	1	1	-1	8.12		7.00	17.50
8	1	1	1	1	8.12	4.94	87.50	87.50
9	-1	-1	-1	-1	4.06	4.70	30.00	75.00
10	1	-1	-1	1	4.06	4.21	28.00	28.00
11	-1	1	-1	1	8.12	5.14	16.00	40.00
12	1	1	-1	-1	8.12	5.31	91.00	91.00
13	-1	-1	1	1	4.06		0.00	0.00
14	1	-1	1	-1	4.06	4.04	98.00	98.00
15	-1	1	1	-1	8.12		6.00	15.00
16	1	1	1	1	8.12	4.86	86.00	86.00

Table 9-3: Data of the experiments with sample C during the gravity test.

RUNS	FACTORS				AQUEOUS pH		RESPONSE	
	x_1	x_2	x_3	x_4	Before	After	V (mL)	% Water
1	-1	-1	-1	-1	4.04	4.26	25.00	62.50
2	1	-1	-1	1	4.04	4.64	87.50	100.00
3	-1	1	-1	1	8.12	6.26	24.00	60.00
4	1	1	-1	-1	8.12	6.50	100.00	100.00
5	-1	-1	1	1	4.04		0.00	0.00
6	1	-1	1	-1	4.04	4.90	74.00	73.00
7	-1	1	1	-1	8.12	6.94	13.00	32.50
8	1	1	1	1	8.12	5.94	14.00	14.00
9	-1	-1	-1	-1	4.04	4.38	31.00	77.50
10	1	-1	-1	1	4.04	6.54	100.00	100.00
11	-1	1	-1	1	8.12	5.05	24.00	60.00
12	1	1	-1	-1	8.12	6.40	100.00	100.00
13	-1	-1	1	1	4.04		0.00	0.00
14	1	-1	1	-1	4.04	4.44	48.00	65.00
15	-1	1	1	-1	8.12	5.15	15.00	37.50
16	1	1	1	1	8.12	5.34	14.00	14.00

Appendix A – Experimental Data

Table 9-4: Data of the experiments with sample U during the gravity test.

RUNS	FACTORS				AQUEOUS pH		RESPONSE	
	x_1	x_2	x_3	x_4	Before	After	V (mL)	% Water
1	-1	-1	-1	-1	4.04	3.94	23.00	57.50
2	1	-1	-1	1	4.04		13.00	13.00
3	-1	1	-1	1	8.12		0.00	0.00
4	1	1	-1	-1	8.12	6.39	100.00	100.00
5	-1	-1	1	1	4.04		0.00	0.00
6	1	-1	1	-1	4.04	3.94	98.00	98.00
7	-1	1	1	-1	8.12		0.00	0.00
8	1	1	1	1	8.12		0.00	0.00
9	-1	-1	-1	-1	4.04	3.87	18.00	45.00
10	1	-1	-1	1	4.04		18.00	18.00
11	-1	1	-1	1	8.12		0.00	0.00
12	1	1	-1	-1	8.12	5.62	100.00	100.00
13	-1	-1	1	1	4.04		0.00	0.00
14	1	-1	1	-1	4.04	3.86	76.00	76.00
15	-1	1	1	-1	8.12		0.00	0.00
16	1	1	1	1	8.12		0.00	0.00

Table 9-5: Data of the experiments with sample V during the gravity test.

RUNS	FACTORS				AQUEOUS pH		RESPONSE	
	x_1	x_2	x_3	x_4	Before	After	V (mL)	% Water
1	-1	-1	-1	-1	4.04	4.28	28.00	70.00
2	1	-1	-1	1	4.04		0.00	0.00
3	-1	1	-1	1	8.12	4.80	14.00	35.00
4	1	1	-1	-1	8.12	5.42	62.50	62.50
5	-1	-1	1	1	4.04		0.00	0.00
6	1	-1	1	-1	4.04		0.00	0.00
7	-1	1	1	-1	8.12		0.00	0.00
8	1	1	1	1	8.12		12.50	12.50
9	-1	-1	-1	-1	4.04	4.59	30.00	75.00
10	1	-1	-1	1	4.04		0.00	0.00
11	-1	1	-1	1	8.12	4.78	14.00	35.00
12	1	1	-1	-1	8.12	5.44	62.50	62.50
13	-1	-1	1	1	4.04		0.00	0.00
14	1	-1	1	-1	4.04		0.00	0.00
15	-1	1	1	-1	8.12		0.00	0.00
16	1	1	1	1	8.12		12.50	12.50

Appendix A – Experimental Data

Table 9-6: Data of the experiments with sample P during the gravity test.

RUNS	FACTORS				AQUEOUS pH		RESPONSE	
	x_1	x_2	x_3	x_4	Before	After	V (mL)	% Water
1	-1	-1	-1	-1	4.04	4.58	25.00	62.50
2	1	-1	-1	1	4.04	4.51	55.00	55.00
3	-1	1	-1	1	8.12		10.00	25.00
4	1	1	-1	-1	8.12	5.74	100.00	100.00
5	-1	-1	1	1	4.04		0.00	0.00
6	1	-1	1	-1	4.04		6.00	6.00
7	-1	1	1	-1	8.12		14.00	35.00
8	1	1	1	1	8.12		0.00	0.00
9	-1	-1	-1	-1	4.04	4.60	25.00	62.50
10	1	-1	-1	1	4.04	4.57	50.00	50.00
11	-1	1	-1	1	8.12		12.00	30.00
12	1	1	-1	-1	8.12	5.79	100.00	100.00
13	-1	-1	1	1	4.04		0.00	0.00
14	1	-1	1	-1	4.04		6.00	6.00
15	-1	1	1	-1	8.12		15.00	37.50
16	1	1	1	1	8.12		0.00	0.00

Table 9-7: Data of the experiments with sample H during the gravity test.

RUNS	FACTORS				AQUEOUS pH		RESPONSE	
	x_1	x_2	x_3	x_4	Before	After	V (mL)	% Water
1	-1	-1	-1	-1	4.04	3.21	25.00	62.50
2	1	-1	-1	1	4.04	3.05	60.00	60.00
3	-1	1	-1	1	8.12	3.34	25.00	62.50
4	1	1	-1	-1	8.12	4.73	66.00	66.00
5	-1	-1	1	1	4.04		0.00	0.00
6	1	-1	1	-1	4.04		0.00	0.00
7	-1	1	1	-1	8.12	3.23	24.00	60.00
8	1	1	1	1	8.12		0.00	0.00
9	-1	-1	-1	-1	4.04	3.06	26	65.00
10	1	-1	-1	1	4.04	3.06	60	60.00
11	-1	1	-1	1	8.12	3.20	25.00	62.50
12	1	1	-1	-1	8.12	5.36	84.00	84.00
13	-1	-1	1	1	4.04		0.00	0.00
14	1	-1	1	-1	4.04		0.00	0.00
15	-1	1	1	-1	8.12	3.10	24.00	60.00
16	1	1	1	1	8.12		0.00	0.00

9.1.2 Critical-electric-field test method

Table 9-8: Data of the experiments with crude oil sample V during the CEF test.

Water cut (Vol.%)	Critical-Electric-Field (V/cm)				Average
	Trial 1		Trial 2		
	Sample 1	Sample 2	Sample 1	Sample 2	
20	47.0	50.0	51.0	52.0	50.00
35	42.0	43.0	40.0	41.0	41.50
50	36.0	35.0	37.0	36.0	36.00
60	33.0	35.0	30.0	32.0	32.50

Table 9-9: Data of the experiments with crude oil sample H during the CEF test.

Water cut (Vol.%)	Critical-Electric-Field (V/cm)				Average
	Trial 1		Trial 2		
	Sample 1	Sample 2	Sample 1	Sample 2	
20	13.0	11.0	13.0	10.0	11.75
35	10.0	11.0	09.0	10.0	10.00
50	08.0	07.0	07.0	09.0	07.75
60	05.0	06.0	04.0	05.0	05.00

Table 9-10: Data of the experiments with crude oil sample C during the CEF test.

Water cut (Vol.%)	Critical-Electric-Field (V/cm)				Average
	Trial 1		Trial 2		
	Sample 1	Sample 2	Sample 1	Sample 2	
20	10.0	09.0	11.0	08.0	09.50
35	09.0	07.0	08.0	09.0	08.25
50	07.0	06.0	05.0	06.0	06.00
60	04.0	03.0	05.0	04.0	04.00

Table 9-11: Data of the experiments with blend 1 during the CEF test.

Water cut (Vol.%)	Critical-Electric-Field (V/cm)				Average
	Trial 1		Trial 2		
	Sample 1	Sample 2	Sample 1	Sample 2	
20	40.00	38.00	41.00	42.00	40.25
35	37.00	38.00	35.00	36.00	36.50
50	30.00	28.00	31.00	32.00	30.25
60	24.00	23.00	21.00	22.00	22.50

Table 9-12: Data of the experiments with blend 2 during the CEF test.

Water cut (Vol.%)	Critical-Electric-Field (V/cm)				Average
	Trial 1		Trial 2		
	Sample 1	Sample 2	Sample 1	Sample 2	
20	85.00	82.00	81.00	83.00	82.75
35	75.00	74.00	72.00	76.00	74.25
50	61.00	64.00	63.00	61.00	62.25
60	49.00	50.00	52.00	53.00	51.00

9.1.3 Centrifuge test method

Table 9-13: Data of the centrifuge experiments with sample V.

Water cut (Vol.%)	Volume of water centrifuged (mL)				Average
	Trial 1		Trial 2		
	Sample 1	Sample 2	Sample 1	Sample 2	
20	1.30	1.30	1.60	1.70	1.48
35	1.80	1.70	2.10	2.00	1.90
50	2.70	2.50	2.80	2.90	2.73
60	3.10	3.20	3.10	3.20	3.15

Table 9-14: Data of the centrifuge experiments with sample H.

Water cut (Vol.%)	Volume of water centrifuged (mL)				Average
	Trial 1		Trial 2		
	Sample 1	Sample 2	Sample 1	Sample 2	
20	2.20	2.30	2.10	2.20	2.20
35	2.50	2.60	2.40	2.60	2.53
50	3.00	3.00	2.90	3.10	3.00
60	3.30	3.40	3.20	3.40	3.33

Table 9-15: Data of the centrifuge experiments with sample H.

Water cut (Vol.%)	Volume of water centrifuged (mL)				Average
	Trial 1		Trial 2		
	Sample 1	Sample 2	Sample 1	Sample 2	
20	2.30	2.80	2.40	2.60	2.53
35	3.60	3.40	3.70	3.50	3.55
50	4.30	4.40	4.40	4.50	4.40
60	6.10	6.60	6.20	6.40	6.33

Appendix A – Experimental Data

Table 9-16: Data of the centrifuge experiments with Blend 1.

Water cut (Vol.%)	Volume of water centrifuged (mL)				Average
	Trial 1		Trial 2		
	Sample 1	Sample 2	Sample 1	Sample 2	
20	1.30	1.20	1.40	1.30	1.30
35	1.50	1.50	1.60	1.70	1.58
50	3.00	2.70	2.80	3.00	2.88
60	3.10	3.50	3.20	3.40	3.30

Table 9-17: Data of the centrifuge experiments with Blend 2.

Water cut (Vol.%)	Volume of water centrifuged (mL)				Average
	Trial 1		Trial 2		
	Sample 1	Sample 2	Sample 1	Sample 2	
20	0.00	0.00	0.00	0.00	0.00
35	0.00	0.00	0.00	0.00	0.00
50	0.00	0.00	0.00	0.00	0.00
60	0.40	0.30	0.20	0.30	0.30

9.2 ROLE OF ORGANIC ACID IN EMULSION STABILITY

9.2.1 Standard graphs for calibration

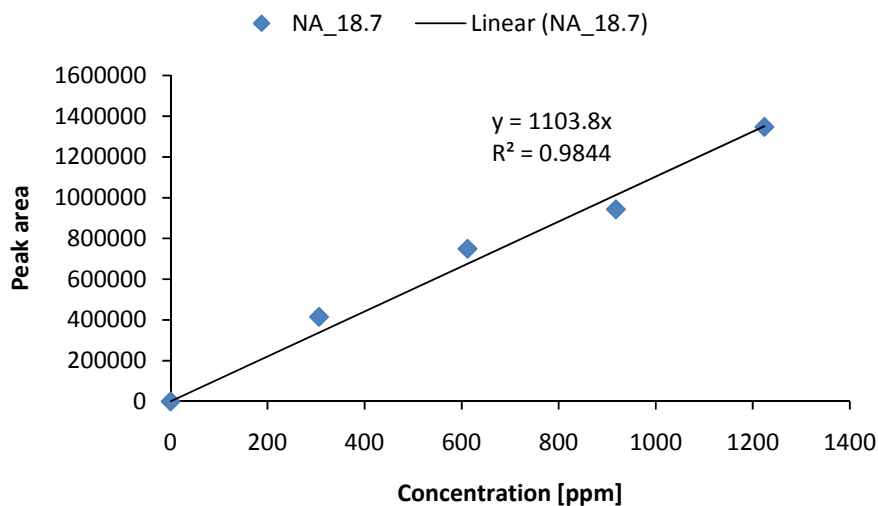


Figure 9-1: Graph of peak area vs. concentration, used for NA_18.7.

Appendix A – Experimental Data

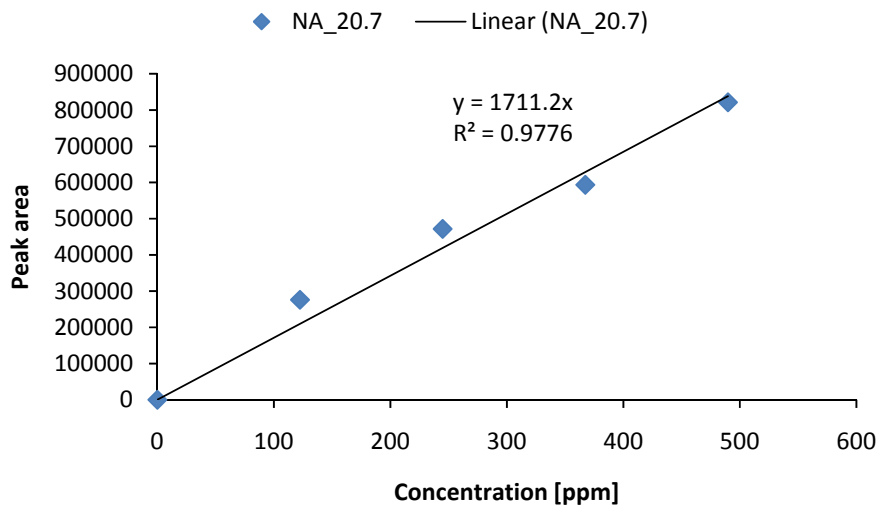


Figure 9-2: Graph of peak area vs. concentration, used for NA_20.7.

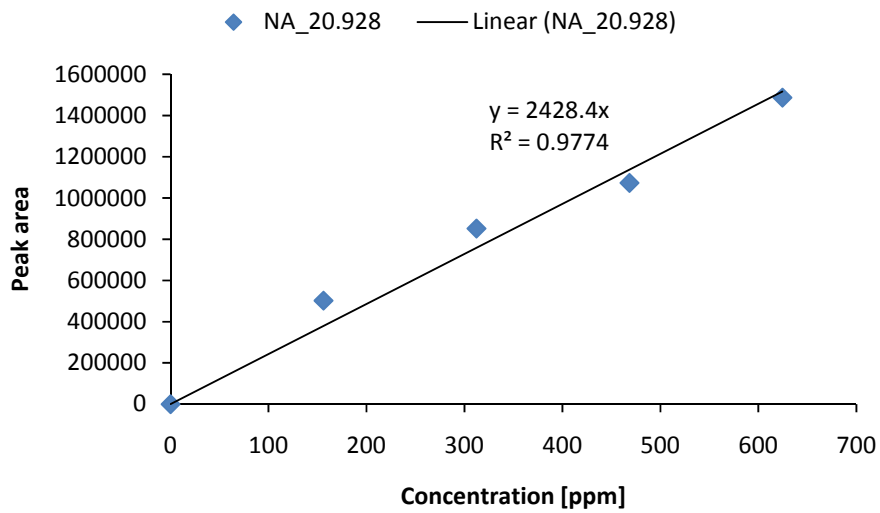


Figure 9-3: Graph of peak area vs. concentration, used for NA_20.928.

Appendix A – Experimental Data

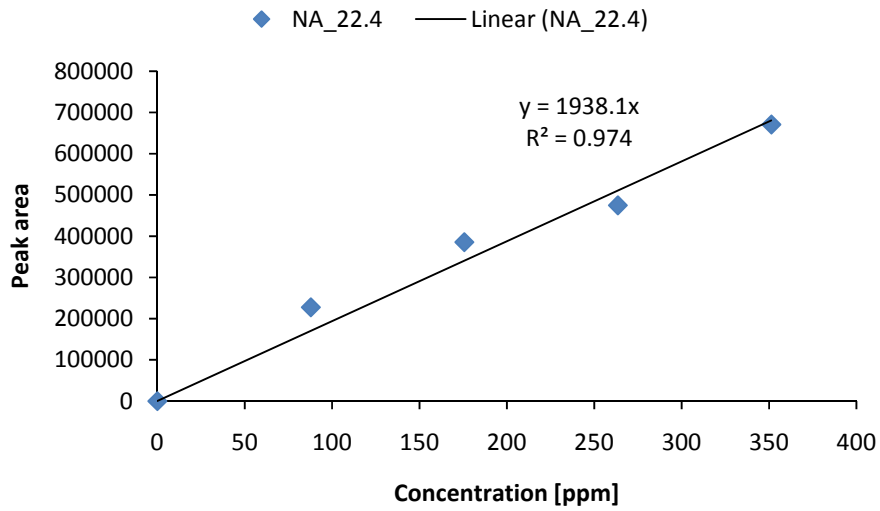


Figure 9-4: Graph of peak area vs. concentration, used for NA_22.4.

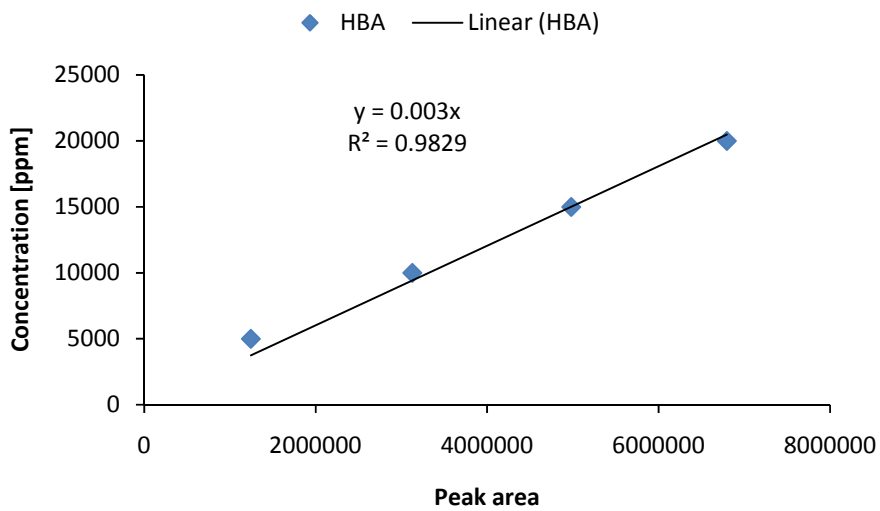


Figure 9-5: Graph of concentration vs. integrated area, used for the HBA samples.

Appendix A – Experimental Data

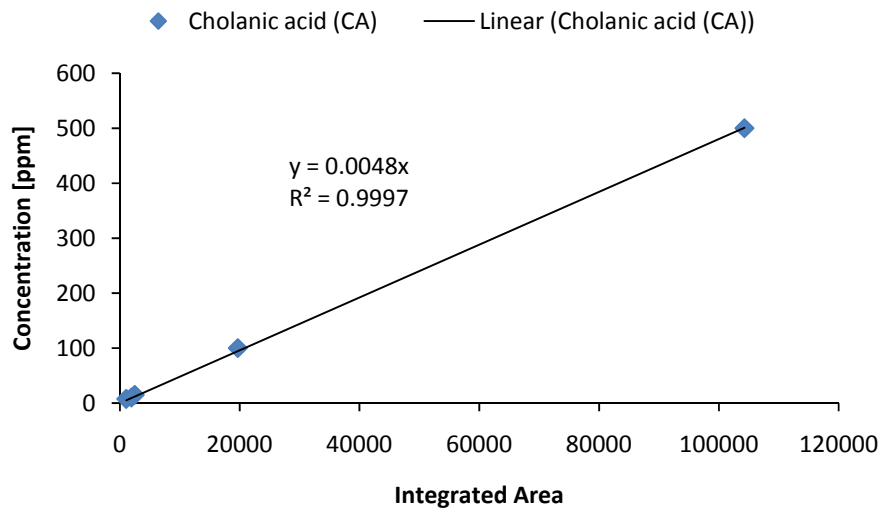


Figure 9-6: Graph of concentration vs. integrated area, used for the CA samples.

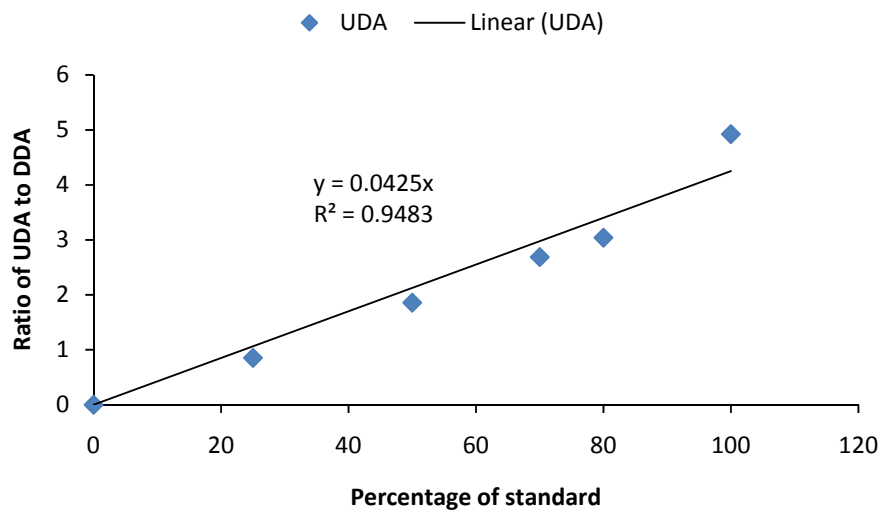


Figure 9-7: Graph of UDA/DDA vs. percentage of standard.

Appendix A – Experimental Data

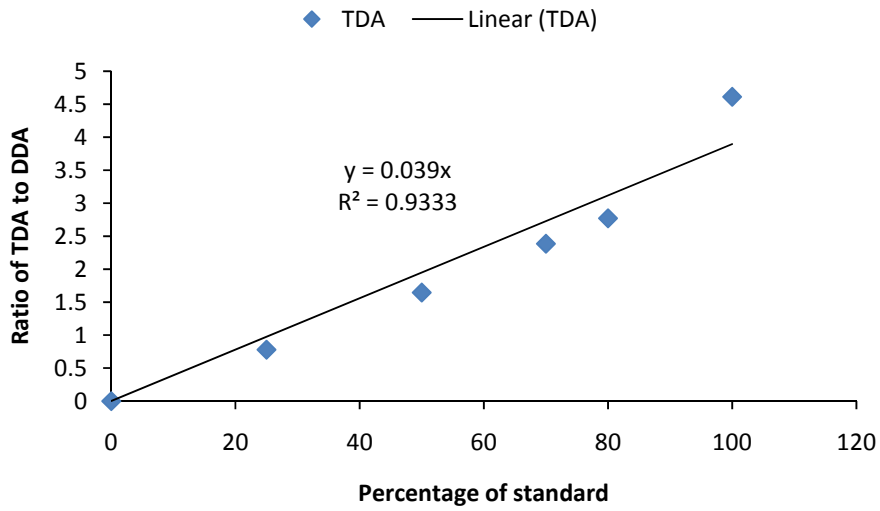


Figure 9-8: Graph of TDA/DDA vs. percentage of standard.

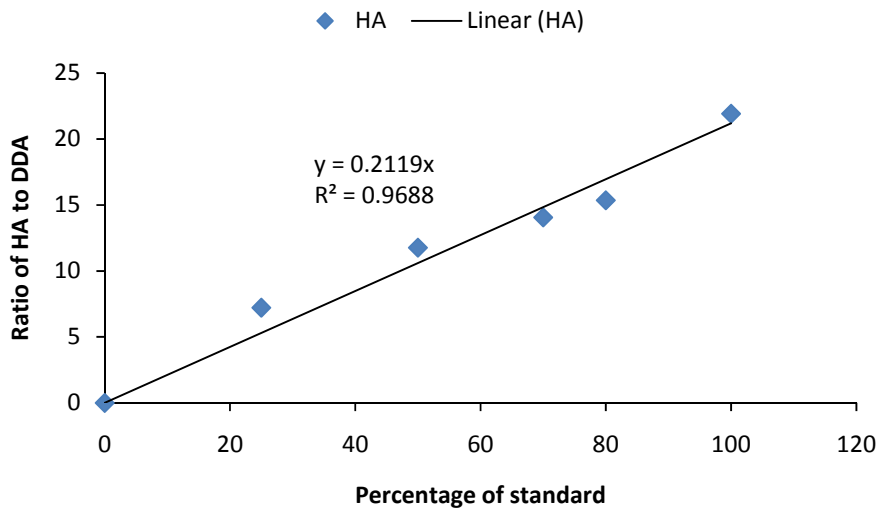


Figure 9-9: Graph of HA/DDA vs. percentage of standard.

9.2.2 Data for naphthenic acid experiments

Table 9-18: Data of the experiments with NA_18.70.

NA_18.70				
pH	C_{f1} [ppm]	C_{f2} [ppm]	$C_{Average}$ [ppm]	Standard deviation
03.07	1277	1205	1241	51
05.43	1094	1171	1132	55
07.21	0988	1052	1020	45
09.14	0902	0824	0863	55
11.26	0127	0120	0124	05

Table 9-19: Data of the experiments with NA_20.70.

NA_20.70				
pH	C_{f1} [ppm]	C_{f2} [ppm]	$C_{Average}$ [ppm]	Standard deviation
03.07	524	503	513	15
05.43	441	491	466	35
07.21	398	419	408	15
09.14	395	375	385	14
11.26	213	194	204	14

Table 9-20: Data of the experiments with NA_20.928.

NA_20.928				
pH	C_{f1} [ppm]	C_{f2} [ppm]	$C_{Average}$ [ppm]	Standard deviation
03.07	661	633	647	20
05.43	554	530	542	17
07.21	506	534	520	20
09.14	502	477	490	18
11.26	337	307	322	21

Appendix A – Experimental Data

Table 9-21: Data of the experiments with NA_22.4.

NA_22.4				
pH	C_{f1} [ppm]	C_{f2} [ppm]	$C_{Average}$ [ppm]	Standard deviation
03.07	375	364	370	07
05.43	336	357	347	15
07.21	288	300	294	08
09.14	282	286	284	03
11.26	277	263	270	10

Table 9-22: Values for the partitioning coefficient of the NA sample.

pH	Partitioning coefficient			
	NA_18.7	NA_20.7	NA_20.9	NA_22.4
03.07	0.44	0.42	0.43	0.42
05.43	0.49	0.48	0.52	0.46
07.21	0.54	0.54	0.54	0.54
09.14	0.61	0.57	0.57	0.56
11.26	0.94	0.77	0.72	0.58

9.2.3 Data for cocktails

Table 9-23: Experimental data for the standard used in the cocktail.

Concentration	Ratio of the acids with DDA			Integrated Area			
	UDA	TDA	HA	UDA	TDA	HA	DDA
0	0	0	0	0	0	0	321587
25	0.853363	0.779386	7.223942	308262	281539	2609519	361232
50	1.858467	1.646677	11.77286	844573	748326	5350131	454446
70	2.688069	2.386589	14.06502	1376087	1221752	7200223	511924
80	3.039367	2.771009	15.36312	1551147	1414190	7840601	510352
100	4.924483	4.61404	21.92603	2964731	2777832	13200323	602039

Appendix A – Experimental Data

Table 9-24: Experimental data for the cocktail samples.

pH	Ratio of the acids with DDA			Integrated Area			
	UDA	TDA	HA	UDA	TDA	HA	DDA
3	4.881864	4.552043	17.29563	2240512	2089142	7937759	458946
5	2.956508	3.319049	12.22088	1436567	1612726	5938125	485900
7	3.331476	3.136648	7.905449	1703067	1603470	4041305	511205
9	3.467008	2.737917	8.345904	1570929	1240572	3781596	453108
11	3.656593	3.049607	7.601736	1813067	1512102	3769207	495835

9.2.4 Data for HBA experiments

Table 9-25: Data of the experiments with HBA samples.

pH	C_{f1} [ppm]	C_{f2} [ppm]	$C_{Average}$ [ppm]	k
3	12287	11687	11987	0.67
5	11324	11503	11414	0.75
7	10803	10653	10728	0.86
9	07853	07925	07889	1.54
11	08076	08052	08064	1.48

9.2.5 Data for CA samples

Table 9-26: Data of the experiments with CA samples, the concentration are based on brine.

pH	C_{f1} [ppm]	C_{f2} [ppm]	$C_{Average}$ [ppm]	k
3	2.15	2.20	2.18	0.00022
5	4.52	4.40	4.46	0.00044
7	5.50	5.60	5.55	0.00056
9	5.09	4.76	4.92	0.00048
11	4.19	4.04	4.12	0.00040

9.3 NOVEL ELECTRIC SEPARATOR EVALUATION

9.3.1 Heptane

Table 9-27: Experimental data of the experiment with heptane in the plant.

VOLTAGE	HEPTANE-AMOUNT OF WATER REMOVED (mL)											
	0.732 Vol% of water			1.25 Vol% of water			2.5 Vol% of water			5 Vol% of water		
	Run 1	Run 2	AVG	Run 1	Run 2	AVG	Run 1	Run 2	AVG	Run 1	Run 2	AVG
0	22.00	24.00	23.00	58.00	60.00	59.00	134	132	133.00	258	262	260
10	28.00	30.00	29.00	60.00	61.00	60.50	147	149	148.00	265	269	267
20	27.00	27.00	27.00	61.00	60.00	60.50	154	153	153.50	279	283	281
40	23.00	23.00	23.00	61.00	61.00	61.00	150	152	151.00	310	304	307
80	22.00	23.00	22.50	62.00	60.00	61.00	148	145	146.50	332	336	334
100	20.00	18.00	19.00	61.00	63.00	62.00	139	141	140.00	348	346	347

AVG: Average

9.3.2 Crown oil at room temperature

Table 9-28: Experimental data for the experiment with vegetable oil at room temperature.

Voltage [V]	Volume of water separated [mL]					
	20% @ Room T, with 1 250 mL of H ₂ O			35 % @ Room T, with 2 500 mL of H ₂ O		
	Run 1	Run 2	Average	Run 1	Run 2	Average
0	98.00	100.00	99.00	490.00	450.00	470.00
20	100.00	108.00	104.00	520.00	500.00	510.00
60	110.00	114.00	112.00	600.00	570.00	585.00
100	125.00	120.00	122.50	700.00	670.00	685.00

9.3.3 Crown oil at $\pm 70^{\circ}\text{C}$

Table 9-29: Experimental data for the experiment with vegetable oil at 70°C .

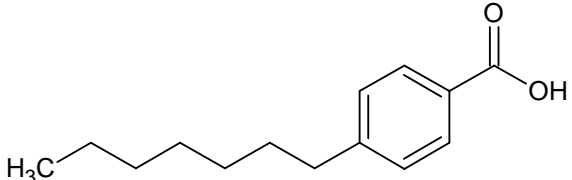
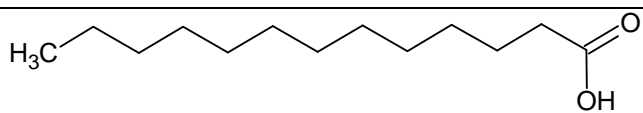
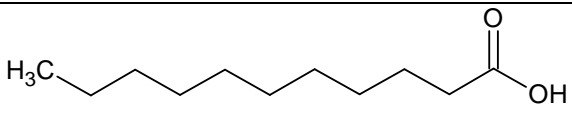
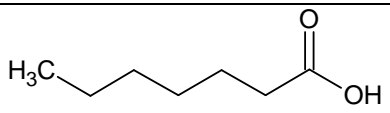
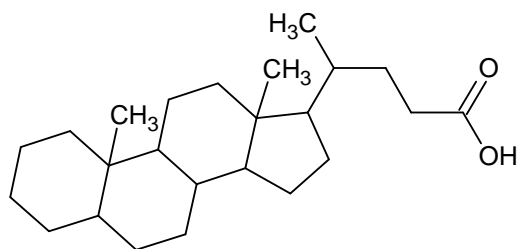
Voltage [V]	Volume of water separated [mL]					
	20% @ $\pm 70^{\circ}\text{C}$, with 1 250 mL of H ₂ O			35 % @ $\pm 70^{\circ}\text{C}$, with 2 500 mL of H ₂ O		
	V ₁	V ₂	Average	V ₁	V ₂	Average
0	150.00	180.00	165.00	550.00	570.00	560.00
20	200.00	230.00	215.00	570.00	590.00	580.00
60	260.00	250.00	255.00	610.00	570.00	590.00
100	300.00	330.00	315.00	690.00	710.00	700.00

9.3.4 Crude oil blend

Table 9-30: Experimental data for the experiments with crude oil blend at 70°C .

Voltage [V]	Volume of water separated [mL]			
	Run 1	Run 2	Average (final)	Initial
0	0	0	0	1898
20	0	0	0	1898
60	50	40	45	1898
100	100	90	95	1898

10 APPENDIX B: CHEMICAL STRUCTURES OF THE ACIDS

Chemical Structure and Name	MW [g/mol]	Source
 <p>4-heptylbenzoic acid (HBA)</p>	220	Sigma-Aldrich
 <p>Tridecanoic acid (TDA)</p>	214	Sigma-Aldrich
 <p>undecanoic acid - (UDA)</p>	185	Sigma-Aldrich
 <p>heptanoic acid - (HA)</p>	130	Sigma-Aldrich
 <p>5β-Cholanic Acid - (CA)</p>	362	Sigma-Aldrich
<p>Naphthenic acid (Mixture of alkylated cyclopentane carboxylic acids)</p>		Sigma-Aldrich

11 APPENDIX C: STATISTICAL ANALYSIS OF THE RESULTS OF THE GRAVITY TEST METHOD

11.1 SAMPLE H CRUDE OIL

The response for this test method was the percentage of brine that separated during the gravity test method. The results of the experiments with sample H crude oil showed that all the factors had a significant effect on the response (at a 95% confidence level) with the stirring speed being the most influential factor in the response, as shown in Figure 11-1. Running the experiment at high stirring speed increased the amount of entrained water in the crude oil, thus a small amount of water was separated under gravity settling. This was evident from the negative sign of the coefficient (say -22.1485), as illustrated in Figures 11-1 and 11-2.

Appendix C: Statistical analysis of the results from gravity test method.

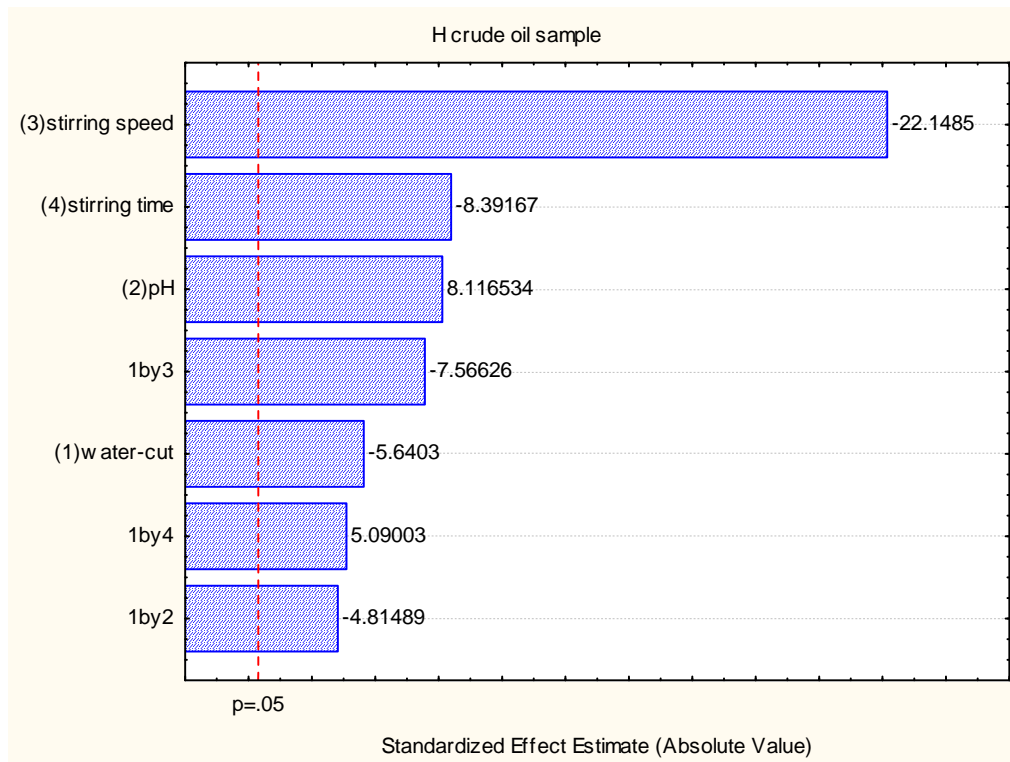


Figure 11-1: Pareto chart of standard effects for the gravity settling method with sample H crude oil.

Figure 11-2 was selected to explain the operating parameters that maximised or minimised the response. The further the variables are from the zero standardised effects (x -axis), the more the effects are in the response. The negative effects from the left-hand side decrease the response, whilst the positive effect increases the response. In order to maximise the response, the stirring speed, stirring time and water cut should be run at low level, whereas the brine pH should be run at high level. Maximising the response (percentage of water separated in the gravity test method) decreases the stability of the emulsion. Therefore, in order to increase the stability of the emulsion in this experiment, the stirring speed, stirring time and the water cut should be run at high level whilst the brine pH should be run at a low level. However, running the experiment at a high brine pH, say 8.0, and a high water-cut, say 50%, increased the emulsion stability; this is reflected in the negative sign of the interaction coefficient between the brine pH and the water cut, as shown in Figure 11-1.

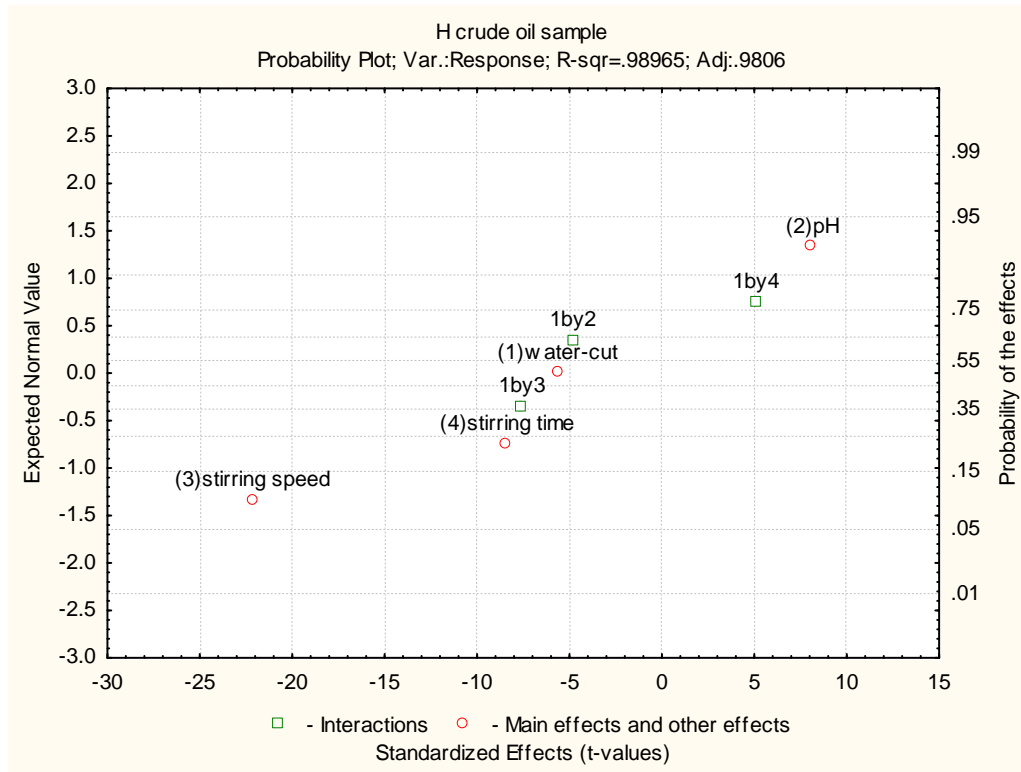


Figure 11-2: Normal probability plot of the results with sample H crude oil.

The model used explained approximately 98.965% of the observed data, as shown in Figure 11-2. The response was then mathematically expressed as shown in Equation 3.01, in Chapter 3.

$$y = 40.16 - 6.41x_1 + 9.22x_2 - 25.16x_3 - 9.53x_4 - 5.47x_1x_2 - 8.59x_1x_3 + 5.78x_1x_4$$

11.2 SAMPLE M CRUDE OIL

The results of the experiment with sample M crude oil showed that all the factors had a significant effect on the response. Water-cut showed the most significant effect on the amount of water separated under gravity; the effects are ranked in a decreasing order from top to bottom in Figure 11-3. The operation of the process at higher water-cut and higher stirring speed simultaneously enhanced the recovery of water under gravity. However, running the experiment at higher stirring speed reduced the amount of water separated. The effect of water-cut overran

Appendix C: Statistical analysis of the results from gravity test method.

all the factors. The operating conditions for the experiments with sample M crude oil are illustrated in Figure 11-4.

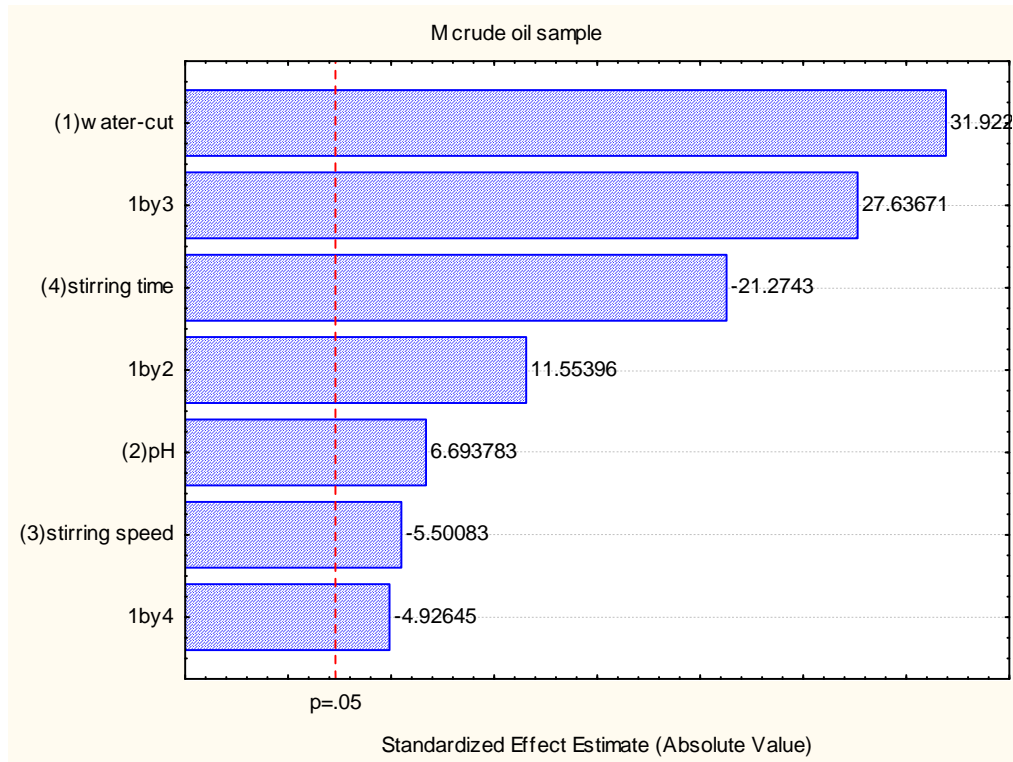


Figure 11-3: Pareto chart of standardised effects for the experiments with sample M crude oil

The higher the amount of water separated during the gravity-test-method the more stable is the emulsion formed. In order to create a stable water-in-oil emulsion, the water cut and the brine pH should be run at their lower level possible, whereas the stirring speed and the stirring time should be run at a higher level, as explained in Figure 11-4. The influence of the water-cut in increasing the percentage of water separated under gravity explains the fact that the sample M crude oil does not mix easily with the prepared brine solution.

Appendix C: Statistical analysis of the results from gravity test method.

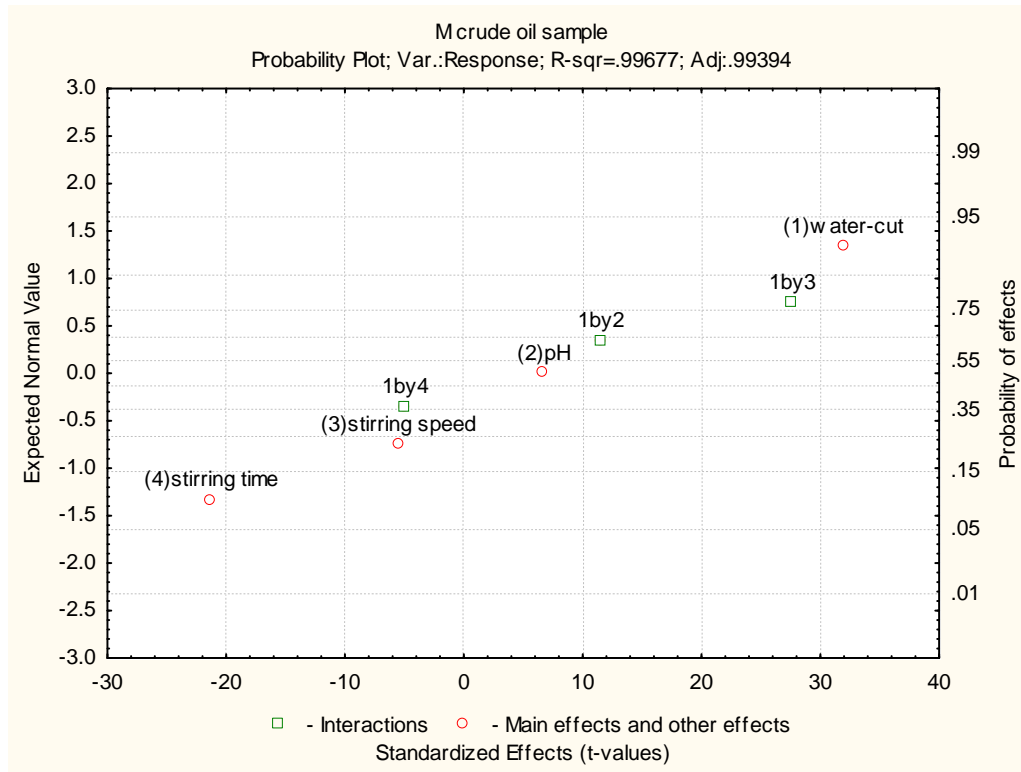


Figure 11-4: Probability plot for the experiment with sample M crude oil.

The influence of the interaction effect on the response is also a matter of concern. The influence of the interaction is shown graphically in Figure 11-5. The distorted plane indicates an influence of the interaction between water cut and the stirring speed. It is clear from this graph that operating at a higher stirring speed while keeping the water-cut at a lower level, decreases the percentage of water in the gravity-test-method, thus increasing the emulsion stability. Running the experiment at higher water cut and lower stirring speed increases the percentage of water in the gravity-test-method, which tended to reduce the emulsion stability. On further running the experiment at higher water cut and higher stirring speed, the percentage of water in the gravity test increased abruptly, as shown in Figure 11-5 in the region where the plane is shifted upward.

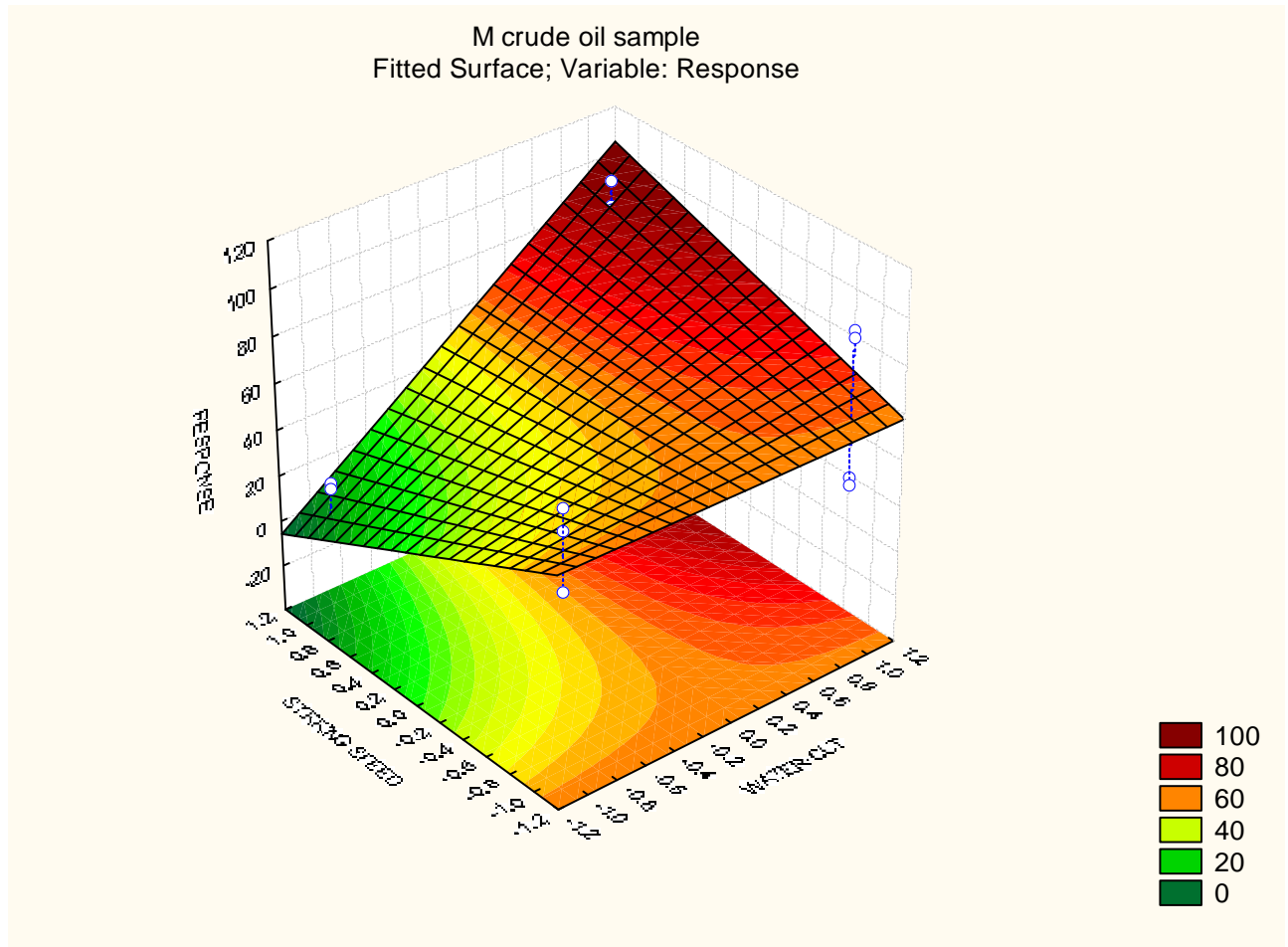


Figure 11-5: Surface response for the results with sample M crude oil.

The model used for this analysis explained approximately 99.677% of the observed data, as shown in Figure 11-4. Here the equation for the model expressed as follows:

$$y = 54.14 + 22.58x_1 + 4.13x_2 - 3.89x_3 - 15.05x_4 + 8.17x_1x_2 + 19.55x_1x_3 - 3.48x_1x_4$$

11.3 SAMPLE U CRUDE OIL

The results from the experiments with sample U crude oil showed that the four factors were significant in the response. All the interactions except the water-cut-stirring-speed interaction were also significant in the response. The factors that affected the response were ranked in

Appendix C: Statistical analysis of the results from gravity test method.

decreasing order as illustrated in Figure 11-6. The stirring time had the biggest effect on the response, followed by the water-cut.

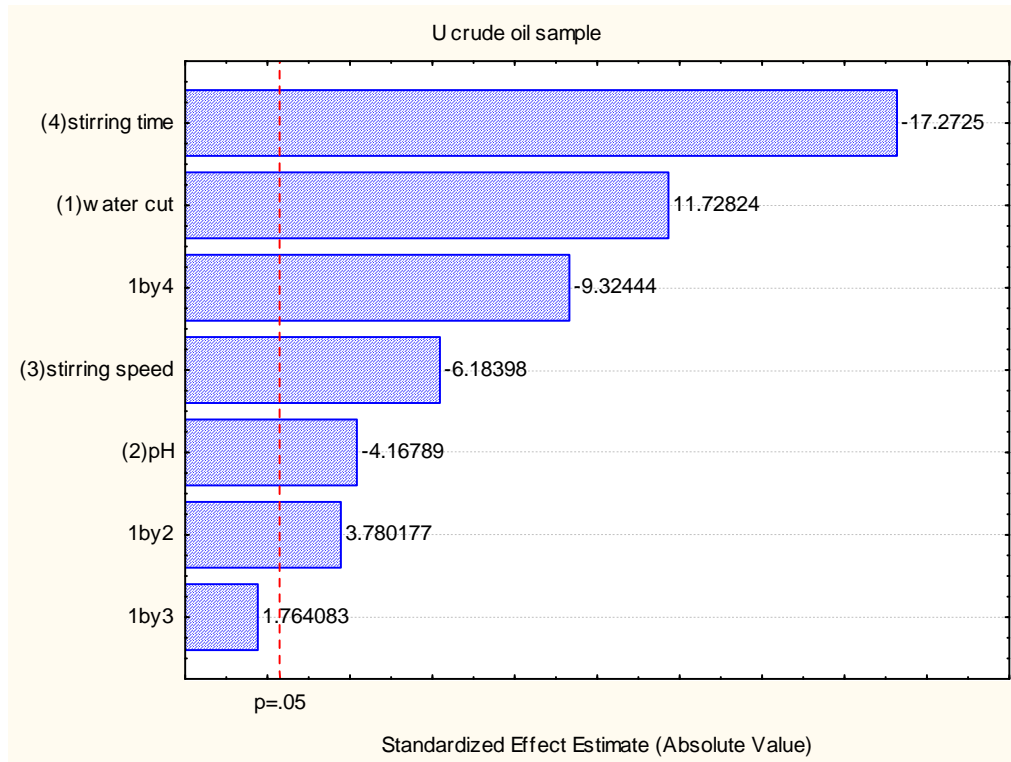


Figure 11-6: Pareto chart of standardised effects for the experiments with sample U crude oil.

Running the experiment at a higher stirring time decreased the response (see Figure 11-7 for further illustration). The response was improved by running the experiment at a higher water cut. Stirring speed and brine pH had a negative effect on the response, but these effects were overruled by the major effects (stirring time and water-cut).

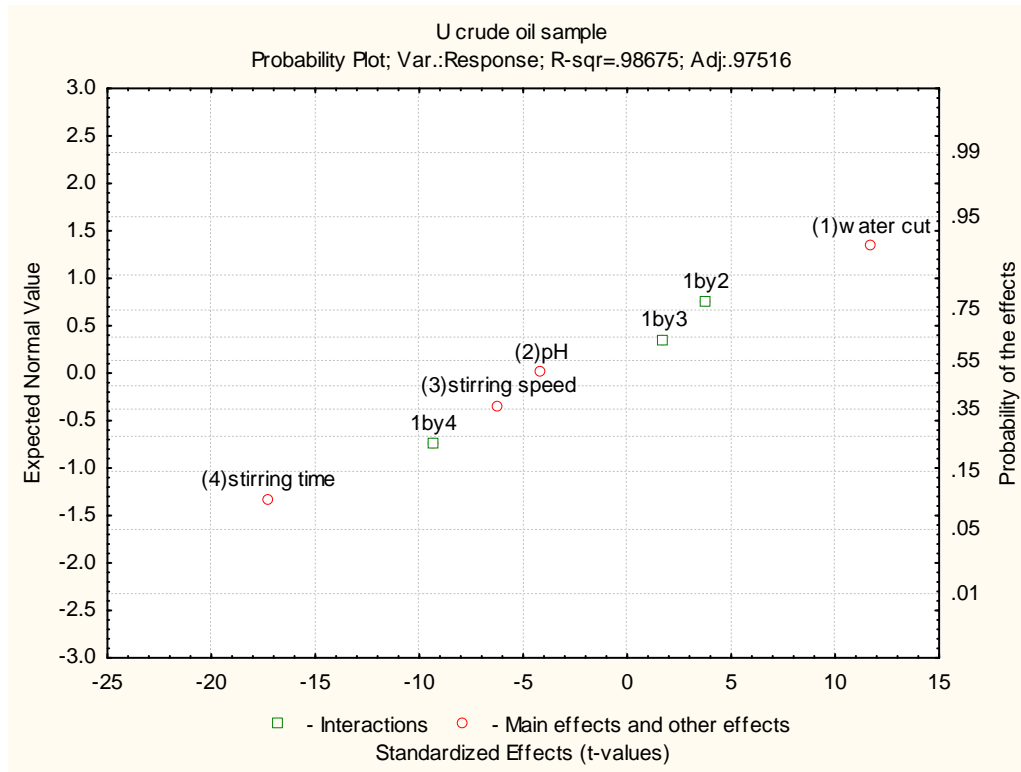


Figure 11-7: Probability plot of the results with sample U crude oil.

The mathematical representation of the response is as follows:

$$y = 31.72 + 18.91x_1 - 6.72x_2 - 9.97x_3 - 27.84x_4 + 6.09x_1x_2 + 2.84x_1x_3 - 15.03x_1x_4$$

11.4 SAMPLE P CRUDE OIL

The results from the experiments with sample P crude oil show that all factors and interactions had a significant effect on the response (the amount of water separated under gravity) (see Figure 11-8 for an illustration).

Appendix C: Statistical analysis of the results from gravity test method.

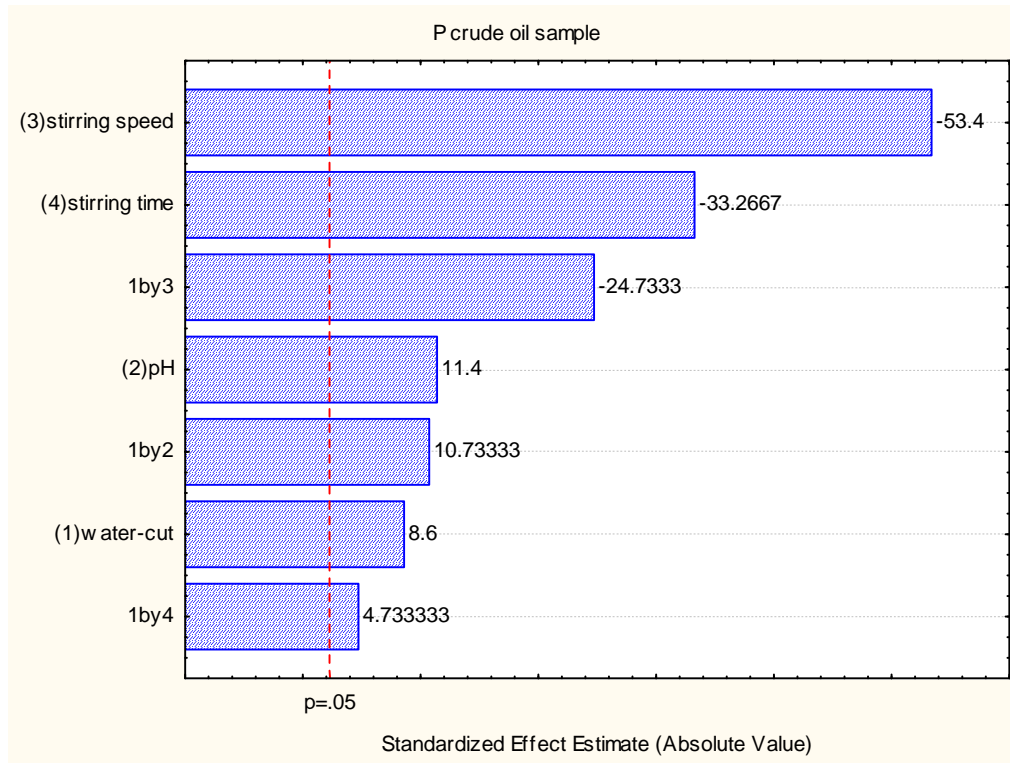


Figure 11-8: Pareto chart of standardised effects of the results with sample P crude oil.

The effects on the response were ranked on the Pareto chart, as illustrated in Figure 11-8. The stirring speed had the highest effect, followed by the stirring time. Both stirring speed and stirring time had a negative effect on the response, whilst the brine pH and the water cut had a positive effect on the response.

The operating parameters are explained using a normal probability plot. Figure 11-9 shows the normal probability plot for the experiment with sample P crude oil. It is clear that, in order to increase the response, the stirring speed and the stirring time should be run at a lower level, whereas the brine pH and the water-cut should be run at higher level, as shown in Figure 11-9.

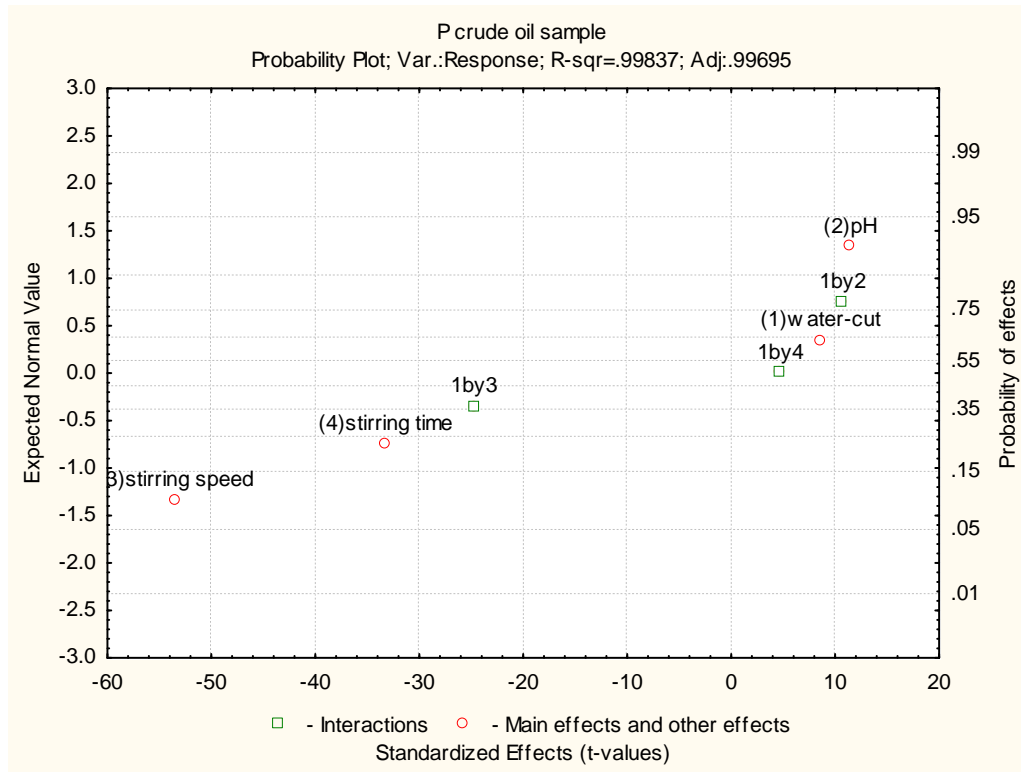


Figure 11-9: Normal probability plot of the experimental results with sample P crude oil.

The effect of the water-cut-stirring-speed interaction is stronger than the effect of the water cut alone and smaller than the effect of the stirring speed. This means that, running the experiment at a higher stirring speed and higher water cut will decrease the response; this overcome the effect of the water alone.

Here the response is represented as follows:

$$y = 35.59 + 4.03x_1 + 5.34x_2 - 25.03x_3 - 15.59x_4 + 5.03x_1x_2 - 11.59x_1x_3 + 2.22x_1x_4$$

11.5 SAMPLE C CRUDE OIL

The results of the experiments with sample C crude oil show that all factors had a significant effect on the response. All the interactions but the water-cut-stirring-speed interaction also had significant effects on the response. The rank of the effects is shown in Figure 11-10. The most influential effect is the stirring speed, followed by the water cut and stirring time. The effect of

Appendix C: Statistical analysis of the results from gravity test method.

the brine pH is small compared to the effects of the stirring speed, water cut and stirring speed, thus it may be ignored for further discussion.

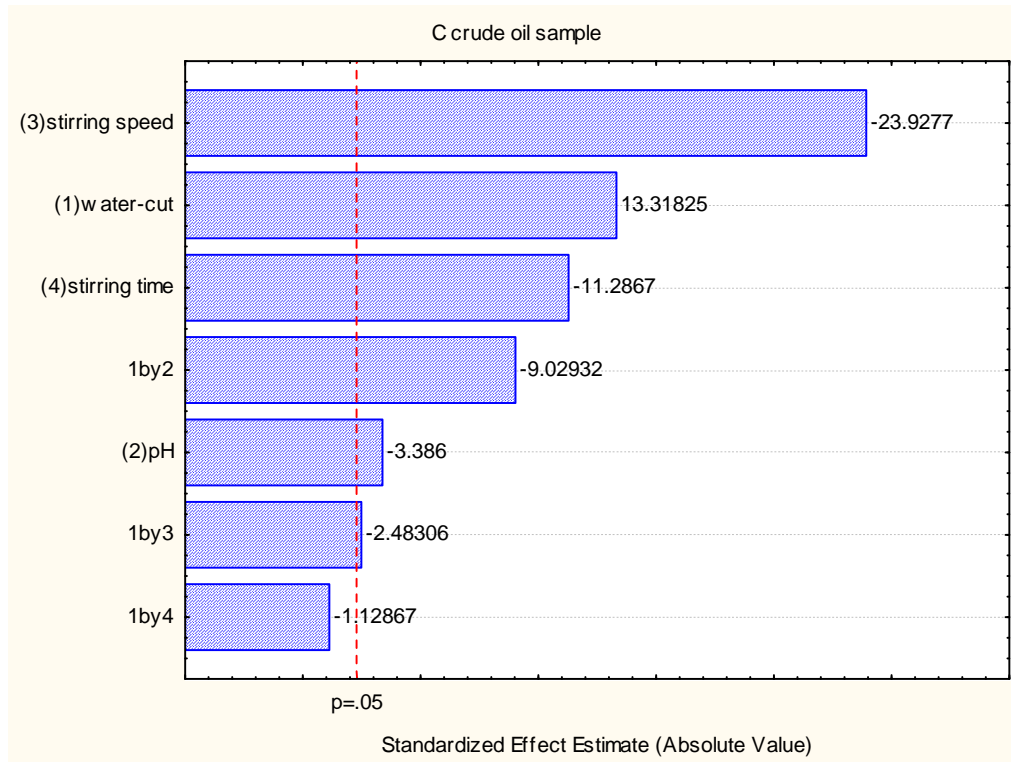


Figure 11-10: Pareto chart of the standardised effects of the experiments with sample C crude oil

The operating parameters are explained using the normal probability plot. Figure 11-11 illustrates the normal probability plot for the experiment with the C crude oil. The stirring speed, stirring time and brine pH had a negative effect on the response, and thus lay on the left-hand side of the normal probability plot graph, as shown in Figure 11-11. The water-cut had a positive effect on the response; this was represented on right-hand side of the normal probability graph. In order to increase the response, the stirring speed, stirring time and brine pH should be run at a lower level whilst the water cut should be run at a higher level.

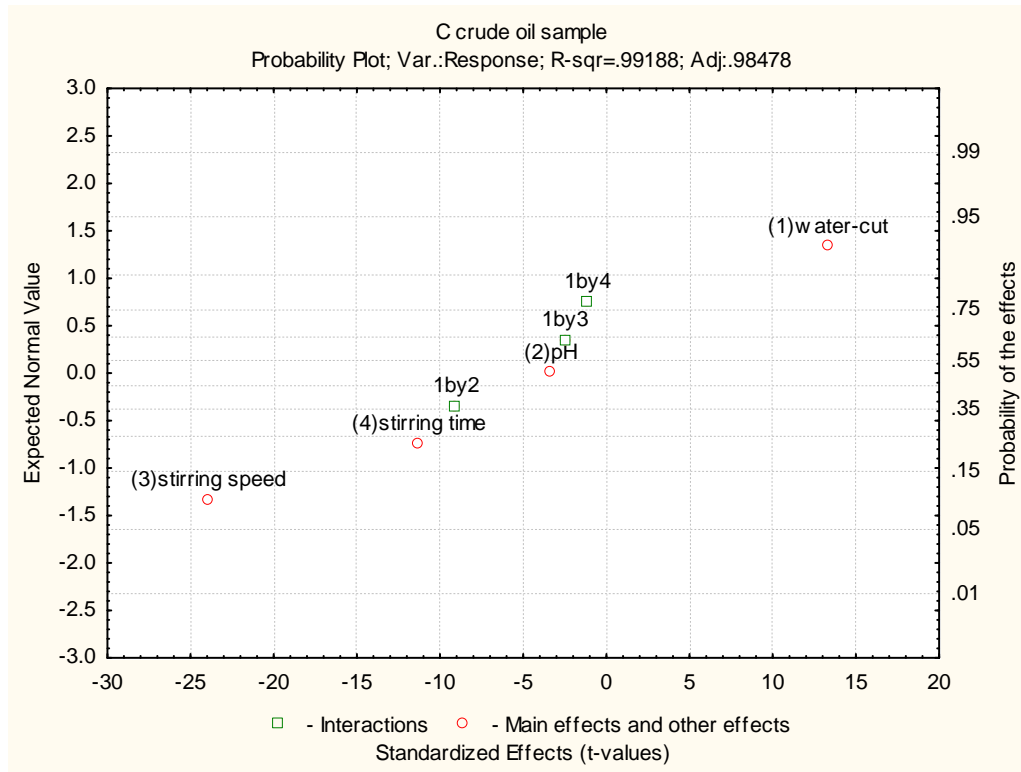


Figure 11-11: Probability plot for the experiments with sample C crude oil.

The response is mathematically expressed as follows:

$$y = 56 + 14.75x_1 - 3.75x_2 - 26.5x_3 - 12.5x_4 - 10x_1x_2 - 2.75x_1x_3 - 1.25x_1x_4$$

11.6 SAMPLE A CRUDE OIL

The experimental results for sample A crude oil show that all factors had a significant effect on the response, as illustrated in Figure 11-12. Only the water-cut-stirring-speed interaction had a significant effect when compared to the other two interactions as shown in Figure 11-12 they lie on the left-hand side of the dashed vertical line ($p = 0.05$). The most influential effect was the stirring speed, followed by the stirring time and brine pH. The water-cut had the least effect on the response.

The stirring speed and stirring time had a negative effect on the response, that is, they decreased the response when these factors were operated at a higher level. However, the water-cut and the

Appendix C: Statistical analysis of the results from gravity test method.

brine pH had a positive effect on the response, that is, when they were operated at a higher level the response increased (see Figure 11-13 for further illustration). In order to increase the response, the stirring speed and the stirring time should be set at a lower level, whilst the water cut and the brine pH should be set at a higher level. The interaction effects had a negligible effect compared to the main effect.

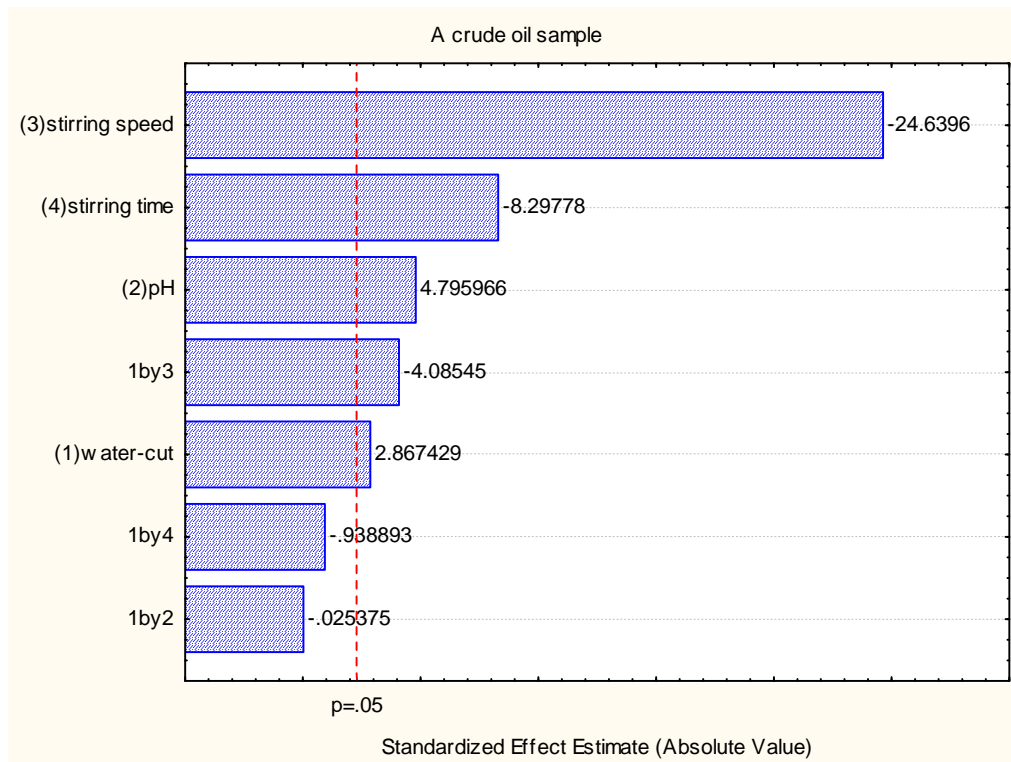


Figure 11-12: Pareto chart of standardised effects of the experiment with sample A crude oil

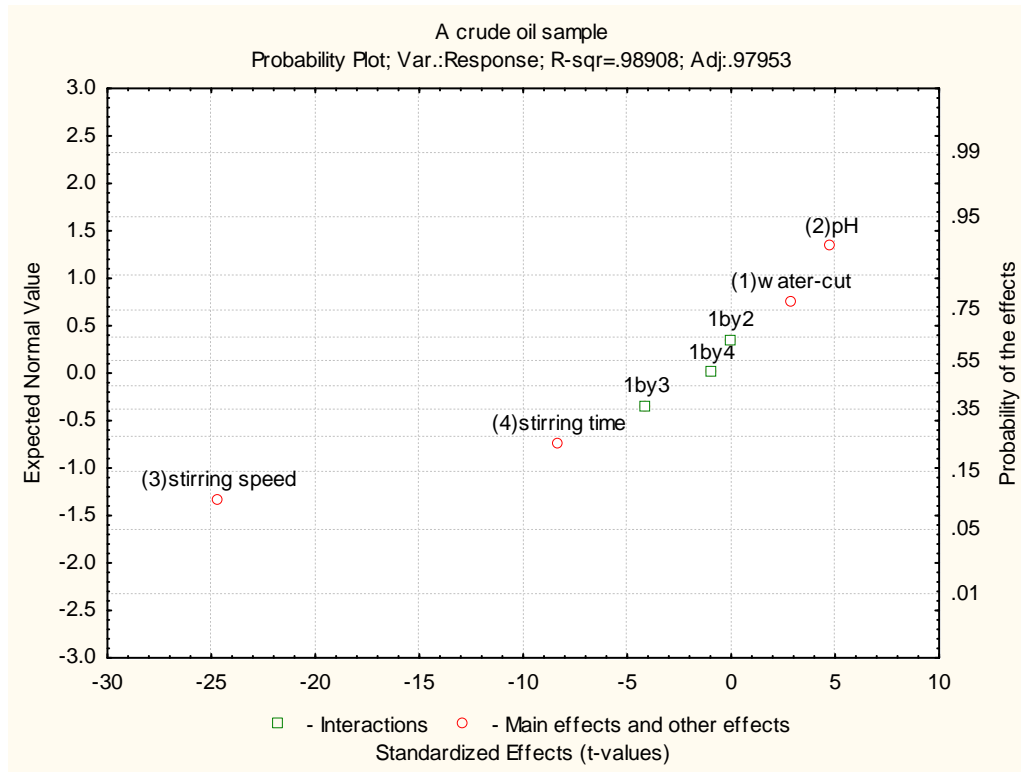


Figure 11-13: Normal probability plot for the results with sample A crude oil

Here the model equation is written as follows:

$$y = 43.84 + 3.53x_1 + 5.91x_2 - 30.34x_3 - 10.22x_4 - 0.03x_1x_2 - 5.03x_1x_3 - 1.16x_1x_4$$

11.7 SAMPLE V CRUDE OIL

The experimental results with sample V crude oil show that all factors and their respective interactions had a significant effect on the response, and the stirring speed had the major effect on the response. The water-cut-pH interaction also had an impact on the response. Figure 11-14 provides an illustration of the effects ranking. The stirring time effect comes after the water-cut-pH interaction.

Appendix C: Statistical analysis of the results from gravity test method.

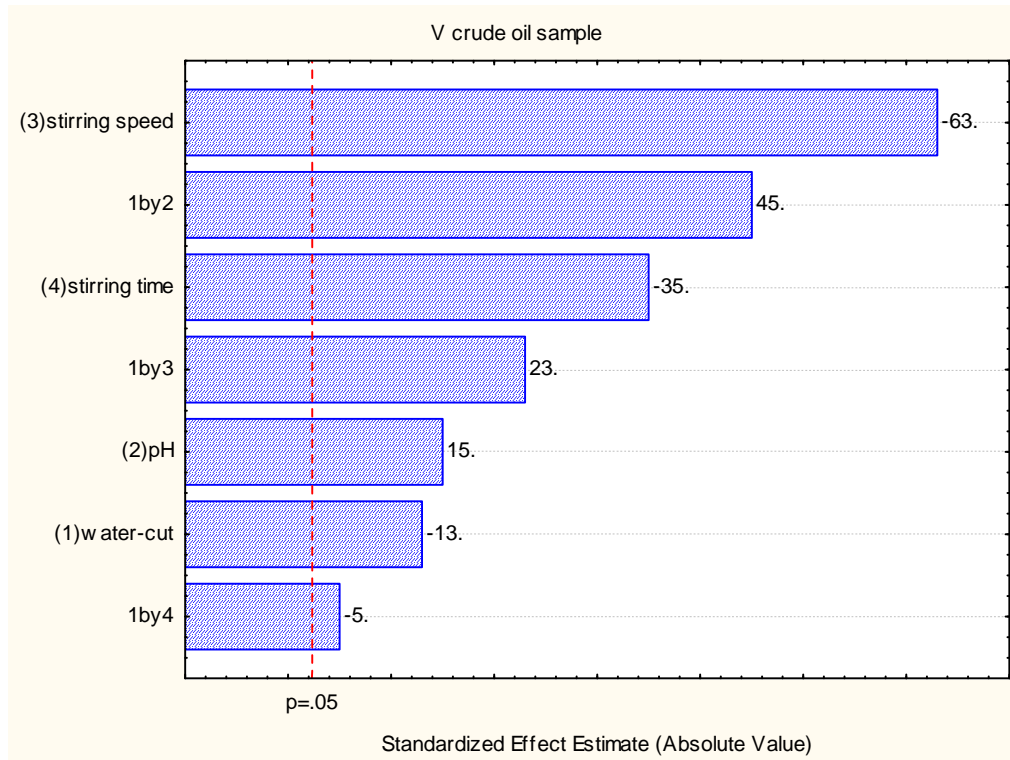


Figure 11-14: Pareto chart of standardised effects for the experiments with sample V crude oil

In order to understand the operating range of the factors and their interactions, the normal probability plot as illustrated in Figure 11-15 was used. It is clear that the stirring speed, stirring time and water cut lie on the left hand side of the normal probability plot, thus inferring a negative effect on the response, that is, the response was decreased when these factors were operated at their higher level. However, the brine pH had a positive effect on the response, which means that the response was increased when the process was operated at higher brine pH.

The interactions in this experiment had quite a significant effect compared to some of the factors. It can be seen from Figure 11-15 that the water-cut-pH interaction lay on the right-hand side, implying that operating the process at both higher water cut and higher brine pH increased the response when the other two factors were operated at a lower level. Furthermore, there is also a positive effect of the water-cut-stirring-speed interaction which implies that operating the process at a higher water cut and stirring speed respectively increases the response when the stirring time is set at a lower level and the brine pH at a higher level. However, the water-cut-stirring-time interaction had a negative effect on the response although it is the least effect of all of the factors but at a confidence level of 95% it was thus considered; the negative effect implies

Appendix C: Statistical analysis of the results from gravity test method.

that operating the process at a higher water-cut and stirring speed decreases the response, provided that the stirring speed is run at a higher level and the brine pH at a lower level.

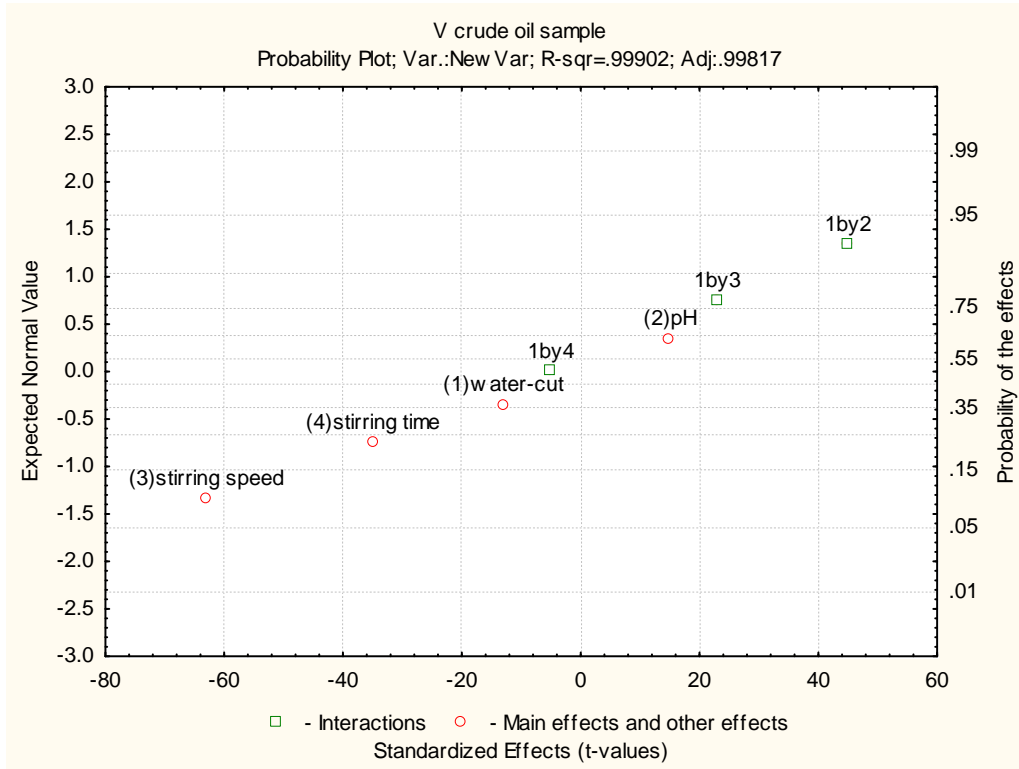


Figure 11-15: Normal probability plot for the results with sample V crude oil

From the analysis done thus far, the conclusion is as follows: In order to increase the response the process should be run at a higher water-cut and brine pH respectively, with the stirring time and stirring speed set at a lower level respectively. This operating condition is explained in a surface response graph in Figure 11-16, in which the interaction effect is visible in the distorted plane and reflected on the curved lines projected onto the pH-water-cut plane.

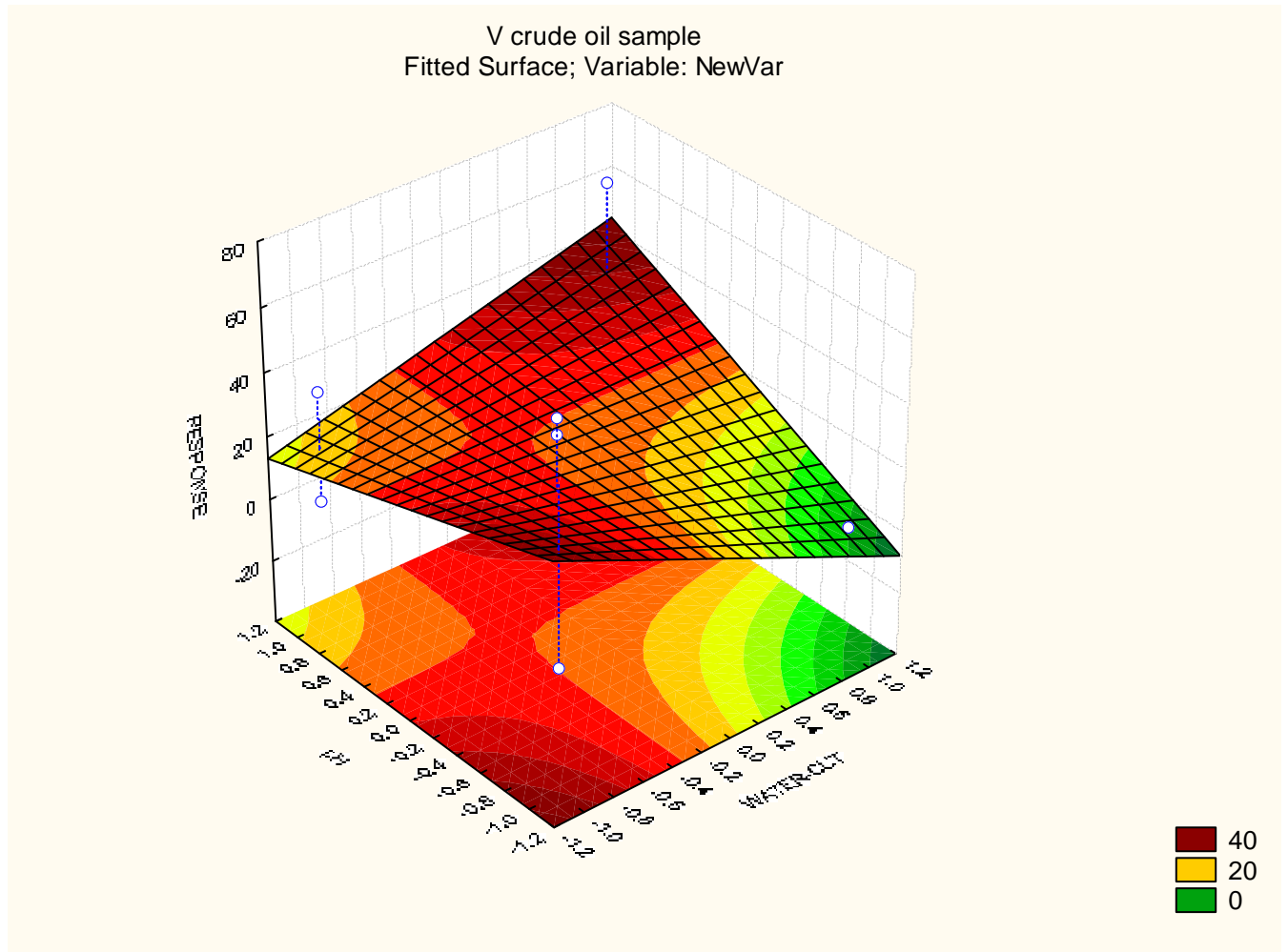


Figure 11-16: Surface response for the results with V crude oil

The response for this experiment is represented mathematically as follows:

$$y = 22.81 - 4.06x_1 + 4.69x_2 - 19.69x_3 - 10.94x_4 + 14.06x_1x_2 + 7.19x_1x_3 - 1.56x_1x_4$$

12 APPENDIX D: EQUIPMENT USED

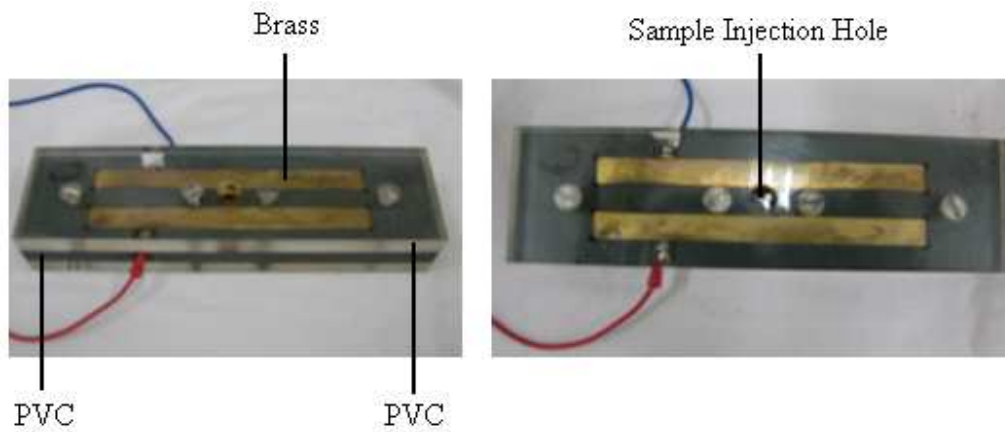


Figure 12-1: The critical electric field cell



Figure 12-2: The electric separator

Appendix D: Equipment used



Figure 12-3: Crude oil blend in the mixing tank



Figure 12-4: The centrifuge used in the experiment

13 APPENDIX E: PUBLISHED PAPER

Andre, A.L.B. & Els, R.E. 2009, 'Study of water-in-crude-oil emulsions, using gravity-settling, critical-electric-field and centrifuge', Paper published in *Chemeca Conference*, Australia.